Master's Thesis

Secondary Organic Aerosol and Ozone Formation Potential from Anthropogenic and Biogenic Volatile Organic Compounds in Ulsan, South Korea, in Summer

Geunwoo Lee

Department of Urban and Environmental Engineering
(Environmental Science and Engineering)

Ulsan National Institute of Science and Technology

2021

Secondary Organic Aerosol and Ozone Formation Potential from Anthropogenic and Biogenic Volatile Organic Compounds in Ulsan, South Korea, in Summer

Geunwoo Lee

Department of Urban and Environmental Engineering
(Environmental Science and Engineering)

Ulsan National Institute of Science and Technology

Secondary Organic Aerosol and Ozone Formation Potential from Anthropogenic and Biogenic Volatile Organic Compounds in Ulsan, South Korea, in Summer

A thesis submitted to
Ulsan National Institute of Science and Technology
in partial fulfillment of the
requirements for the degree of
Master of Science

Geunwoo Lee

12/10/2020

Approved by

Advisor
Prof. Sung-Deuk Choi

Secondary Organic Aerosol and Ozone Formation Potential from Anthropogenic and Biogenic Volatile Organic Compounds in Ulsan, South Korea, in Summer

Geunwoo Lee

This certifies that the thesis of Geunwoo Lee is approved.

12/10/2020

signature

Advisor; Thesis Committee Chair: Prof. Sung-Deuk Choi

signature

Thesis Committee Member: Prof. Chang-Keun Song

signature

Thesis Committee Member: Prof. Sang Seo Park

Abstract

A large quantity of anthropogenic and biogenic volatile organic compounds (VOCs) is emitted in Ulsan because Ulsan has huge multi-industrial complexes in its eastern coastal area and high mountainous regions in the western hinterland. Some of the VOCs are oxidized and form tropospheric ozone and secondary organic aerosol (SOA) in the atmosphere. Not only high temperature and radiation but also the transport of VOCs from their sources could aggravate the photochemical oxidation reactions in the atmosphere in Ulsan in summer. Despite the environmental importance of photochemical reactions of VOCs, few studies on photochemical VOCs in Ulsan have been carried out. The objectives of this study are to investigate the spatial concentration levels of photochemical VOCs, estimate the formation potentials of ozone and SOA, and propose further research to figure out how much VOCs have contributed to high tropospheric ozone and particulate matter episodes in Ulsan, South Korea, in summer.

Hybrid VOC monitoring was conducted with diffusive passive samplers (Radiello, Instituti Clinici Scientifici Maugeri, Itay) and active pumped adsorbent tube samplers (Sequential tube sampler-25, PerkinElmer, UK) at 17 sites (5 industrial, 6 rural, 6 urban sites) and three sites (1 control, 1 industrial, 1 rural site), respectively, in Ulsan from May to August 2020. Through the hybrid VOC sampling, the temporal and spatial resolution of Ulsan VOC monitoring was highly improved. The target VOCs were selected as photochemical assessment monitoring stations (PAMS) ozone precursor 53 VOCs (36 aliphatics and 17 aromatics). Both anthropogenic VOCs like benzene, toluene, ethylbenzene, and o,m,p-xylene (BTEX) and a biogenic VOC, isoprene, were included. All 240 VOC adsorbent samples were analyzed with a thermal desorber-coupled gas chromatography/mass spectrometer (TD-GC/MS, UNITY series 2, Markes, UK-7890B/5977A, Agilent, USA). Every sampling trip had field blank samples to track any contaminations from the whole analytical process. A 3:1 signal to noise ratio was applied to the quantification of VOCs. The concentration spatiotemporal distribution of the VOCs was comprehensively interpreted with the data of 16 meteorological observation stations in Ulsan, considering the physicochemical properties of the 53 VOCs.

From May to August, the atmospheric temperature in Ulsan increased except for in July because July is the rainy period. Heavy rain was observed in July, causing relatively low temperatures and radiation. Due to the land-sea breeze in Ulsan, the transport of VOCs from industrial areas to highly urbanized areas occurred in the daytime while transport of VOCs from mountainous areas to the urban region occurred in the nighttime. Criteria air pollutants (CAPs) in rural and industrial sites were compared. Although the concentration of fine particulate matter ($PM_{2.5}$) did not show statistically

significant differences between the sites, NO_2 was higher, and O_3 was lower in the industrial site than in the rural sites. Also, O_3 and the fine particulate matter to coarse particulate matter (PM_{10}) ratio, whose change could indicate the secondary aerosol formation, showed strong diurnal variations in the rural sites but not in the industrial site. These differences in the concentration levels of NO_2 and O_3 and the diurnal variation between industrial and rural sites need to be contemplated in a further SOA and O_3 formation study in Ulsan.

Total VOCs (TVOCs), BTEX, and aliphatics exhibited significantly higher concentrations in industrial sites than in rural and urban sites. However, isoprene, a well known biogenic VOC (BVOC), showed a higher concentration in rural sites than in industrial and urban sites. This was obvious due to the BVOCs being emitted from the vegetation. In addition, isoprene concentrations had strong diurnal cycles depending on temperature and solar radiation. In order to identify the source and aging status of BTEX in each site, diagnostic ratios were applied to the BTEX concentration in each sampling site. Toluene to benzene ratio and m,p-xylene to ethylbenzene ratio were used as indicators for traffic emission and aging, respectively. BTEX in automobile and shipbuilding industrial areas were highly affected by fresh and non-traffic sources while BTEX in the harborside petrochemical industrial area were mostly influenced by fresh and traffic sources. Most rural and urban sites were affected by aged both traffic and non-traffic BTEX sources.

The top 5 VOC contributors of ozone and SOA formation potentials (OFP and SOAFP) in different sites were compared in this study. In urban and rural sites, toluene, ethylbenzene, and xylenes (TEX) were dominant in the top 5 OFP contributors. In addition to TEX, n-octane and 3-methylpentane significantly contributed to OFP in industrial sites. Regardless of the sites, TEX made the biggest contribution to SOAFP. OFP and SOAFP from VOCs were highest in petrochemical and automobile industrial areas, respectively, in this study. However, the estimated formation potential of O_3 and SOA could not explain the spatiotemporal variations of O_3 and SOA based on the observed data. To improve the accuracy of the estimations, more VOCs, especially BVOCs, should be included in VOC monitoring and a better methodology to calculate formation potential with meteorological conditions needs to be developed.

In conclusion, TEX largely influenced OFP and SOAFP in Ulsan in the summer. While controls for TEX over the Ulsan need to be enhanced to reduce photochemical oxidation reactions forming O_3 and SOA, the study on BVOCs such as isoprenes and terpenes, is also needed due to the lack of understanding BVOCs in Ulsan. In order to improve the estimation of O_3 and SOA formation, the key factors, such as meteorological conditions and atmospheric composition, should be investigated and considered in a non-linear way like through a machine learning approach.

Contents

List of Figures

List of Tables

1. Introduction

1.1. Environmental importance of volatile organic compounds in Ulsan

Ulsan is one of the largest multi-industrial cities in South Korea, emitting about 8,100 tons of the most varied chemicals a year (7.63 ton/y/km^2) among metropolitan cities in Korea (Figure 2) (NICS, 2018). Ulsan is the south-eastern coastal area of the Korean Peninsula. The residential population is about 1.1 million and the area is 1,061.54 km^2 based on the report from Ulsan City Hall in 2020 (Ulsan, 2020). Urban areas were developed and urbanized along with the Taehwa river located in the middle of the city. The eastern coastal part of Ulsan consists of multi-industrial complexes involving petrochemical, automobile, shipbuilding, and non-ferrous metal industries, whereas the western inland part of Ulsan is mostly an agricultural area surrounded by mountainous regions with more than 1,000km height of peaks (Figure 1). Therefore, various air pollutant emissions from both anthropogenic and biogenic sources are expected to influence the atmospheric composition in Ulsan. This should be investigated to effectively improve the air quality of Ulsan.

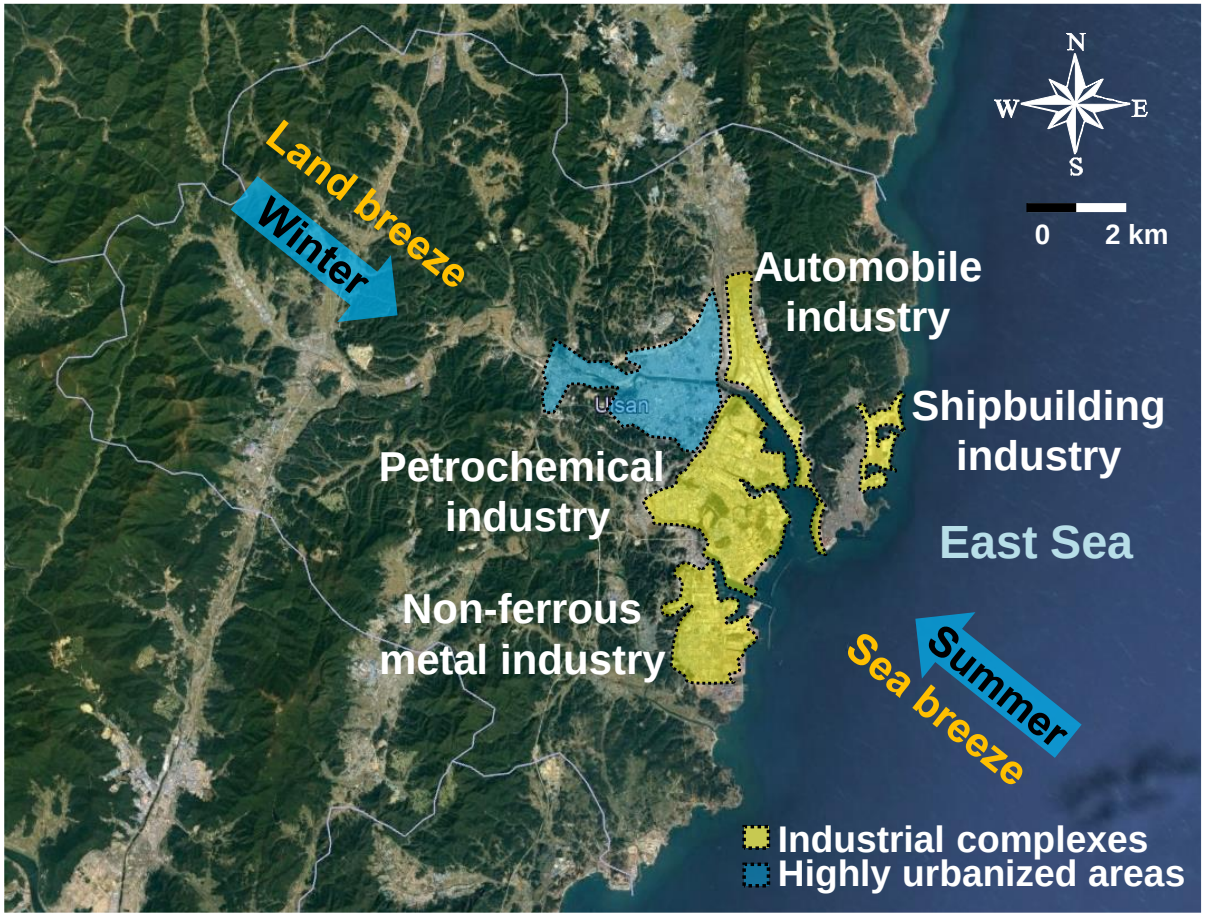

Figure 1. Geographical and meteorological conditions of Ulsan

Seasonal synoptic meteorological patterns and diurnal sea-land breezes are important for understanding the air quality of Ulsan because of its geographical location. While the westerlies are dominant in the Korean Peninsula, the North Pacific high grows in warm periods and the southeasterly blows while transporting air pollution from industrial to residential areas. The sea breeze enhances air pollution transport during the daytime. Due to these meteorological characteristics in Ulsan, there was an extremely high air pollution episode with hourly maximum concentration of 132 μg/m^3, 117 ppb in fine particulate matter (< 2.5 μm diameter, $PM_{2.5}$) and ozone (O_3), respectively, in July 2018 (MOE, 2020; NIER, 2018). According to the National Institute of Environmental Research (NIER), Ulsan and neighbouring Busan regions exhibit high concentrations of $PM_{2.5}$ and O_3 due to photochemical formation reactions of secondary organic aerosols (SOA) from volatile organic compounds (VOCs) under air stagnation conditions (NIER, 2018). Hence, it is important to determine the degree to which VOCs affect the air quality through photochemical reactions in the atmosphere in Ulsan in summer.

1.2. VOC Monitoring

The Korean government has monitored VOCs, environmentally important pollutants in terms of both their toxicity and photochemical reactivity creating ozone and SOA, through two types of monitoring stations. Toxic VOCs have been monitored along with other toxic chemicals like polycyclic aromatic hydrocarbons (PAHs) by hazardous air pollutants (HAPs) monitoring stations whereas the VOCs with high photochemical reactivity have been observed with other relevant compounds by photochemical assessment monitoring stations (PAMS). The two VOC monitoring systems have different target compounds and stations based on their objectives (Table 1). The 40 HAPs monitoring stations were established over the nation, three of which in Ulsan. But only 18 PAMS have been operated in Korea and there is no photochemical assessment monitoring station in Ulsan. They are differently distributed all over the country (Figure 3). Even though Ulsan has been suffering from the photochemical oxidation reactions of VOCs emitted from various industrial activities, only hazardous toxic VOCs have been monitored, not photochemical reactive VOCs. Therefore, PAMS VOCs should be monitored and studied to resolve the photochemical reaction issue in summer.

For the VOC monitoring studies, three kinds of sorbent-based air sampling methods are widely used over the world (Woolfenden, 2010). The first method is whole-air sampling into sorbent focusing traps of analytical instrument, which involves most of station monitoring systems mentioned above. It generally provides continuous and high-quality managed VOC compositional data at the fixed

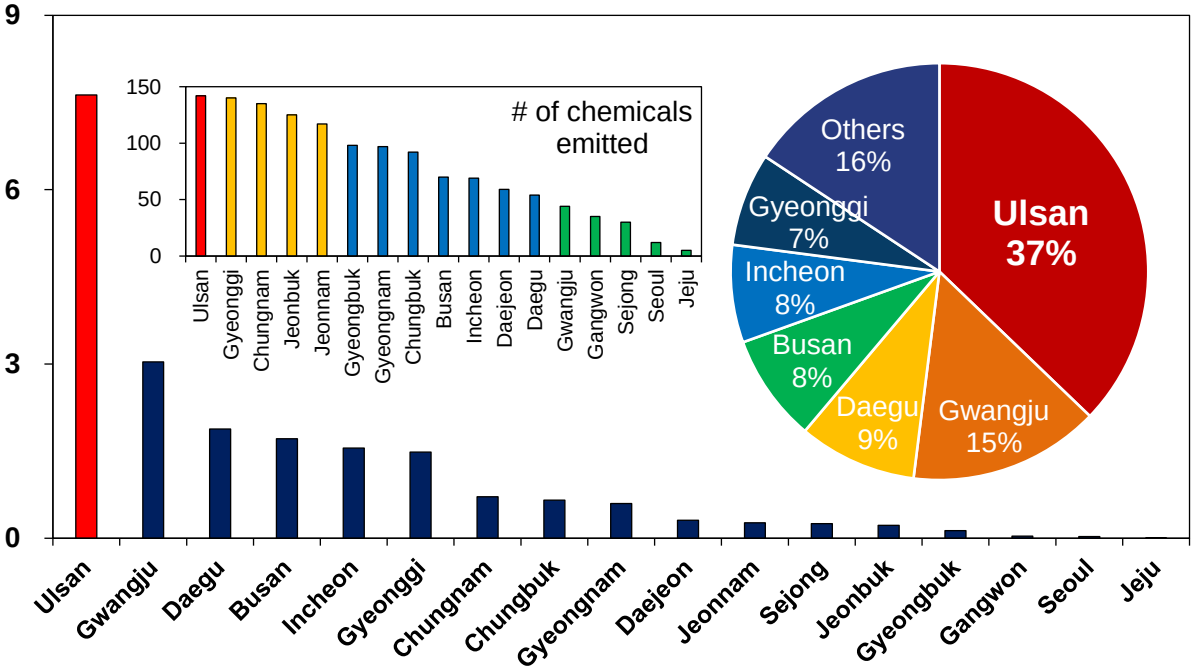

Figure 2. PRTR information in South Korea, 2018

stations. Because it carries considerable cost to operate the monitoring stations, it is difficult to get VOC distribution at high spatial-resolution with the whole-air sampling methods.

Table 1. General information of HAP monitoring stations and PAMS

Monitoring station	Target compounds	# of stations
HAP monitoring	HAP VOCs (16), PAHs (16)	40
PAMS	Precursor VOCs (56), NO_x, NO_y, PM_{10}, $PM_{2.5}$, O_3, CO, Carbonyls	18

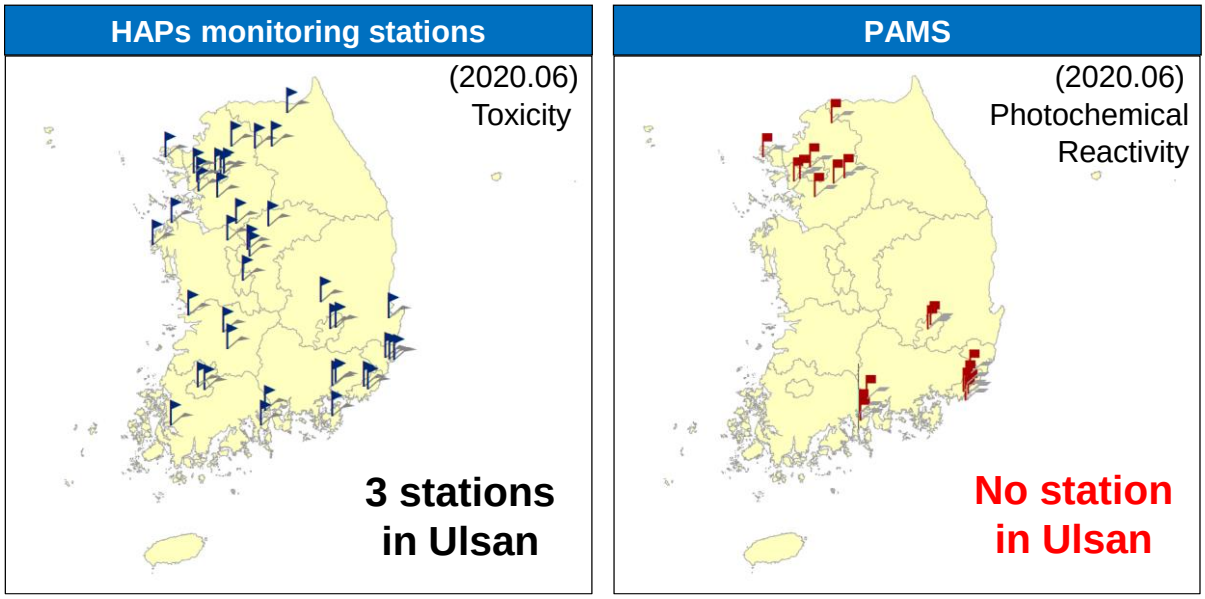

Figure 3. Governmental VOC monitoring systems in South Korea

To customize VOC sampling for the specific objectives of individual study, pumped active sampling and diffusive passive sampling are appropriate methods in terms of the cost of the monitoring. Pumped active sampling onto sorbent tubes can provide high quality of data in temporal resolution because it enables to collect sequential samples with specific time interval and sampling rate. Although the active sampling does not require the operation cost as much as monitoring stations does, it is limited to monitor a huge area with many active samplers since it is high-maintenance with a pump-coupled sampler and power supply for each site. Diffusive passive sampling onto sorbent cartridges could make up for the limitations of pumped active sampling. Diffusive passive samplers are reasonable price and low-maintenance, which allows the spatial resolution of the VOC monitoring to substantially increase. Nonetheless, the diffusive passive sampling has some limitations in time resolution of the monitoring and quantitative accuracy of target compounds. Because the advantages of the active and passive sampling methods are complementary to the disadvantages of each sampling method, the hybrid sampling, which is a combined method with both active and passive sampling, is able to highly improve the monitoring capacity with high temporal and spatial resolution of data.

1.3. Sources of VOCs

Large amount of VOCs is emitted into the atmosphere from both the anthropogenic and biogenic sources (Atkinson, 2000). The anthropogenic VOCs are originated from fugitive emission of gasoline, combustion including vehicle exhaust and fossil-fueled power plant emission, fuel storage and transport, solvent usage, and industrial operations. In addition, plants emit large amount of biogenic VOCs such as isoprene and terpenes for a crucial role in plants interaction with biotic and abiotic factors (Atkinson, 2000; Vivaldo et al., 2017).

Ulsan has anthropogenic and biogenic VOC sources because of huge multi-industrial (petrochemical, automobile, shipbuilding, and non-ferrous metal) areas and dense forest areas, as mentioned above. Particularly, petrochemical industry is well known as one of important VOC sources and the product painting processes with solvent-based paints in shipbuilding and automobile industry cause significant emissions of VOC to the atmosphere (Kim, 2011; Malherbe & Mandin, 2007). In addition, large quantity of petroleum including crude oil and petrochemical relevant products is loading and unloading at the Ulsan port. These operations are also emitting lots of VOCs around the port (USEPA, 1995). Biogenic emission rates are quite various depending on the vegetation species, but isoprene (C_5) and monoterpenes (C_{10}) are the prominent compounds (Kesselmeier & Staudt, 1999).

1.4. Previous studies on the VOCs in Korea

The Korea-US Air Quality Study (KORUS-AQ) is an intensive air quality monitoring campaign conducted in Korea in spring 2016 (Kim et al., 2018; Nault et al., 2018; NIER & NASA, 2017; Schroeder et al., 2020). Because one of main goals of KORUS-AQ was to invenstigate the ozone photochemistry and aerosol evolution, the KORUS-AQ provided meaningful background knowledge (Kim et al., 2018). Aromatic VOCs, particularly toluene, are key components dominantly contributing to SOA and tropospheric ozone formation in Korea (Kim et al., 2018; Nault et al., 2018; NIER & NASA, 2017; Schroeder et al., 2020). According to the HAPs monitoring system, the last 5-year average (from 2015 to 2019) concentration of toluene was second highest in Ulsan, 3.28 ppb (NIER, 2019).

In spite of the atmospheric environmental vulnerability from VOC emissions in Ulsan, a few studies investigated the atmospheric VOC composition in Ulsan. Kim et al. carried out an intensive field monitoring at two sites in Ulsan and analyzed health risk of them in June 1996 (Kim et al., 1998). This research provided a comprehensive concentration levels of hazardous air pollutants including VOCs. Na et al. sampled C_2-C_9 VOCs and analyzed the mean and daily concentration of the VOCs in an industrial site and a downtown site (Na et al., 2001). A high spatial distribution of 28 VOCs was seasonally studied in Ulsan by Kim et al. (Kim et al., 2019). In the study, the industrial emission effect on the VOC concentrations in Ulsan was investigated by diagnostic ratio and principal component analysis of VOCs. A comprehensive hazardous air pollutants (HAPs) monitoring and health risk assessment were conducted at 5 sites in Ulsan (Baek et al., 2020). They provided major cancer risk and non-cancer risk contributors from the result of risk analysis. There is one study concerning about photochemical oxidation SOA formation reactions of VOCs in Ulsan. Numerical sensitivity simulations of SOA formation from VOCs with VOC emission data were researched in the study (Yang et al., 2020). Whereas one study dealt with the photochemical oxidation reactions of VOCs, the others previous studies on the VOCs in Ulsan focused on their toxicity and health risk.

1.5. Formation of secondary organic aerosol and ozone from VOCs

Although understanding the toxicity of VOCs themselves in a city is a crucial issue to make a policy protecting people from exposure of the hazardous air pollutants, the research on the photochemical oxidation reactions forming SOA and ozone of VOCs are getting an important issue in Ulsan in summer as mentioned in section 1.1. The VOCs emitted from anthropogenic and biogenic sources could generate SOAs by reacting with the oxidants such as hydroxyl radical, ozone, nitrate radical and increase O_3 concentration level by changing the balance between NO and NO_2 with organic peroxy radicals (RO_2) in the atmosphere (Figure 4). RO_2 can replace the role of O_3 oxidizing NO to NO_2 and the loss of O_3 is hindered by the oxidizing capacity of RO_2. As a result, the level of O_3 concentrations in the atmosphere increases. These oxidization mechanisms of VOCs have broadly been investigated using laboratory flow reaction chamber experiments and chemical reaction modeling (NIER & NASA, 2017).

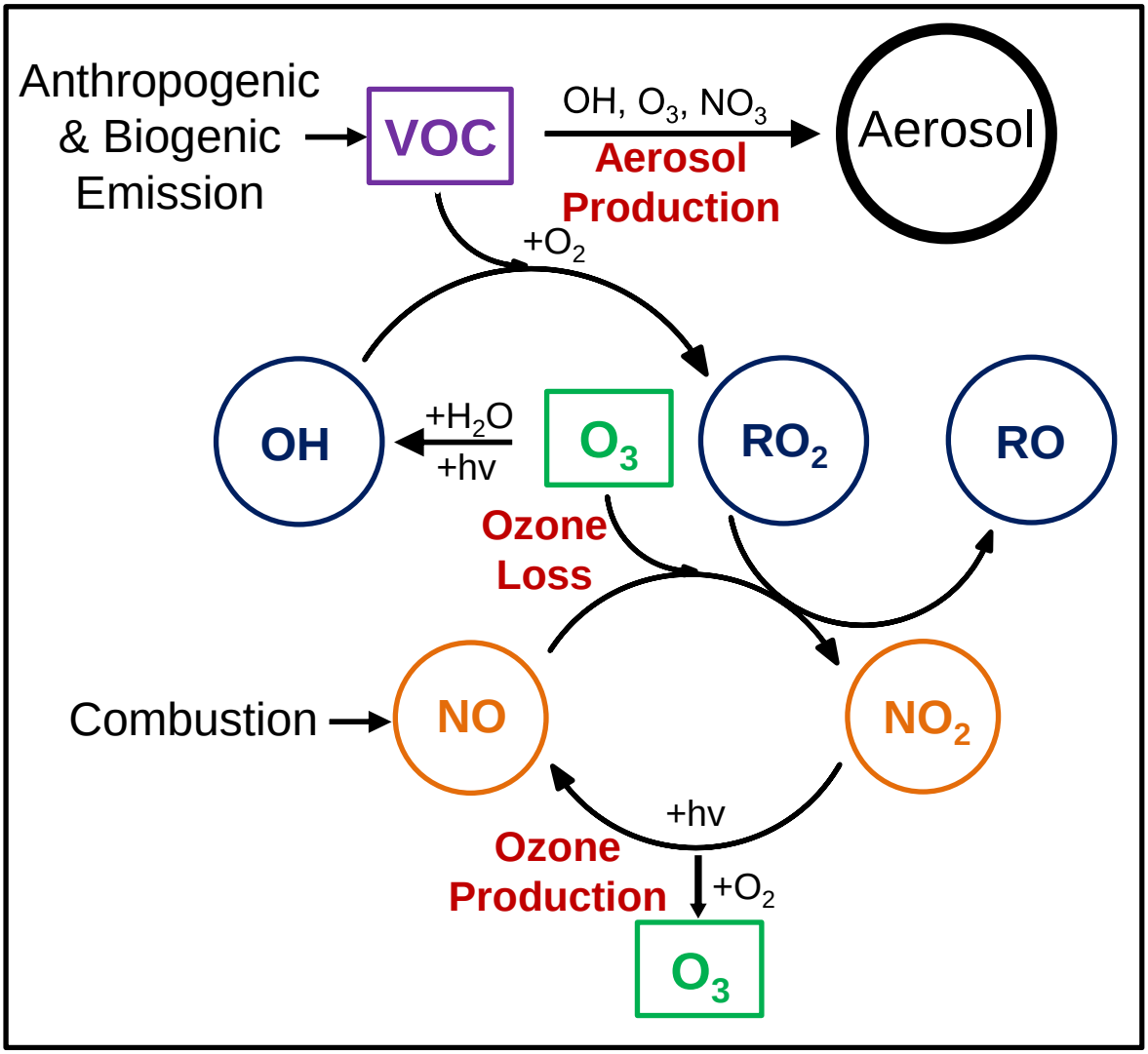

Figure 4. Schematic diagram of tropospheric ozone and SOA chemistry

There are three methods commonly used to evaluate ozone formation potential of speciated VOCs. Maximum incremental reactivity method indicates a maximum incremental reactivity under adjusted NO_X conditions through empirical kinetic modeling approach which is a single-cell box modeling to simulate how ozone is created in 1-day episodes (Carter, 1994; Farshad et al., 2013; Hoekman, 1992). This MIR value shows the maximum potential the VOC have in certain adjusted NO_X conditions. The second is the reactivity-based method, a propylene (C_3H_6)-equivalent concentration for each VOC species i (Propy-Equiv (i)) (Chameides et al., 1992).When a VOC species, i, produces ozone, the concentration C_i and reaction rate with OH radical (Lee et al., 2020) are the dominant factors. Therefore, the OH-reactivity rate normalized with propylene and concentration only are considered. The other is a photochemical ozone creating potential (POCP) developed by R. G. Derwent and M. E. Jenkin (1991). POCP was calculated by the Harwell Photochemical Trajectory Model (PTM) using a Lagrangian approach. POCP is a relative index of ozone creation with a VOC species to that with ethylene (C_2H_4) because it is an appropriate ozone precursor with medium reactivity to OH radical for the normalization (Derwent & Jenkin, 1991). These three methods for calculating ozone formation potential are slightly different but the values for VOC species from them highly positively correlated with one another (0.01 significant level, 2-tailed, Pearson correlation coefficient).

The three concepts for estimating SOA formation potential from VOCs are widely used in previous studies. One is a fractional aerosol coefficients (FAC) defined by D. Grosjean and J. H. Seinfeld (1989). It means the mass of SOA formation divided by the mass of VOC estimated by Teflon film chamber experiments. Another is a SOA yield method which is similar to FAC. SOA yield values are based on smog chamber experiments and estimates by Grosjean and Seinfeld using structure-reactivity relationship (Grosjean & Seinfeld, 1989; Pandis et al., 1992). The other is SOA potential (SOAP) developed by Derwent et al., which is a propensity of each VOC to form SOA on an equal mass emitted basis relative to toluene. Toluene is a convenient compound for normalization because it is well characterized in emission sources and widely regarded as an important man-made SOA precursor (Derwent et al., 2010). It was determined by the same PTM running method as POCP indexes were previously calculated. The three SOA potential estimation methods also showed the positive Pearson correlation coefficient with one another with 0.01 significant level.

1.6. Objectives of this study

Ulsan is one of the largest multi-industrial cities with the highest chemical emission rates in South Korea. In addition to anthropogenic emissions, large quantity of biogenic VOCs is emitted from huge mountainous areas. To make matters worse, the synoptic and diurnal meteorological conditions including the seasonal wind direction and land-sea breeze circulation in summer allow the VOCs emitted from biogenic and anthropogenic sources to move to central highly urbanized areas of Ulsan. The VOCs cause adverse effects with not only the toxicity of VOCs itself but also photochemical oxidation reactivity forming SOA and ozone. However, few studies on the photochemical reactions of VOCs in Ulsan were conducted and the mechanism of them remained unclear and poorly understood (Baek et al., 2020; Kim et al., 2019; Kim et al., 1998; Na et al., 2001; Yang et al., 2020). Therefore, this study scrutinized thoroughly the concentration of ozone precursor VOCs in industrial, rural, and urban sites, Ulsan with the hybrid (active/passive) sampling, estimated the formation potentials of ozone and SOA, and evaluated potential risks from the SOA and ozone formation in Ulsan in summer. The objectives of this study are to investigate the VOC concentration and ozone and SOA formation potential from VOCs in Ulsan in summer, to conduct a comprehensive analysis of O_3 and SOA formation with meteorological conditions, and to suggest how we control SOA and O_3 formation and a future research direction of follow-up studies to explain how VOCs reacts with oxidants and generates ozone and SOA in the atmosphere in Ulsan.

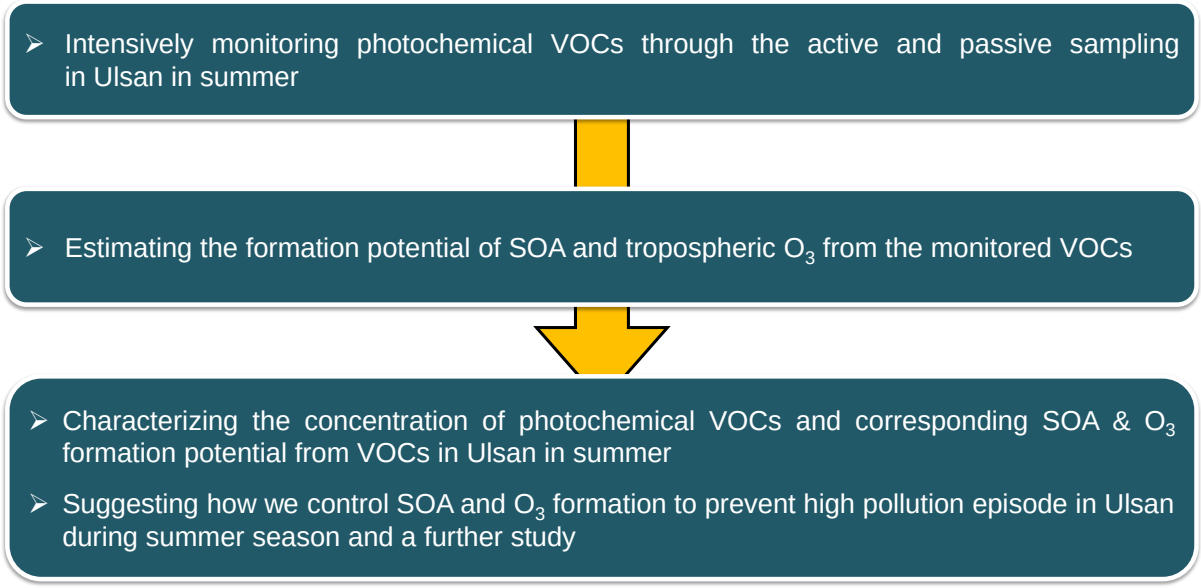

Figure 5. Objectives of this study

2. Materials and Methods

2.1. VOC sampling

2.1.1. Sampling sites

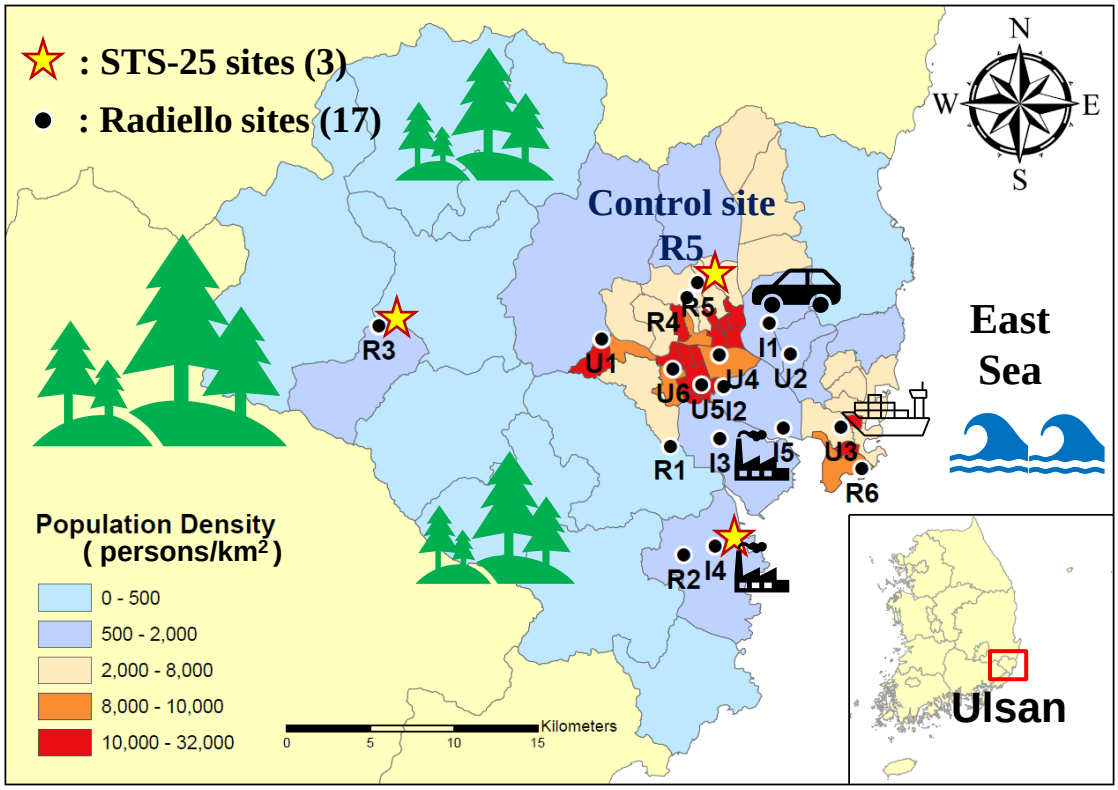

Figure 6. Sampling areas and sites

To monitor PAMS ozone precursor VOCs from both anthropogenic and biogenic emissions with the high spatial and temporal resolution, we have selected 17 sites as considering the monitoring sites from the government, previous studies in Ulsan, accessibility of sites, pollutant release and transfer register (PRTR), and demographics (Figure 6). We classified the 17 sampling sites as five industrial sites, six urban sites, and six rural sites according to the extent of development in the neighborhood. I1 is located in the automobile industrial complex and U2 is a residential area beside the automobile industrial complex. U3 and R6 could be affected by the shipbuilding industrial activities due to the short distance from the complex. R6 is a fishing village in the neighborhood of the shipbuilding complex. While I2, I3, and I5 are classified as industrial sites related to the petrochemical industrial complex, I3 is in the center of the petrochemical industrial area and I5 is the site affected by harbor loading and unloading activities. I4 exists in the non-ferrous metal industrial complex and it is quite close to the petrochemical industrial area. R1 and R2 are rural villages nearby huge industrial complexes but they are surrounded by forest areas. Although they are residential areas, R4 and R5

were classified as rural sites because there is no obvious local emission source except for the expected emission from small traffic volume, and most areas in the vicinity are restricted in urban development. U1, U4, U5, and U6 represent large residential and various commercial districts with high population density, more than 8,000 persons per km^2. U1 is approximately 1 km distant from the tollgate of Ulsan highway. R3 is at the agricultural village surrounded by forest. The Busan-Seoul Expressway, which is one of the heaviest traffic Expressway in Korea, passes through this village with about 1 km distance from the R3.

2.1.2. Active and passive air samplers

The active and passive hybrid VOC monitoring was conducted in Ulsan with the two different samplers. For the active sampling, we used the sequential tube sampler (STS-25, PerkinElmer, UK) coupled with the mini pump VOCs sampler (MP-Σ30KNII, SIBATA, Japan). APK multi-bed sorbent tubes (KT50603, KNR, South Korea), Carbotrap 300-equivalent or more, were used to collect the PAMS ozone precursor 53 VOCs. KT50603 is an adsorbent tube packed with Carbograph 1, Carbograph 2, and Carbosieve SIII. USEPA has evaluated a VOC sampling with the combination of STS-25 and 3-stage sorbent tubes as a very good precision for the collection of VOCs (Albert J. and Demtrios J., 1993). STS-25 enables a sequential tube sampling with a specific time interval and the flow rate is automatically corrected as standard conditions by the mini pump VOCs sampler.

Enhancing the cost-effectiveness of high spatial-resolution VOC monitoring in Ulsan, passive air samplers for VOCs, adsorbing cartridges for VOCs (RAD 145, Radiello, Italy), were used. The calculation of diffusive Radiello sampler's sampling rate is expressed as :

$$Q = \frac{m}{tC} = D\frac{S}{I} = D\frac{2\pi h}{\ln\frac{r_d}{r_a}}$$

Q [$l \cdot min^{-1}$]: the sampling rate

m [ug]: mass

C [$ug \cdot l^{-1}$]: the concentration at the diffusive surface

S [mm^2]: the diffusive surface

I [mm]: the path length between diffusive surface and adsorbing surface

S/I [mm]: the geometrical constant of the sampler

D [$cm^2 \cdot sec^{-1}$]: the diffusion coefficient

h [cm]: the height of the cylinder

$\mathbf{r_d}$ [mm]: radius of the diffusive cylindrical surface

$\mathbf{r_a}$ [mm]: radius of the adsorbing surface

* $\frac{2\pi h}{ln\frac{r_d}{r_a}}$: $geometric\ constant\ of\ radiello\ or\ diffusive\ path\ length$

Due to the loss of the diffusivity by the diffusive body in actual sampling conditions, the actual diffusive path length was estimated from the empirical experiments by the manufacturer, Instituti Clinici Scientifici Maugeri . The sampling rate for several VOCs such as benzene and toluene is provided in the user manual of Radiello (ICSM, 2019). The sampling rate for VOCs non-included in the manual was calculated by the above equation and diffusive coefficient in the air from the literature (Tang et al., 2015). The summary of sampling rates is shown at Table 2.

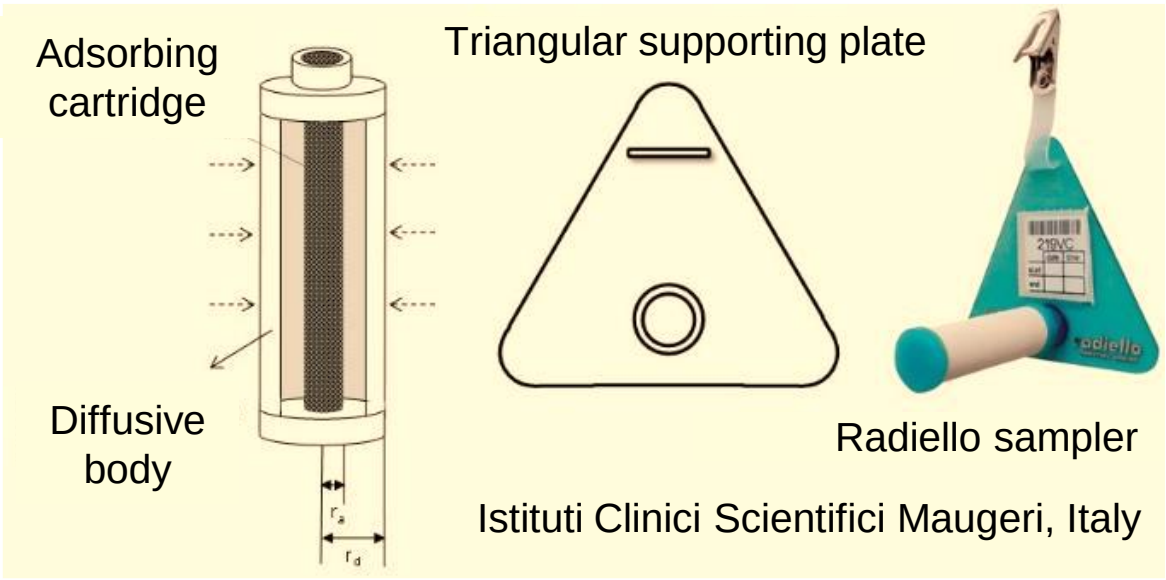

Figure 7. Schematic diagram of a Radiello sampler

STS-25, PerkinElmer, UK

MP-Σ30KNⅡ, SIBATA, Japan

KT50603, KNR, South Korea

Figure 8. Active sampling instruments and an active sampling picture

Table 2. Sampling rates of VOCs for Radiello

No.	Compound	Sampling Rate at 298K Q_{298K}, [ml min^{-1}]	No.	Compound	Sampling Rate at 298K Q_{298K}, [ml min^{-1}]
1	Isobutane	31.8[3)]	27	n-Heptane	25.3 [2)]
2	1-Butene	37.2[3)]	28	Methylcyclohexane	25.8 [3)]
3	n-Butane	33.6[3)]	29	2,3,4-Trimethylpentane[1)]	23.7 [3)]
4	trans-2-Butene	37.2[3)]	30	Toluene	30.0 [2)]
5	cis-2-Butene	37.2[3)]	31	2-Methylheptane	22.9 [3)]
6	iso-Pentane	31.8[3)]	32	3-Methylheptane[1)]	22.9 [3)]
7	1-Pentene	32.7[3)]	33	n-Octane	24.1 [2)]
8	n-Pentane	29.1[3)]	34	Ethylbenzene	25.7 [2)]
9	Isoprene	32.7[3)]	35	m,p-Xylenes	26.6 [2)]
10	trans-2-Pentene[1)]	32.7[3)]	36	Styrene	27.1 [2)]
11	cis-2-Pentene[1)]	32.7[3)]	37	o-Xylene	24.6 [2)]
12	2,2-Dimethylbutane[1)]	26.9[3)]	38	n-Nonane	21.0 [2)]
13	Cyclopentane	31.4[3)]	39	Isopropylbenzene	22.8 [3)]
14	2,3-Dimethylbutane	26.9 [3)]	40	n-Propylbenzene	22.8 [3)]
15	2-Methylpentane	31.8 [3)]	41	m-Ethyltoluene	23.4 [3)]
16	3-Methylpentane[1)]	31.8 [3)]	42	p-Ethyltoluene	23.4 [3)]
17	1-Hexene	32.7 [3)]	43	1,3,5-Trimethylbenzene	22.4 [3)]
18	n-Hexane	25.5 [2)]	44	o-Ethyltoluene	23.4 [3)]
19	Methylcyclopentane	27.8 [3)]	45	1,2,4-Trimethylbenzene	21.9 [2)]
20	2,4-Dimethylpentane	24.6 [3)]	46	n-Decane	22.3 [2)]
21	Benzene	26.8 [2)]	47	1,2,3-Trimethylbenzene[1)]	22.2 [3)]
22	Cyclohexane	27.6 [2)]	48	m-Diethylbenzene[1)]	21.9 [3)]
23	2-Methylhexane	24.6 [3)]	49	p-Diethylbenzene	21.9 [3)]
24	2,3-Dimethylpentane[1)]	24.6 [3)]	50	n-Undecane	12.0 [2)]
25	3-Methylhexane	24.6 [3)]	51	n-Dodecane	16.6 [3)]
26	2,2,4-Trimethylpentane	23.7 [3)]			

[1)] The estimated diffusion coefficient with isomer's diffusion coefficient

[2)] Radiello User Manual 2019

[3)] The estimated sampling rate with the average of geometrical constant

2.1.3. Sampling methods

In order to investigate the formation potential of SOA and ozone over the Ulsan, we have monitored PAMS ozone precursor 53 VOCs at 17 sites for passive sampling and three sites for active sampling in summer, 2020. The passive sampling periods can be summarized as follows: May (2020.05.22-29, 8 days), June (2020.06.19-26, 8 days), July (2020.07.21-28, 8 days), and August (2020.08.18-25, 8 days). The passive sampling was based on the duplicate sampling at 17 sites for better accuracy and representability of the sampling. Every starting and ending time of samplings was recorded and the sampling volume was calculated by multiplying the sampling rate with the sampling duration of each sample. The sampling rate was corrected along with the average temperature at the nearest meteorological observation station from each sampling site during the specific sampling periods. The list of meteorological observation stations used in the correction of the sampling rate was provided in Table 3.

The active VOC sampling was complementarily conducted with the sequential tube sampler coupled with a mini pump (STS-25/MP-∑30KNII) to enhance the temporal-resolution of VOC monitoring in Ulsan. All of the adsorbent tubes used in active sampling had been conditioned by the tube conditioner (APK1200, KNR) at 340℃ with the highly-purified N_2 (99.999 %, purity) 50 mL/min flow for 2 hrs, sealed in a glass vial with a screw cap, and stably stored in a desiccator since used. The VOCs had actively been collected during the following periods: May (2020.05.20-25, 6 days), June (2020.06.19-24, 6 days), July (2020.07.21-28, 8 days). The scheme of the active sequential VOC sampling was planned to intensively monitor diurnal characteristics of VOCs, especially the difference of day and night, while the 24 hrs of a day were split into four sampling sessions with the 6 hr-interval, that are the afternoon (A), evening (E), night (N), and morning (M). The diurnal cycle of the sampling time was set at local time as follows: A (14:00 ~ 20:00), E (20:00 ~ 02:00), N (02:00 ~ 08:00), and M (08:00 ~ 14:00) (Figure 9). To monitor any contaminations, each trip for both active and passive sampling included two field blank samples. The cartridges and adsorbent tubes had been carried to the laboratory in an insulated bag filled with sufficient ice packs after the sampling and been stored in a refrigerator under the 4 ℃ and -21 ℃ condition, respectively, until analyzed.

Table 3. Sampling site information

No.	Site ID	Coordinate		Description	Meteorological observation station
		UTM_X (Easting, m)	UTM_Y (Northing, m)		
1	I1	533661.26	3935153.15	streamside	PO 8184
2	I2	530937.00	3931355.00	rooftop	PO 8183
3	I3	530716.00	3928240.00	roadside	PO 8172
4	I4	530426.04	3921801.84	rooftop	PO 8170
5	I5	534512.90	3928842.84	seashore	AWS 898
6	R1	527755.01	3927782.29	rooftop	PO 8164
7	R2	528551.07	3921285.24	rooftop	PO 8161
8	R3	510319.50	3934973.46	rooftop	PO 8185
9	R4	528742.74	3936681.73	rooftop	ASOS 152
10	R5	529378.89	3937548.84	rooftop	ASOS 152
11	R6	539208.93	3926427.63	seashore	AWS 901
12	U1	523641.75	3934174.01	rooftop	PO 8177
13	U2	534934.00	3933277.32	rooftop	PO 8184
14	U3	537941.15	3928922.87	rooftop	PO 8178
15	U4	530686.60	3933233.43	rooftop	PO 8179
16	U5	529625.75	3931464.54	rooftop	PO 8173
17	U6	527900.08	3932390.53	rooftop	PO 8180

* Yellow rows indicate both active and passive sampling sites

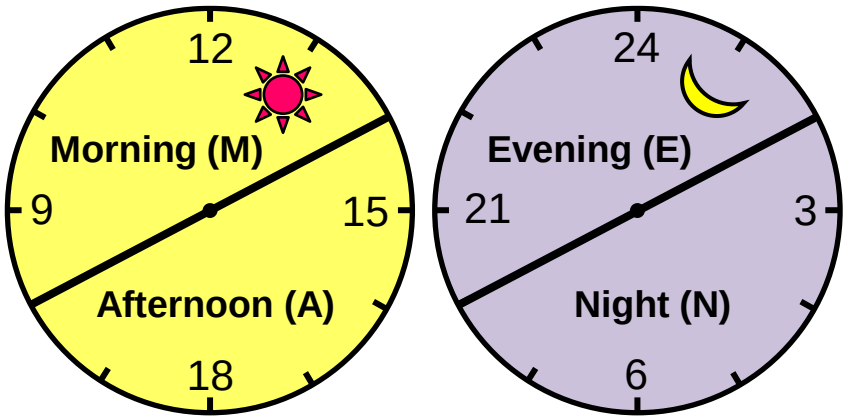

Figure 9. Temporal cycle of the active sequential VOC sampling

Figure 10. Pictures of active and passive VOC sampling

2.1.4. Meteorological and criteria air pollution monitoring stations

The data of meteorological conditions in Ulsan during the samplings were obtained from the observation stations of automated synoptic observing system (ASOS) and automatic weather system of Korea Meteorological Administration (KMA)(KMA, 2020b). The 13 observation stations of public office (PO) also were utilized to improve the spatial resolution of the meteorological data. These stations are under the normalized meteorological observation environments and quality management (KMA, 2020b). The list of observation stations used in this study was shown in Table 3 above. The 17 urban CAPs monitoring stations provided air quality data including PM_{10}, $PM_{2.5}$, O_3, and NO_2 over the Ulsan from May to August 2020 (MOE, 2020). Both meteorological and atmospheric compositional data were used in the integrated interpretations of the study on the formation potential of SOA and ozone.

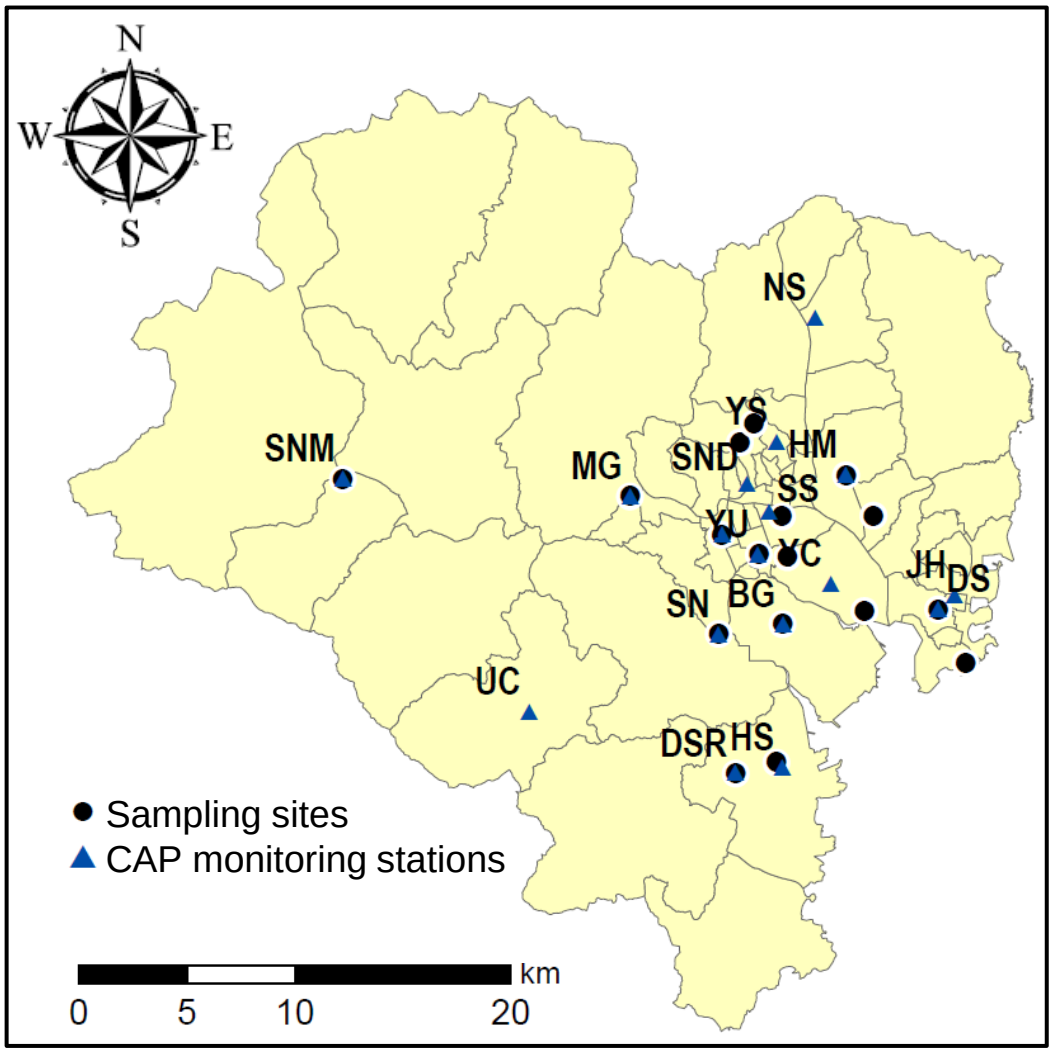

Figure 11. CAP monitoring stations and sampling sites

2.2. Analysis and Quality Assurance/Quality Control (QA/QC)

2.2.1. Target VOCs

The ozone precursor/PAMS Mix, 57 compounds, was used as a native standard in this study. However, the light VOCs with C_2 - C_3, and C_2 were not detected in passive and active air samples, respectively, because the RAD 145 cartridges and multi-bed sorbent tubes could not stably capture the VOCs in the conditions of this study. In addition, the n-hexane (C_6H_{14}) was not included in our target compounds due to the contamination from the prevalent use of the n-hexane solvent in our analytical laboratory. The total 53 VOCs analyzed in this study are 36 aliphatics (15 alkanes, 8 n-alkanes, 4 cycloalkanes, and 9 alkenes) and 17 aromatics as follows: propylene, propane, isobutene, 1-butene, n-butane, trans-2-butene, cis-2-butene, iso-pentane, 1-pantene, n-pentane, isoprene, trans-2-pentene, cis-2-pentene, 2,2-dimethylbutane, cyclopentane, 2,3-dimethylbutane, 2-methylpentane, 3-methylpentane, 1-hexene, methylcyclopentane, 2,4-dimethylpentane, benzene, cyclohexane, 2-methylhaxane, 2,3-dimethlypentane, 3-methylhexane, 2,2,4-trimethylpentane, n-heptane, methylcyclohexane, 2,3,4-trimethylpentane, toluene, 2-methylheptane, 3-methylheptane, n-octane, ethylbenzene, m-xylene, p-xylene, styrene, o-xylene, n-nonane, isopropylbenzene, n-propylbenzene, m-ethyltoluene, p-ethyltoluene, 1,3,5-trimethylbenzene, o-ethyltoluene, 1,2,4-trimethylbenzene, n-decane, 1,2,3-trimethylbenzene, m-diethylbenzene, p-diethylbenzene, n-undecane, and n-dodecane. The majority of them in ambient air are considered anthropogenic VOCs but isoprene (C_5H_8) is emitted in immense quantities from vegetation. The characteristics of anthropogenic and biogenic VOCs were investigated by 52 VOCs and isoprene, respectively, in this study.

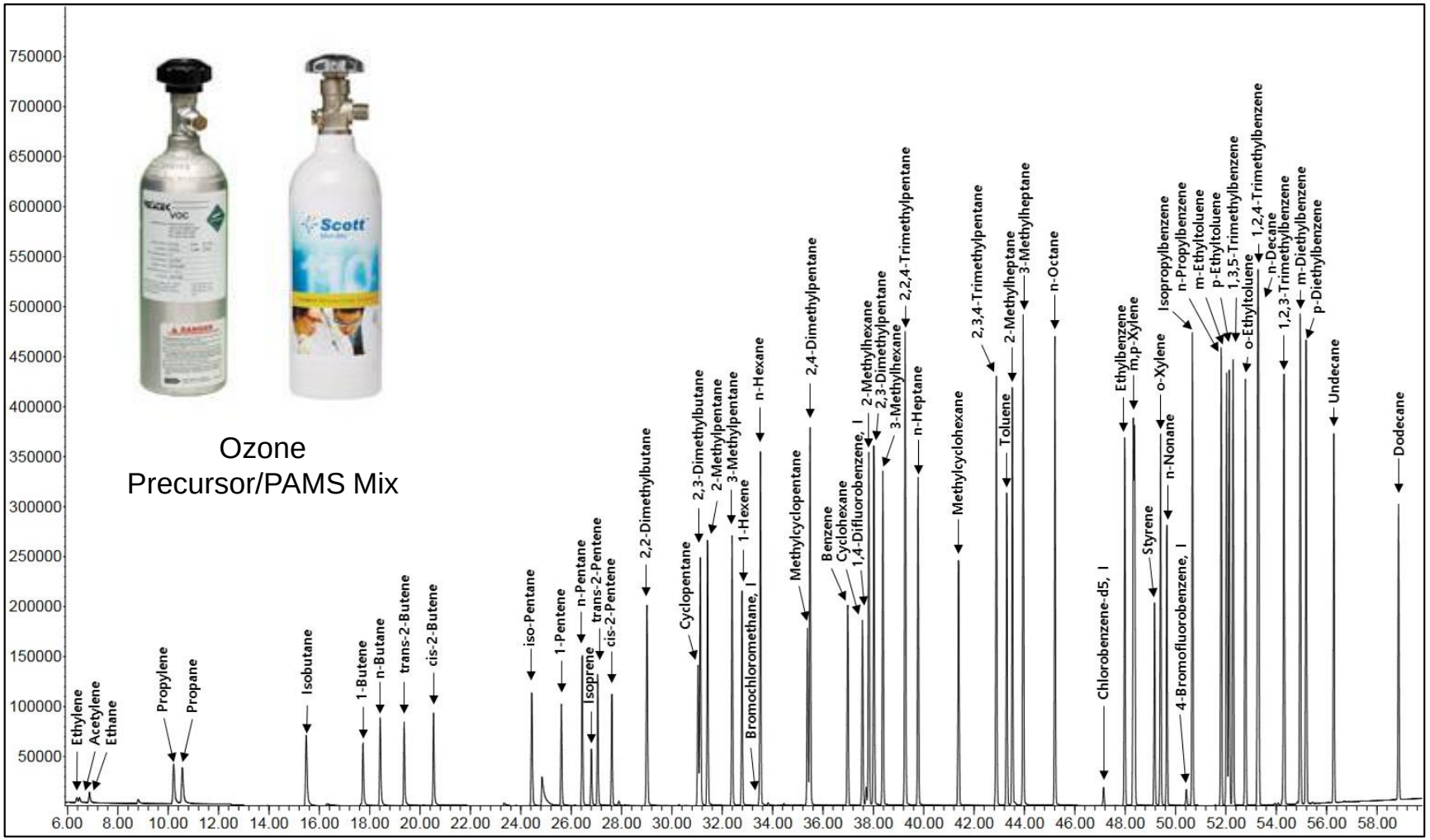

Figure 12. Chromatogram of a calibration standard sample

Table 4. Physical-chemical properties of target VOCs

No.	#C	Compound	Group	[1)] M.W.	M..P.	B.P.	F.R.	D.	Vapor pressure		Solubility			log K_{OW}	Henry's law constant	[1)] $k_{OH,298}$	[1)] Life time
									P^S	P_L	S	C^S	C_L				
1	3	Propylene	Alkene	42.1	-185.3	-47.7		0.514						1.8		26.3	2.1
2	3	Propane	Alkane	44.1	-187.6	-42.1										1.2	48.3
3	4	Isobutane	Alkane	58.1	-159.4	-11.7	1	0.557	357,000	357,000	49	0.84	0.84	2.8	120,435	2.3	23.7
4	4	1-Butene	Alkene	56.1	-185.3	-6.3	1	0.595	297,000	297,000	222	3.96	3.96		25,610	31.4	1.8
5	4	n-Butane	n-Alkane	58.1	-138.3	-0.5	1	0.579	243,000	243,000	61	1.06	1.06	2.9	95,915	2.5	21.9
6	4	trans-2-Butene	Alkene	56.1	-139.3	3.7										64.0	0.9
7	4	cis-2-Butene	Alkene	56.1	-138.9	3.7										56.4	1.0
8	5	iso-Pentane	Alkane	72.2	-159.8	27.9	1	0.619	91,640	91,640	48	0.66	0.66	2.3	138,320	3.9	14.3
9	5	1-Pentene	Alkene	70.1	-165.1	30.0	1	0.641	85,000	85,000	148	2.11	2.11	2.2	40,280	31.4	1.8
10	5	n-Pentane	n-Alkane	72.2	-129.7	36.1	1	0.626	68,400	68,400	39	0.53	0.53	3.5	128,180	3.9	14.1
11	5	Isoprene	Alkene	68.1	-145.9	34.0	1	0.681	73,300	73,300	642	9.42			7,780	101.0	0.6
12	5	trans-2-Pentene	Alkene	70.1	-140.2	36.3										67.0	0.8
13	5	cis-2-Pentene	Alkene	70.1	-151.4	36.9	1	0.656	66,000	66,000	2					65.0	0.9
14	6	2,2-Dimethylbutane	Alkane	86.2	-98.8	49.7	1	0.649	42,600	42,600	18	0.21	0.21	3.8	199,515	2.3	24.0
15	6	2,3-Dimethylbutane	Alkane	86.2	-128.1	57.9	1	0.662	32,010	32,010	19	0.22	0.22	3.9	144,422	6.2	9.0
16	5	Cyclopentane	Alkane	70.1	-93.4	49.3	1	0.745	42,400	42,400	166	2.37	2.37	3.0	17,915	5.2	10.8
17	6	2-Methylpentane	Alkane	86.2	-153.6	60.3	1	0.632	28,200	28,200	14	0.16	0.16	2.8	176,097	5.6	9.9
18	6	3-Methylpentane	Alkane	86.2	-162.9	63.3	1	0.664	25,300	25,300	13	0.15	0.15	3.6	170,330	5.7	9.8
19	6	1-Hexene	Alkene	84.2	-139.8	63.5	1	0.673	24,800	24,800	50	0.59	0.59	3.4	41,743		
20	6	Methylcyclopentane	Cycloalkane	84.2	-142.4	71.8	1	0.749	18,300	18,300	43	0.51	0.51	3.4	35,815	8.8	6.3
21	7	2,4-Dimethylpentane	Alkane	100.2	-119.5	80.5	1	0.673	13,100	13,100	4	0.04	0.04	3.1	323,312	5.1	10.9
22	6	Benzene	Aromatic	78.1	5.5	80.1	1	0.877	12,700	12,700	1780	22.79	22.79	2.1	557	1.2	45.2
23	6	Cyclohexane	Cycloalkane	84.2	6.6	80.7	1	0.779	13,014	13,014	58	0.69	0.69	3.4	18,885	7.5	7.4
24	7	2-Methylhexane	Alkane	100.2	-118.2	90.0	1	0.679	8,780	8,780	3	0.03	0.03		346,370	6.8	8.2
25	7	2,3-Dimethylpentane	Alkane	100.2												4.9	11.4
26	7	3-Methylhexane	Alkane	100.2	-119.4	92.0	1	0.687	8,210	8,210	3	0.03	0.03		249,290	7.2	7.8
27	8	2,2,4-Trimethylpentane	Alkane	114.2	-107.3	99.2	1	0.692	6,560	6,560	2	0.02	0.02		307,110	3.7	15.1
28	7	n-Heptane	n-Alkane	100.2	-90.6	98.4	1	0.684	6,110	6,110	3	0.03	0.03	5.0	208,955	7.2	7.8
29	7	Methylcyclohexane	Cycloalkane	98.2	-126.6	100.9	1	0.769	6,180	6,180	15	0.15	0.15	3.9	40,185	10.4	5.3

Continued. Table 4

No.	#C	Compound	Group	[1)] M.W.	M..P.	B.P.	F.R.	D.	Vapor pressure		Solubility			log K_{OW}	Henry's law constant	[1)] $k_{OH,\ 298}$	[1)] Life time
									P^S	P_L	S	C^S	C_L				
30	8	2,3,4-Trimethylpentane	Alkane	114.2	-109.2	113.5	1	0.719	3,600	3,600	2	0.01	0.01		205,614	7.0	7.9
31	7	Toluene	Aromatic	92.1	-95.0	110.6	1	0.867	3,800	3,800	515	5.59	5.59	2.7	680	6.0	9.3
32	8	2-Methylheptane	Alkane	114.2	-109.0	117.7	1	0.698	2,600	2,600	1	0.01	0.01		349,410	8.2	6.8
33	8	3-Methylheptane	Alkane	114.2	-120.5	118.9	1	0.708								8.6	6.5
34	8	n-Octane	n-Alkane	114.2	-56.8	125.7	1	0.703	1,800	1,800	1	0.01	0.01	5.2	311,536	8.7	6.4
35	8	Ethylbenzene	Aromatic	106.2	-95.0	136.2	1	0.867	1,270	1,270	152	1.43	1.43	3.1	887	7.1	7.8
36	8	m-Xylene	Aromatic	106.2	-47.8	139.1	1	0.884	1,100	1,100	160	1.51	1.51	3.2	730	19.0	4.7
37	8	p-Xylene	Aromatic	106.2	13.3	138.4	1	0.861	1,170	1,170	215	2.02	2.02	3.2	578	19.0	4.7
38	8	Styrene	Aromatic	104.1	-30.7	145.0	1	0.906	880	880	250	2.40	2.40	3.0		58.0	1.0
39	8	o-Xylene	Aromatic	106.2	-25.2	144.5	1	0.880	1,170	1,170	220	2.07	2.07	3.2	565	13.7	4.1
40	9	n-Nonane	n-Alkane	128.3	-53.5	150.8	1	0.718	571	571	0	0.00	0.00	5.7	332,880	10.2	5.5
41	9	Isopropylbenzene	Aromatic	120.2	-96.0	152.4	1	0.862	610	610	50	0.42	0.42	3.6	1,466	6.5	8.6
42	9	n-Propylbenzene	Aromatic	120.2	-99.6	159.2	1	0.862	450	450	52	0.43	0.43	3.7	1,040	6.0	9.3
43	9	m-Ethyltoluene	Aromatic	120.2	-95.6	161.3	1	0.865	391	391						19.2	2.9
44	9	p-Ethyltoluene	Aromatic	120.2	-62.4	162.0	1	0.861	395	395	95	0.79	0.79	3.6	500	12.1	4.6
45	9	1,3,5-Trimethylbenzene	Aromatic	120.2	-44.7	164.7	1	0.880	325	325	50	0.42	0.42	3.6	781	57.5	1.0
46	9	o-Ethyltoluene	Aromatic	120.2	-79.8	165.2	1	0.881	330	330	75	0.62	0.62	3.6	529	12.3	4.5
47	9	1,2,4-Trimethylbenzene	Aromatic	120.2	-43.8	169.4	1	0.876	270	270	57	0.47	0.47	3.6	569	32.5	1.7
48	10	n-Decane	n-Alkane	142.3	-29.6	174.2	1	0.730	175	175	0	0.00	0.00	6.3	478,840	11.6	4.8
49	9	1,2,3-Trimethylbenzene	Aromatic	120.2	-25.4	176.1	1	0.894	200	200	70	0.58	0.58	3.6	343	32.7	1.7
50	10	m-Diethylbenzene	Aromatic	134.2	-83.9	181.1		0.860								14.2	3.9
51	10	p-Diethylbenzene	Aromatic	134.2	-42.8	183.7		0.862								14.2	3.9
52	11	n-Undecane	n-Alkane	156.3	-25.5	195.9	1	0.740	52	52	0	0.00	0.00		2,039,835	13.2	4.2
53	12	n-Dodecane	n-Alkane	170.3	-9.6	216.3	1	0.749	18	18	0	0.00	0.00	6.8	829,570		

* abbreviation : #C (carbon number), M.P. (melting point), B.P. (boiling point), F.R. (fugacity ratio), D. (density)

** unit : M.W.[g mol^{-1}], M.P.,B.P.[°C], D.[g cm^{-3}], P^S,P_L[Pa], S[g m^{-3}], C^S,C_L[mol m^{-3}], Henry's law constant[Pa m^3 mol^{-1}], $k_{OH,\ 298K}$ [10^{12} cm^3 $moledule^{-1}$ s^{-1}], lifetime[h]

*** references : [1)]USEPA (2003), [the other parameters)]Mackay et al. (2006)

Table 5. Retention times and monitoring ions of target VOCs for GC/MS

No.	Group	Compound	Retention time (mins)	Target ion (m/z)	Qualifier ion (m/z)
1	Alkene	Propylene	10.027	41	39
2	Alkane	Propane	10.374	29	27
3	Alkane	Isobutane	15.245	43	41
4	Alkene	1-Butene	17.349	41	56
5	n-Alkane	n-Butane	18.121	43	41
6	Alkene	trans-2-Butene	19.048	41	56
7	Alkene	cis-2-Butene	20.197	41	56
8	Alkane	iso-Pentane	24.038	43	41
9	Alkene	1-Pentene	25.206	42	55
10	n-Alkane	n-Pentane	26.027	43	42
11	Alkene	Isoprene	26.393	67	68
12	Alkene	trans-2-Pentene	26.644	55	70
13	Alkene	cis-2-Pentene	27.204	55	70
14	Alkane	2,2-Dimethylbutane	28.584	43	57
15	Alkane	Cyclopentane	30.698	42	55
16	Cycloalkane	2,3-Dimethylbutane	30.708	43	42
17	Alkane	2-Methylpentane	30.978	43	42
18	Alkane	3-Methylpentane	31.953	57	56
19	Alkene	1-Hexene	32.339	41	56
20	Halogenated alkane	Bromochloromethane **(IS)**	33.005	83	85
21	Cycloalkane	Methylcyclopentane	34.919	56	41
22	Alkane	2,4-Dimethylpentane	35.035	43	57
23	Aromatic	Benzene	36.499	78	77
24	Cycloalkane	Cyclohexane	37.089	56	84
25	Halogenated aromatic	1,4-Difluorobenzene **(IS)**	37.237	114	63
26	Alkane	2-Methylhexane	37.374	43	85
27	Alkane	2,3-Dimethylpentane	37.553	56	43
28	Alkane	3-Methylhexane	37.911	43	71
29	Alkane	2,2,4-Trimethylpentane	38.785	57	56

Continued. Table 5

No.	Group	Compound	Retention time (mins)	Target ion (m/z)	Qualifier ion (m/z)
30	n-Alkane	n-Heptane	39.302	43	57
31	Cycloalkane	Methylcyclohexane	40.882	55	83
32	Alkane	2,3,4-Trimethylpentane	42.399	43	71
33	Aromatic	Toluene	42.799	91	92
34	Alkane	2-Methylheptane	43.052	43	57
35	Alkane	3-Methylheptane	43.473	43	57
36	n-Alkane	n-Octane	44.737	43	41
37	Halogenated aromatic	Chlorobenzene-d5 **(IS)**	46.645	117	82
38	Aromatic	Ethylbenzene	47.482	91	106
39	Aromatic	m-Xylene	47.82	91	106
40	Aromatic	p-Xylene	47.82	91	106
41	Aromatic	Styrene	48.657	104	103
42	Aromatic	o-Xylene	48.895	91	106
43	n-Alkane	n-Nonane	49.17	43	57
44	Halogenated aromatic	4-Bromofluorobenzene **(IS)**	49.92	174	95
45	Aromatic	Isopropylbenzene	50.158	105	120
46	Aromatic	n-Propylbenzene	51.302	91	120
47	Aromatic	m-Ethyltoluene	51.51	105	120
48	Aromatic	p-Ethyltoluene	51.619	105	120
49	Aromatic	1,3,5-Trimethylbenzene	51.772	105	120
50	Aromatic	o-Ethyltoluene	52.252	105	120
51	n-Alkane	n-Decane	52.798	43	57
52	Aromatic	1,2,4-Trimethylbenzene	52.743	105	120
53	Aromatic	1,2,3-Trimethylbenzene	53.78	105	120
54	Aromatic	m-Diethylbenzene	54.435	119	105
55	Aromatic	p-Diethylbenzene	54.653	119	105
56	n-Alkane	Undecane	55.766	57	43
57	n-Alkane	Dodecane	58.32	57	43

* Each color filter indicates a group for the same internal standard compound.

2.2.2. TD-GC/MS

For the instrumental analysis of the 53 target compounds, a thermal desorber-coupled gas chromatography/mass spectrometer (TD-GC/MS, UNITY series 2, Markes, UK–7890B/5977A, Agilent, USA) was used. Every VOC sample had been conditioned in a desiccator filled with the adequate amount of silica gel at laboratory room temperature, about 22 ℃, for more than 24 hrs, in order to dry any moisture which could be condensed at the surface of samples due to the difference of temperature between the room and the fridge.

TO-14A internal standard/tuning mix and Ozone Precursor Mix/PAMS from the Scott/Air Liquide gas, which includes four compounds (bromochloromethane, 1,4-diflourobenzene, Chlorobenzene, and 4-bromofluorobenzene), were used as internal standard (IS) and calibration standard (CS), respectively. The standard gases were injected into all of the samples and 7 calibration standard samples with a standard gas dilutor (APK 6100, KNR, South Korea). After the injection of internal standards, the samples were loaded in an automated thermal desorber. The primary thermal desorption (tube desorption) was conducted at 320 ℃ from a tube to a cold trap and the secondary thermal desorption of the cold trap transferred the final gas sample to GC/MS with a 3.5:1 split ratio at 300 ℃.

RTX-1 (105 m length x 0.25 mm (id), 1 μm thickness) was selected for the gas chromatography of the target compounds. The GC oven temperature program proceeded from -45 ℃ with a cryogenic liquefied nitrogen system to 250 ℃. The ionization and acquisition mode of the mass spectrometer detector was the electron ionization (EI) and selected ion monitoring mode, respectively. The target ions are classified into five SIM groups and the total run time was 59.17 min for the GC/MS analysis. The detailed conditions of TD-GC/MS instrumental analysis were provided in Table 6 below.

APK1200, KNR, South Korea

APK6100, KNR, South Korea

UNITY series 2, Markes, UK - 7890B/5977A, Agilent, USA

Figure 13. TD-GC/MS and instruments for the pretreatment

Table 6. TD-GC/MS analytical conditions

Parameter		Condition		
Gas	Carrier gas	Helium (99.999 %, purity), 2 ml/min		
	Purge gas	Nitrogen (99.999%, purity)		
	Cryogenic gas	Liquefied nitrogen		
TD	Purge flow rate	50 ml/min		
	Purge time	1 min		
	Flow path temperature	170 ℃		
	Tube desorption	320 ℃		
	Tube desorption flow rate	50 ml/min		
	Tube desorption time	10 min		
	Cryogenic trap temperature	-30 ℃		
	Cryogenic trap hold	5 min		
	Trap high	300 ℃		
	Heating rate	Max		
	Trap flow	50 ml/min		
	Trap split flow	5 ml/min		
	Trap split ratio	3.5 : 1		
GC	Column	RTX-1, 100% dimethyl polysiloxane, 105 m x 0.25 mm (id), 1 μm thickness		
	Oven temperature program	-45 ℃ hold for 4 min		
		4.5 ℃/min to 125 ℃		
		9 ℃/min to 250 ℃, hold for 3.5 min		
	Total run time	59.17 min		
MS	Mass mode	Ionization EI mode at 70 eV, acquisition SIM mode, solvent delay 3.00 min		
	Selected ion monitoring	Group	Time (min)	Selected ions (m/z)
		Group 1	03.00-13.00	25, 26, 27, 29, 39, 41
		Group 2	13.00-34.30	41, 42, 43, 49, 55, 56, 57, 67, 68, 70, 130
		Group 3	34.30-46.10	41, 43, 55, 56, 57, 63, 71, 77, 78, 83, 84, 85, 91, 82, 114
		Group 4	46.10-50.90	43, 57, 82, 91, 95, 103, 104, 105, 106, 117, 120, 174
		Group 5	50.90-59.17	43, 57, 91, 105, 117, 120
	MS quad temperature	150 ℃		
	MS source temperature	230 ℃		

2.2.3. QA/QC

Quality assurance and quality control (QA/QC) were carried out with field blank and duplicate sampling, internal standard method, and method detection limit (MDL). All of the VOC samples we collected in Ulsan included field blank samples to track any contamination during the whole process of research activities including the sampling preparation, sampling trip, storage, and analytical experiment in the lab. The MDL was applied to the calculation of VOC concentrations by the signal to noise ratio of 3 to 1 in the chromatograph. In order to improve the stability of instrumental analysis, the internal standard method was used to quantify the VOC concentrations of samples. The duplicate air sampling at each site was applied to the passive diffusive cartridge sampling for accurate sampling because the passive air sampling is less accurate than the active air sampling.

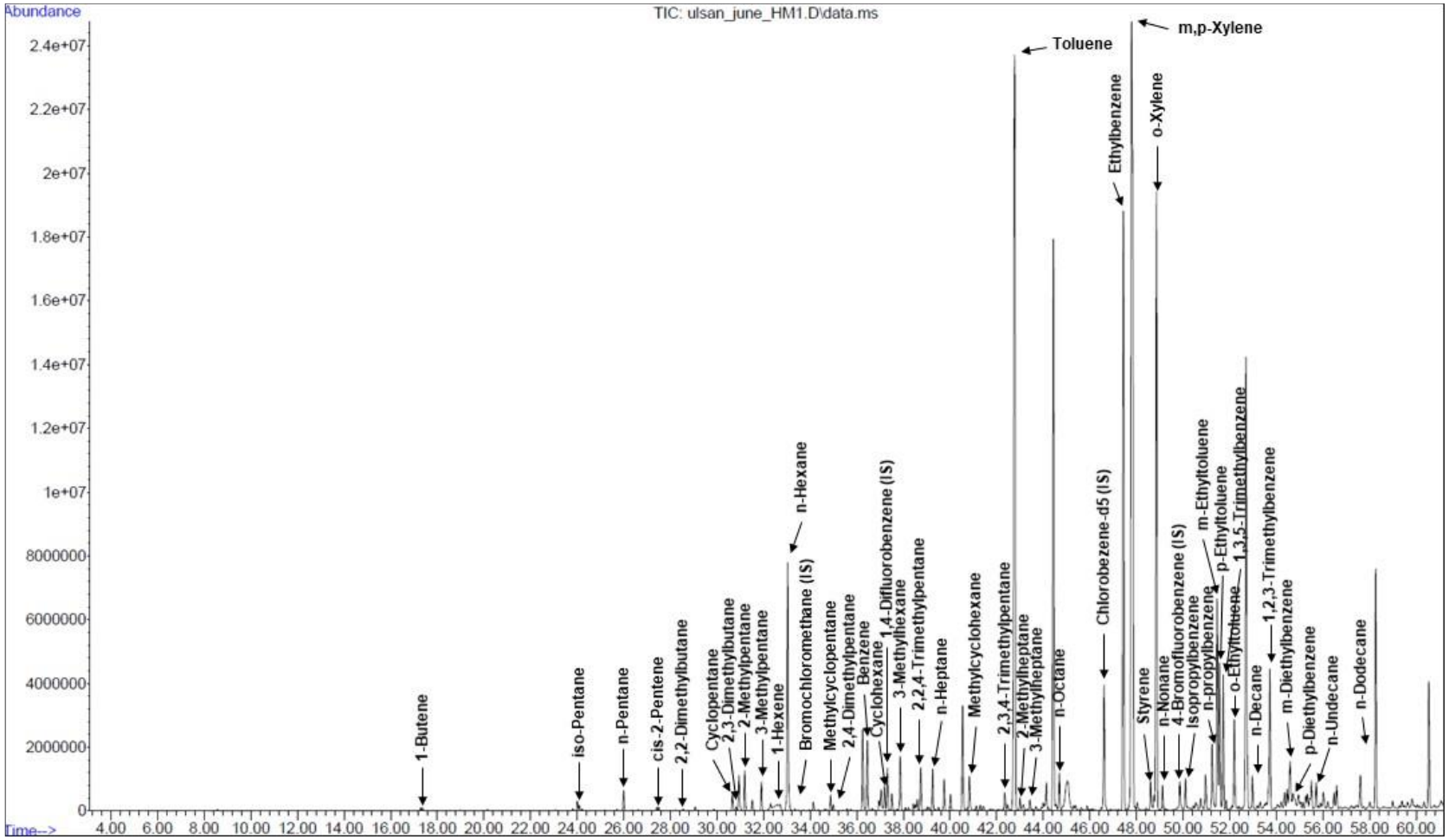

Figure 14. Chromatogram of a Radiello sample

2.3. Estimation of SOA and ozone formation

2.3.1. Ozone formation potential (OFP)

The concept of photochemical ozone creation potential introduced by R.G. Derwent in 1991 was used to calculate ozone formation potential based on the concentration of VOCs in Ulsan (Derwent & Jenkin, 1991). Even though there are other frequently used methods such as MIR or Prop-Equiv, POCP is the most appropriate method for characterizing the relative ozone potentials among them. The OFP was calculated as follows:

$$\mathrm{OFP} = \sum(\mathrm{concentration}_i \times \mathrm{POCP}_i)$$

The compilation of the last updated POCP was provided by R.G. Derwent et al. in 2007 (Derwent et al., 2007). The R.G. Derwent et al. calculated POCP index, using the formula:

$$\mathrm{POCP}_i = \frac{Mean\ O_{3i} - Mean\ O_{3base\ case}}{Mean\ O_{3ethylene} - Mean\ O_{3base\ case}} \times 100$$

POCP refers to the relative additional creation of ozone from a VOC, i, to the creation of ethylene (C_2H_4) compared to the ozone creation under the base case. The list of POCP index used in this study was provided in Table 7. The alkenes with < C_7, aromatics with > C_7 have high POCP (over their average 56.9), in general.

2.3.2. SOA formation potential (SOAFP)

Among three methods widely used of estimating SOA formation potentials, SOA yield, FAC, and SOAP, the SOAP index was utilized to estimate SOAFP in Ulsan for this study. Similarly to POCP index, the SOAP expresses the relative increment in SOA concentration with a VOC to that with toluene (Derwent et al., 2010). According to the previous study, the SOAPs were estimated using the equation:

$$\mathrm{SOAP}_i = \frac{Increment\ in\ SOA\ mass\ concentration\ with\ species, i}{Increment\ in\ SOA\ with\ toluene} \times 100$$

The SOAFP used in this study was calculated using the equation as follows:

$$\mathrm{SOAFP} = \sum(Concentration_i \times SOAP_i)$$

SOAFP enabled us to analyze the spatial and temporal characterization of SOA formation in Ulsan based on the VOC concentrations.

Table 7. Compilation of the SOAPs, FACs, SOA Yields, POCPs, Propy-Equivs, and MIRs for 56 VOCs

			Reference	Derwent, 2010	Grosjean, 1989	Pandis, 1992	Derwent, 2007	Chameides, 1992	Carter, 1994
No.	# of Carbons	Compound	Group	SOAP	FAC_NO_X (%)	SOA Yield ($\mu g\ m^{-3}\ ppm^{-1}$)	POCP	Propy -Equiv	MIR
1	2	Ethylene	Alkene	1.3	0	0	100	0.32	7.40
2	2	Acetylene	Alkyne	0.1	0		7	0.03	0.50
3	2	Ethane	Alkane	0.1	0		8	0.01	0.25
4	3	Propylene	Alkene	1.6	0	0	117	1.00	9.40
5	3	Propane	Alkane	0	0	0	14	0.04	0.48
6	4	Isobutane	Alkane	0	0	0	28	0.08	1.21
7	4	1-Butene	Alkene	1.2	0	0	104	1.19	8.90
8	4	n-Butane	n-Alkane	0.3	0	0	31	0.09	1.02
9	4	trans-2-Butene	Alkene	4	0	0	116	2.43	10.00
10	4	cis-2-Butene	Alkene	3.6	0	0	113	2.14	10.00
11	5	iso-Pentane	Alkane	0.2	0	0	34	0.14	1.38
12	5	1-Pentene	Alkene	0	0	0	95	1.19	6.20
13	5	n-Pentane	n-Alkane	0.3	0	0	40	0.14	1.04
14	5	Isoprene	Alkene	1.9	0	0	114	3.80	9.10
15	5	trans-2-Pentene	Alkene	3.1	0	0	111	2.55	8.80
16	5	cis-2-Pentene	Alkene	3.1	0	0	109	2.47	8.80
17	6	2,2-Dimethylbutane	Alkane		0	0	22	0.08	6.40
18	6	2,3-Dimethylbutane	Alkane		0	0		0.19	2.40
19	5	Cyclopentane	Alkane		0	0	50	0.22	1.07
20	6	2-Methylpentane	Alkane	0	0	0	41	0.20	1.50
21	6	3-Methylpentane	Alkane	0.2	0	0	43	0.20	1.50
22	6	1-Hexene	Alkene	0	0.34	0	88	1.41	4.40
23	6	n-Hexane	n-Alkane	0.1	0	0	40	0.20	0.98
24	6	Methylcyclopentane	Cycloalkane		<0.17	17	49	0.29	2.80
25	7	2,4-Dimethylpentane	Alkane		0	0		0.18	1.50
26	6	Benzene	Aromatic	92.9	<=1	0	10	0.05	0.42
27	6	Cyclohexane	Cycloalkane	0	0.17	17	28	0.27	1.28
28	7	2-Methylhexane	Alkane	0	0	0	32	0.26	1.08

Continued. Table 7

No.	# of Carbons	Compound	Group	SOAP	FAC_NO_X (%)	SOA Yield ($\mu g\ m^{-3}\ ppm^{-1}$)	POCP	Propy -Equiv	MIR
29	7	2,3-Dimethylpentane	Alkane	0.4	0	0		0.25	1.31
30	7	3-Methylhexane	Alkane	0	0	0	42	0.25	1.40
31	8	2,2,4-Trimethylpentane	Alkane		0.73	98		0.13	0.93
32	7	n-Heptane	n-Alkane	0.1	0.06	7	35	0.26	0.81
33	7	Methylcyclohexane	Cycloalkane		1	120	65	0.37	1.80
34	8	2,3,4-Trimethylpentane	Alkane		0	98		0.25	1.60
35	7	Toluene	Aromatic	100	5.4	424	44	0.21	2.70
36	8	2-Methylheptane	Alkane		0.5	98	34	0.35	0.96
37	8	3-Methylheptane	Alkane		0.5	98	37	0.53	0.99
38	8	n-Octane	n-Alkane	0.8	0.06	98	34	0.31	0.60
39	8	Ethylbenzene	Aromatic	111.6	5.4	440	46	0.27	2.70
40	8	m,p-Xylene	Aromatic	75.8	3.15	299.5	79	0.71	7.40
41	8	Styrene	Aromatic	212.3	0		5	2.21	2.20
42	8	o-Xylene	Aromatic	95.5	5	428	78	0.52	6.50
43	9	n-Nonane	n-Alkane	1.9	1.5	236	34	0.37	0.54
44	9	Isopropylbenzene	Aromatic	95.5	0.4	334	32	0.24	2.20
45	9	n-Propylbenzene	Aromatic	109.7	1.6	138	38	0.22	2.10
46	9	m-Ethyltoluene	Aromatic	100.6	2.6		78	0.71	
47	9	p-Ethyltoluene	Aromatic	69.7	2.5		63	0.45	
48	9	1,3,5-Trimethylbenzene	Aromatic	13.5	2.9	577	107	2.16	10.10
49	9	o-Ethyltoluene	Aromatic	94.8	5.6		73	0.45	
50	9	1,2,4-Trimethylbenzene	Aromatic	20.6	2	251	110	1.24	8.80
51	10	n-Decane	n-Alkane	7	2	348	36	0.42	0.46
52	9	1,2,3-Trimethylbenzene	Aromatic	43.9	3.6	496	105	1.24	8.90
53	10	m-Diethylbenzene	Aromatic		6.3			0.84	
54	10	p-Diethylbenzene	Aromatic		6.3			0.61	
55	11	n-Undecane	n-Alkane	16.2	2.5	479	36	0.47	0.42
56	12	n-Dodecane	n-Alkane	34.5	3	626	33	0.50	0.38

2.4. Approaches to data analysis

2.4.1. Comparison of the data distributions

Comparing two groups, when the data shows a distribution, the Wilcoxon rank-sum test, also known as Mann-Whitney U test, was used in this study. Because such a group shown in the results of this study does not follow the normal distribution, the median of each group was compared. Each result of comparisons was provided with its significant level according to the p-value.

2.4.2. Source and aging identification

Diagnostic ratio of BTEX enables to identify which source is dominant from traffic and non-traffic pollution and exhibit relative aging extent of the pollution. To determine traffic or non-traffic source, toluene to benzene (T/B) ratio is commonly used because benzene is well known as a traffic source and toluene is mostly used in non-traffic activities such as painting (Kim et al., 2019; Liu et al., 2008; Miller et al., 2012). Even though many studies suggested their own criteria from 1 to 4.3, the criteria could be different depending on the combination of local emission sources (Jaars et al., 2014; Miller et al., 2012; Miller et al., 2011; Tiwari et al., 2010; Yurdakul et al., 2013). It allows the sources to be tracked to confirm which is more dominantly contributed between traffic and nontraffic sources. The m,p-xylene to ethylbenzene (X/E) ratio could indicate how aged the VOC sources are. This is because the atmospheric stability of m,p-xylene and ethylbenzene are different enough to exhibit the elapsed time of the VOC emission from each other (Kim et al., 2019; Nelson & Quigley, 1983). Therefore, monthly diagnostic ratio analysis for each site was carried out to identify VOC source characteristics at industrial, urban, and rural site.

3. Results and Discussions

3.1. Criteria air pollutants (CAPs) with meteorological data

3.1.1. Meteorological conditions

As time goes from May to August 2020, the average temperature has continuously increased, except for July because of a rainy period, also known as ‘Changma’ in Korean, which included the July sampling time. The heavy precipitation was recorded in July 2020, accompanying the high relative humidity, large cloud cover, and weak solar radiation, which are unfavorable conditions for the photochemical formation reactions of SOA and ozone. Ambient air temperature, relative humidity, and solar radiation had strong diurnal cycles, which is that the temperature and radiation are high in the daytime and low in the nighttime, but humidity is low in daytime and high in the nighttime. Considering the effect of land-sea breeze transferring the high concentrations of VOCs emitted from the industrial complex in Ulsan, the most favorable conditions for the formation of SOA and ozone are expected to be made during the daytime. As Figure 15, the gentle northwestern wind, less than 3 m/s, was dominant at nighttime. When the Sun heated land, the wind from the eastern coastal area with more than 3 m/s was developed. Therefore, it would be critical that the characteristics of the diurnal and nocturnal transportation of VOCs emitted and the heavy rainfall in the rainy period affect the photochemical SOA and ozone formation reactions in Ulsan during summertime.

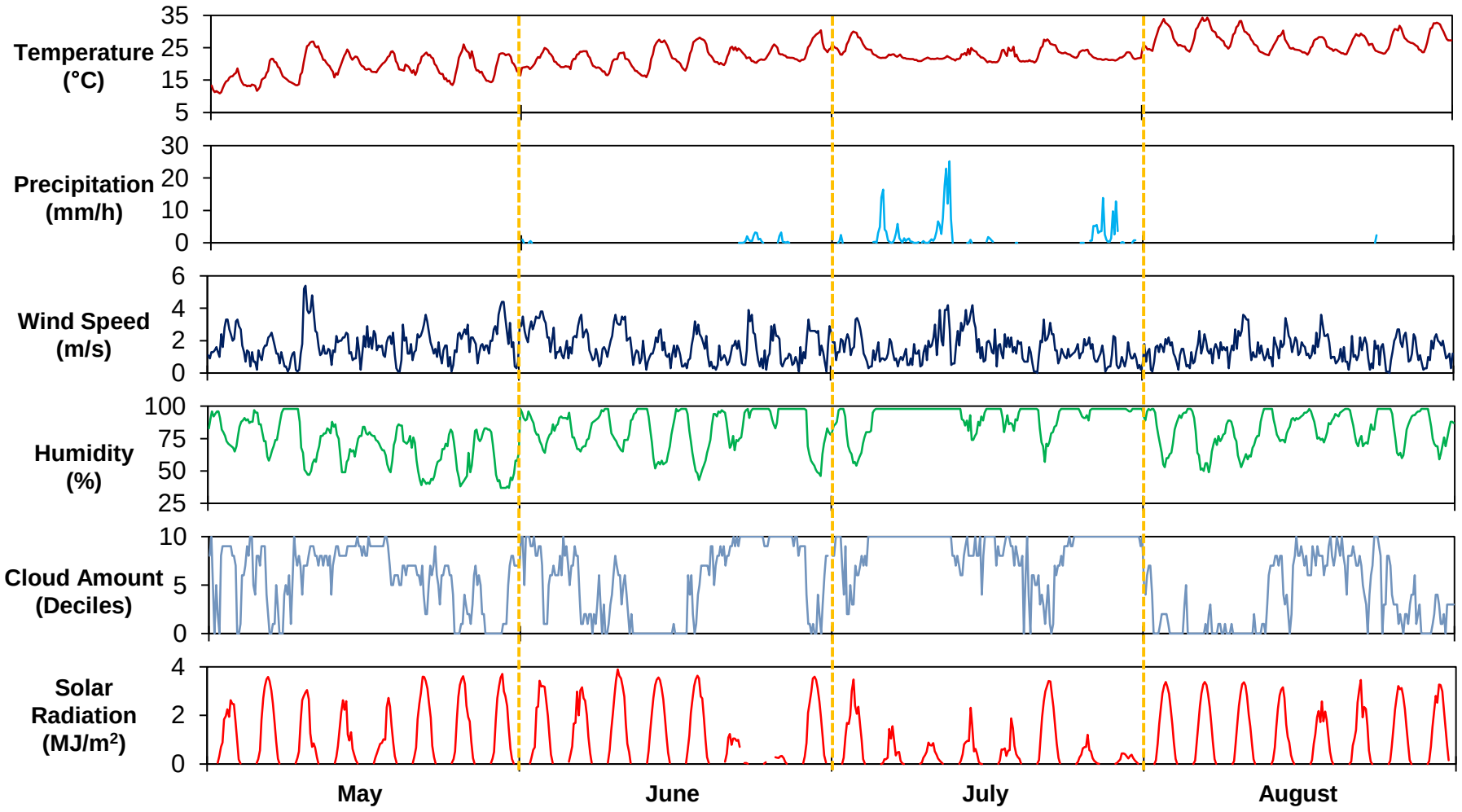

Figure 15. Summary of meteorological conditions

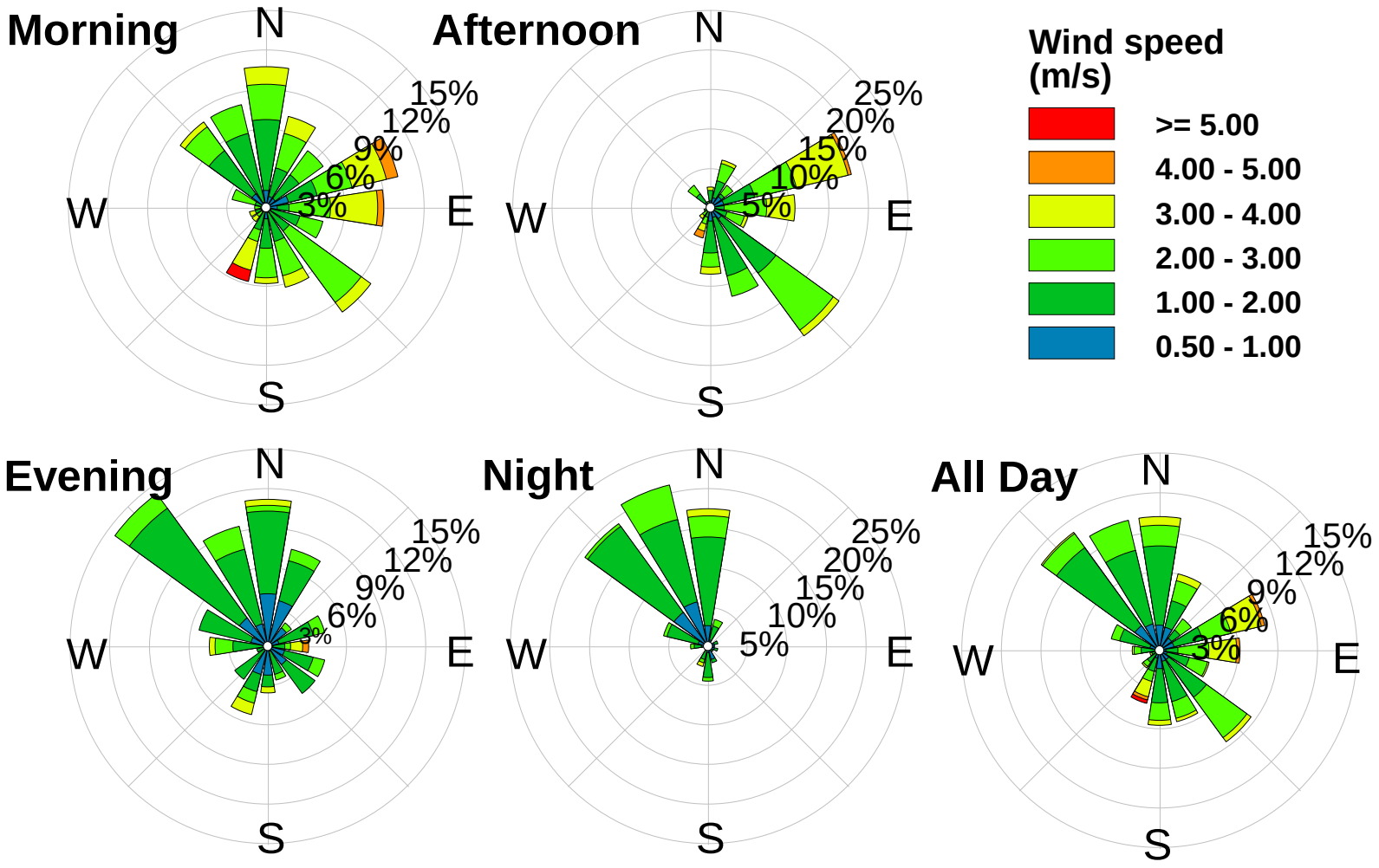

Figure 16. Diurnal wind cycle in Ulsan

3.1.2. Spatial distribution of CAP concentrations

The concentrations of both coarse (< 10 μm diameter, PM_{10}) and fine (< 2.5 μm diameter, $PM_{2.5}$) particulate matter and SO_2 were high in the non-ferrous metal and petrochemical industrial complexes. According to the Clean air policy support system (CAPSS), most emissions of particulate matter and SO_2 are concentrated in the areas because those industrial processes require high heat sources from the coal combustion (NCFDI, 2017). The carbon monoxide showed high concentrations in the vicinity of main roads connected to industrial areas, which has a large traffic volume of heavy vehicles. The spatial distribution of O_3 and NO_2 was inversely proportional to each other. These two pollutants are highly affected by complex photochemical oxidation reactions and O_3 is known as an oxidant oxidizing NO to NO_2 in the atmosphere (Figure 4). So, we could not directly infer the reasons why they exhibit a high concentration in a specific area but the NO_2 is considered traffic-related pollutants involved in vehicle exhaust as a form of NO_x since urban and industrial areas exhibited higher NO_2 concentration than rural areas.

Korean criteria for the CAPs, which have been controlled with annual standard, were applied to the monthly CAPs concentrations conservatively. PM_{10}, NO_2, and SO_2 did not exceed their annual criteria, 50 μg/m^3, 30 ppb, and 20 ppb, respectively. However, $PM_{2.5}$ was the only CAP that exceeded its annual criteria, 15 μg/m^3, in most areas. Although it is possible to satisfy the annual concentration criteria when the annual average concentration data is evaluated rather than monthly average concentration, it is obvious that there is the largest risk in $PM_{2.5}$ among CAPs in Ulsan in Summer. Assuming that the loss rate such as depositions of PM_{10} and $PM_{2.5}$ is the same to each other, the change of $PM_{2.5}/PM_{10}$ ratio means an additional increment of $PM_{2.5}$ in the atmosphere, which is highly related to the secondary organic aerosol formation. Regarding the ratio in July with heavy rain as the ratio of local primary emission sources, the most SOA formations occurred in August, under the strongest solar radiation and highest temperature condition among the sampling periods and the $PM_{2.5}/PM_{10}$ ratio is more than 0.8 in rural areas. This indicates the SOA formation might mainly contribute to the $PM_{2.5}$ concentration level in rural sites in August.

The spatial differences of $PM_{2.5}$, O_3, and NO_2 concentration at three sites, R3, R5, and I4, were intensively compared to characterize the variation of them. R5 is a control site without an obvious local pollution source, R3 is a rural site including the Seoul-Busan expressway, and I4 is in the non-ferrous metal industrial complex emitting a lot of anthropogenic pollutants to the atmosphere. However, in Figure 18, there is no significant difference in the $PM_{2.5}$ concentration among the three sites but there are statistically significant differences in NO_2 and O_3 concentration between the industrial site (I4) and two rural sites (R3 and R5) in the result of Wilcoxon rank-sum tests. This indicates that the oxidation reactions are different depending on the site use because of the various

site-specific atmospheric composition of NO_x, oxidants, VOCs, and others.

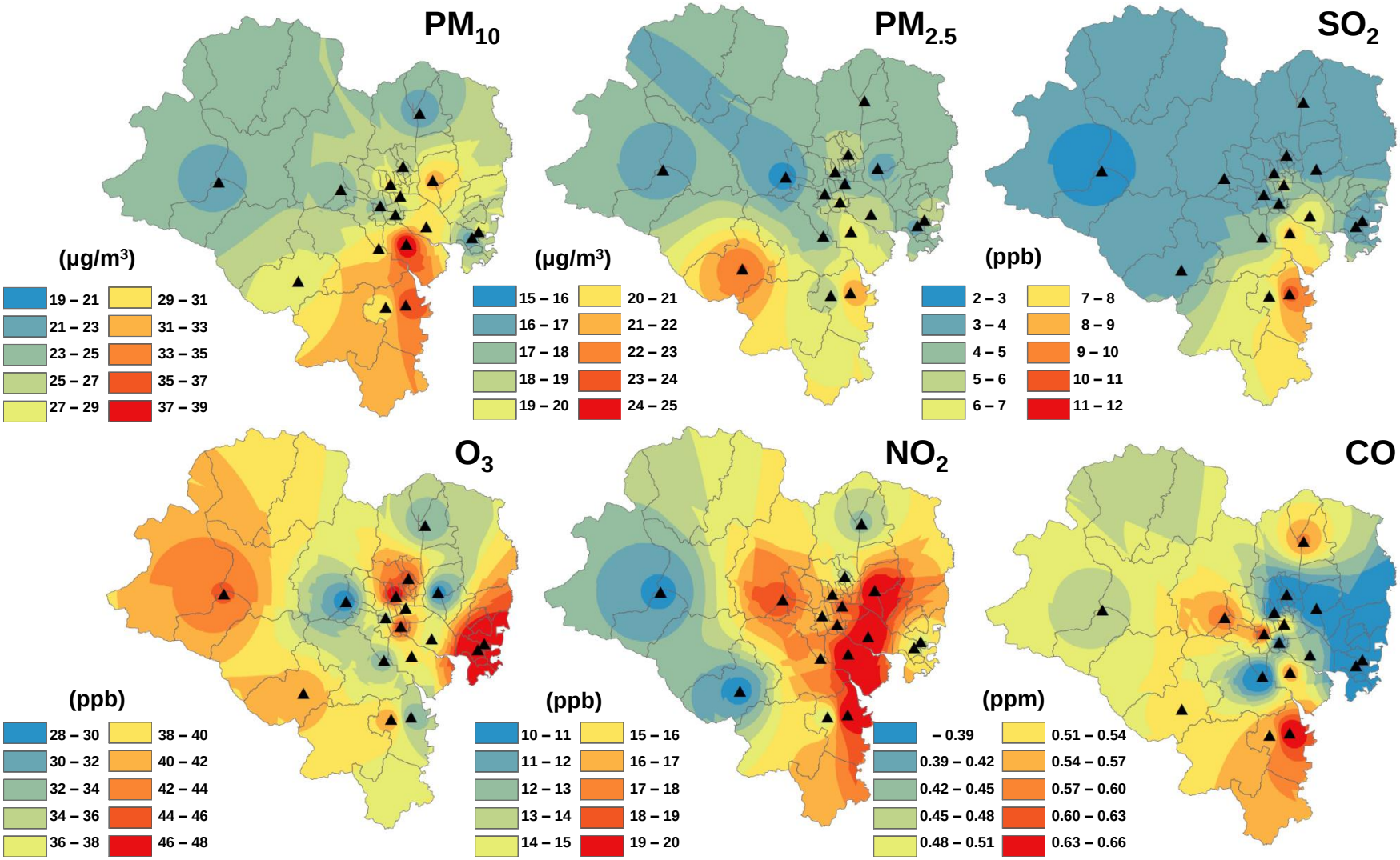

Figure 17. Spatial distribution of CAPs

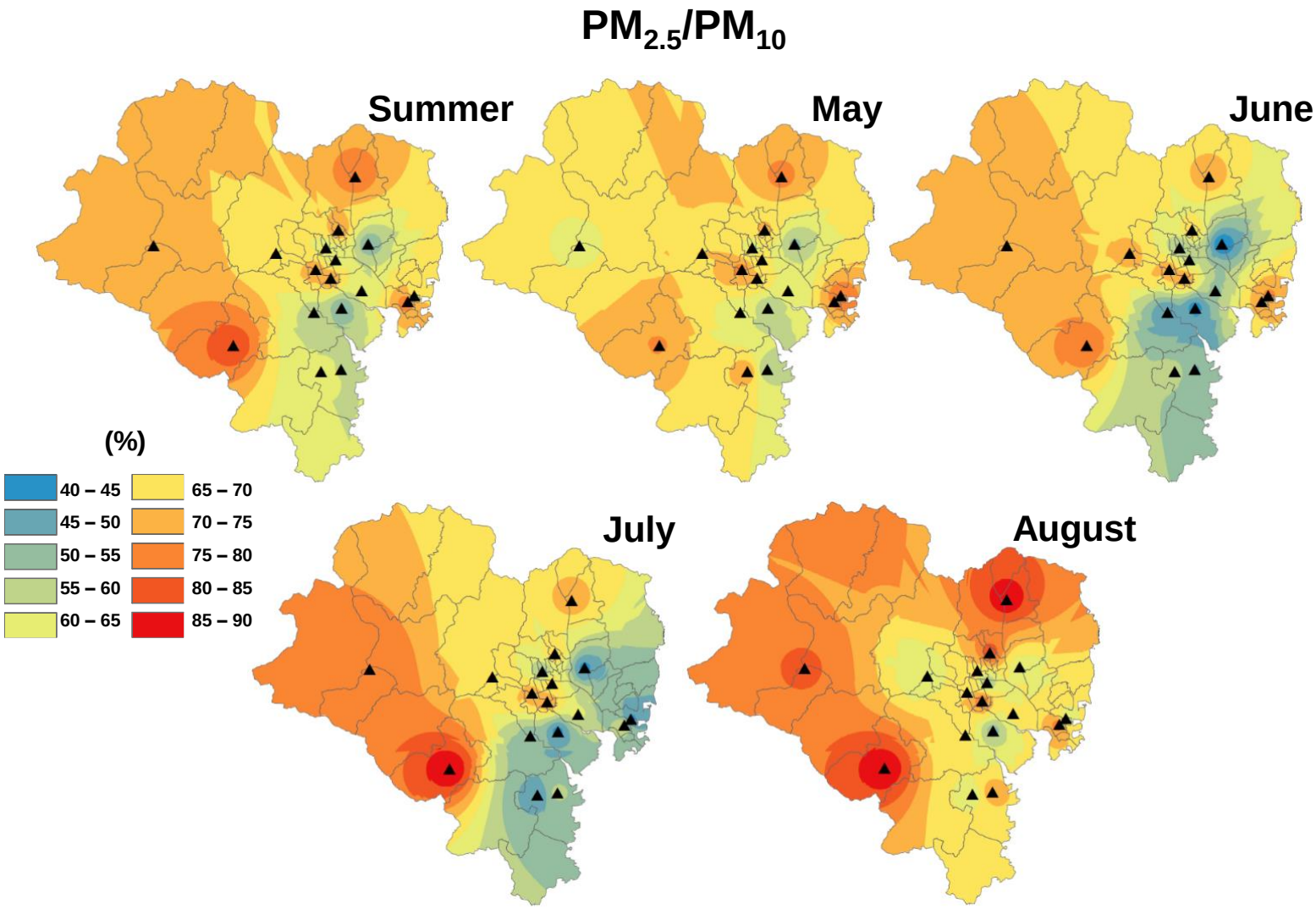

Figure 18. Monthly spatial distribution of $PM_{2.5}/PM_{10}$ ratio

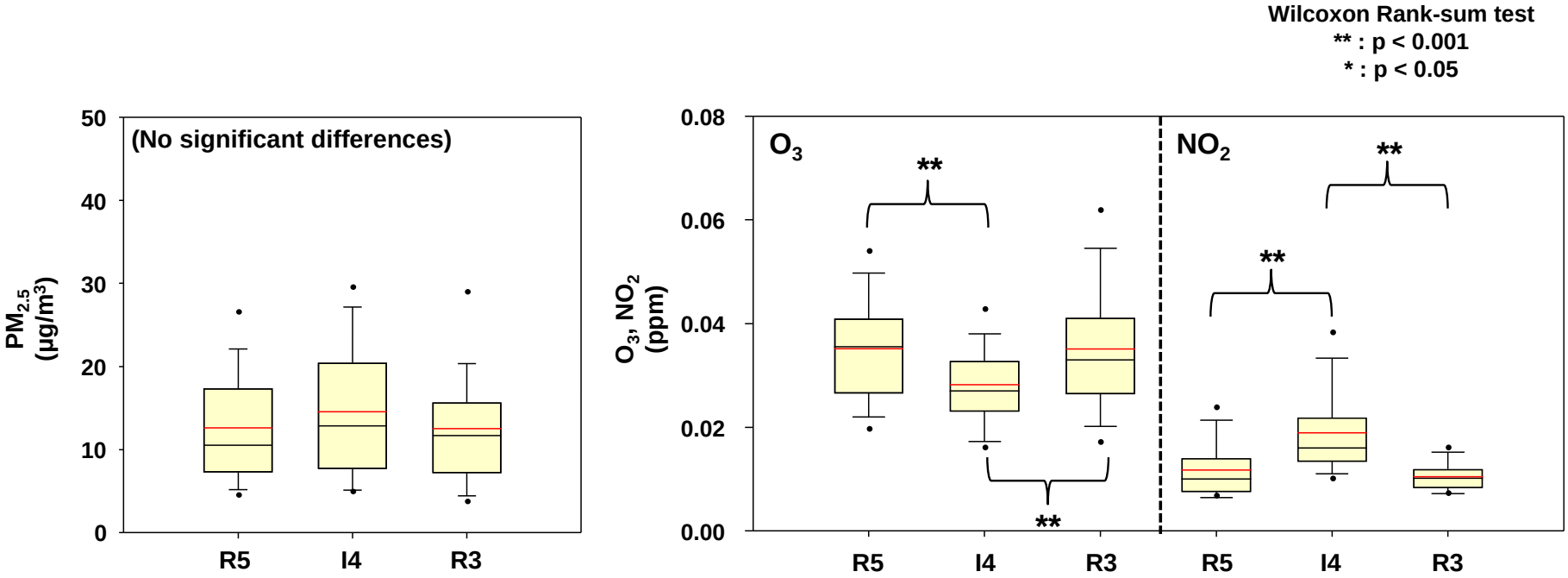

Figure 19. Concentration levels of $PM_{2.5}$, O_3, and NO_2 at 3 sites

3.1.3. Diurnal cycle in CAP concentrations

Figure 20 shows the diurnal trend of CAP concentrations at R5, I4, and R3 during the sampling period with the 6 hr-average concentration. PM_{10} and $PM_{2.5}$ are positively correlated in three sites but do not have any strong diurnal pattern of them. As we expected the photochemical oxidation reactions are dominant in the daytime, O_3 has a strong diurnal cycle, high during daytime and low during nighttime, at all three sites. The variance of O_3 concentration is much larger at rural sites (R3, R5) than that of the industrial site (I4) due to the favorable conditions for the ozone formation. NO_2, and SO_2 do not show any clear diurnal trend but CO and SO_2 at I4 show diurnal high and nocturnal low cycle because of the land-sea breeze circulation.

The 6 hr-average concentrations of CO at all three sites did not exceed the 9 ppm (8 hr-average) criteria however the 6 hr-average concentration of O_3 exceeded 60 ppb (8 hr-average) several times. The O_3 concentration at I4 and R5 could not satisfy the criteria only once, July-21 afternoon when the overall air quality was poor in Ulsan due to the air stagnation from the inverse layer. On the other hand, the ozone concentration at R3 exceeded 60 ppb (8 hr-average) four times during the sampling periods.

One of the interesting points that the diurnal cycles of CAPs gave is that there is a significant increase in the $PM_{2.5}/PM_{10}$ ratio while ozone concentration decreases at night. These phenomena are represented as the patterns that the O_3 concentration line of rural sites approaches the $PM_{2.5}/PM_{10}$ ratio line at the daytime and moves away at the nighttime. Even though the mechanism of the phenomena is not clearly understood yet, it might be associated with the oxidation reactions of VOCs emitted by vegetation when the wind directions are considered.

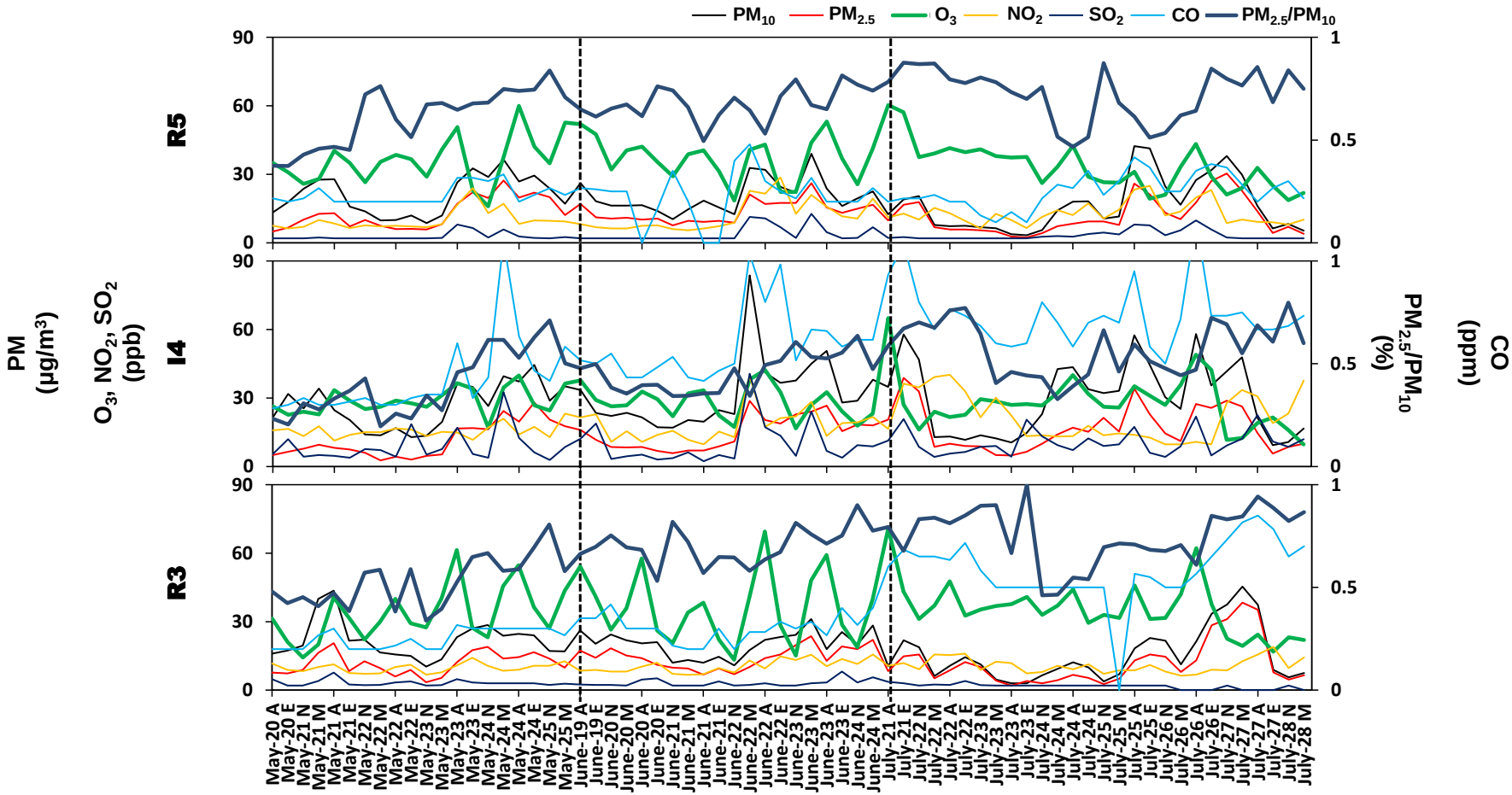

Figure 20. Diurnal cycles in CAP concentrations at 3 sites

3.2. Spatial and temporal distributions of VOCs

3.2.1. Spatial distribution of VOC concentrations

The level of total VOC (TVOC), benzene, toluene, ethylbenzene, and o,m,p-xylene (BTEX), and aliphatics in the industrial sites (I1-I5) was quite high (average 214.78, 53.72, 142.94 μg/m^3, respectively), which is statistically significantly different ($p < 0.001$) from their concentrations at the rural and urban sites (average 50.16, 17.84, 22.32 μg/m^3 and 65.03, 28.91, 22.89 μg/m^3, respectively). The level of VOCs at urban sites is slightly higher than that of VOCs at rural sites but not statistically different from that of VOCs at the sites. However, the level of isoprene concentration had a distinct distribution from other VOCs in Ulsan. The rural sites have the highest concentration of isoprene among all sampling sites. The spatial distribution of isoprene in Ulsan reflected the physical distance from forest areas emitting BVOCs.

Sites I3 and I4 have significantly higher TVOC concentrations than other sites in Ulsan, the former representing a site strongly influenced by petrochemical industrial emissions and the latter a site highly affected by non-ferrous metal industrial emissions in the vicinity of petrochemical plants. The most predominant source of aliphatics like paraffins and olefins in Ulsan is the petrochemical industrial activities including refinery and cracking processes. However, toluene, ethylbenzene, and o,m,p-xylene (TEX), the representatives of aromatics, are prevalent in the automobile and shipbuilding industry complex (I1), north-eastern Ulsan. That is because TEX are widely used to spray paint on the surface of the bodies of cars and ships. The characteristics of isoprene in Ulsan are defined by Figure 22, Figure 23, Figure 24, and Figure 24. The rural sampling sites, R1 to R5, except for R6, have a high concentration of isoprene because the rural sites are surrounded by vegetation; R6 is at a fishing village distant from forest areas. Also, in the cloudiest period, June, there was a large drop in the concentration of isoprene in the rural areas. It shows specific characteristics of vegetation emissions of isoprene, compared to anthropogenic emission which is not related to cloud cover and proximity to a forest area; the emission of isoprene is strongly temperature-dependent.

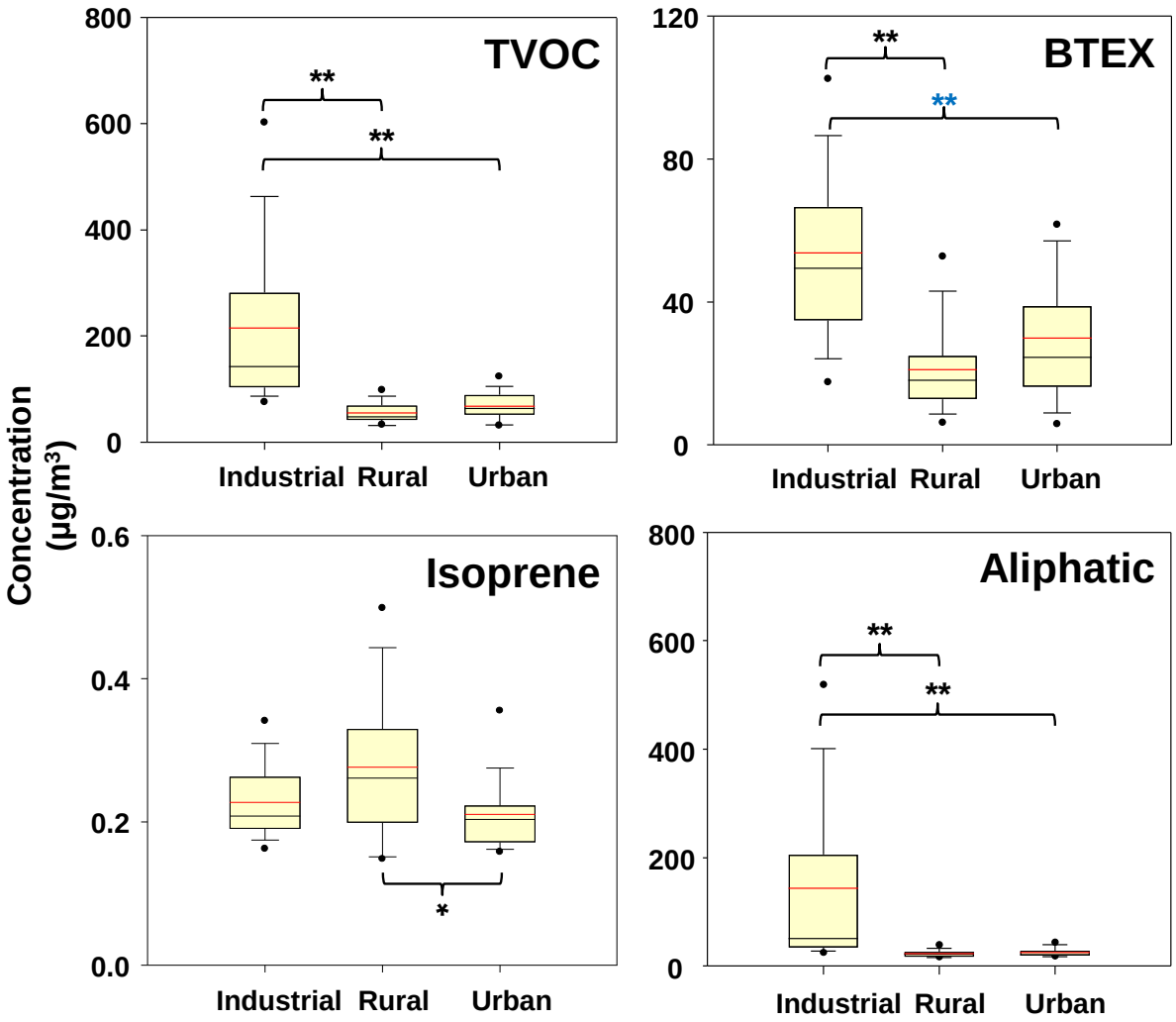

Figure 21. Concentration levels of TVOC, BTEX, isoprene, and aliphatics

Wilcoxon Rank-sum test
**** : p < 0.001**
*** : p < 0.05**
(* for Student t-test)

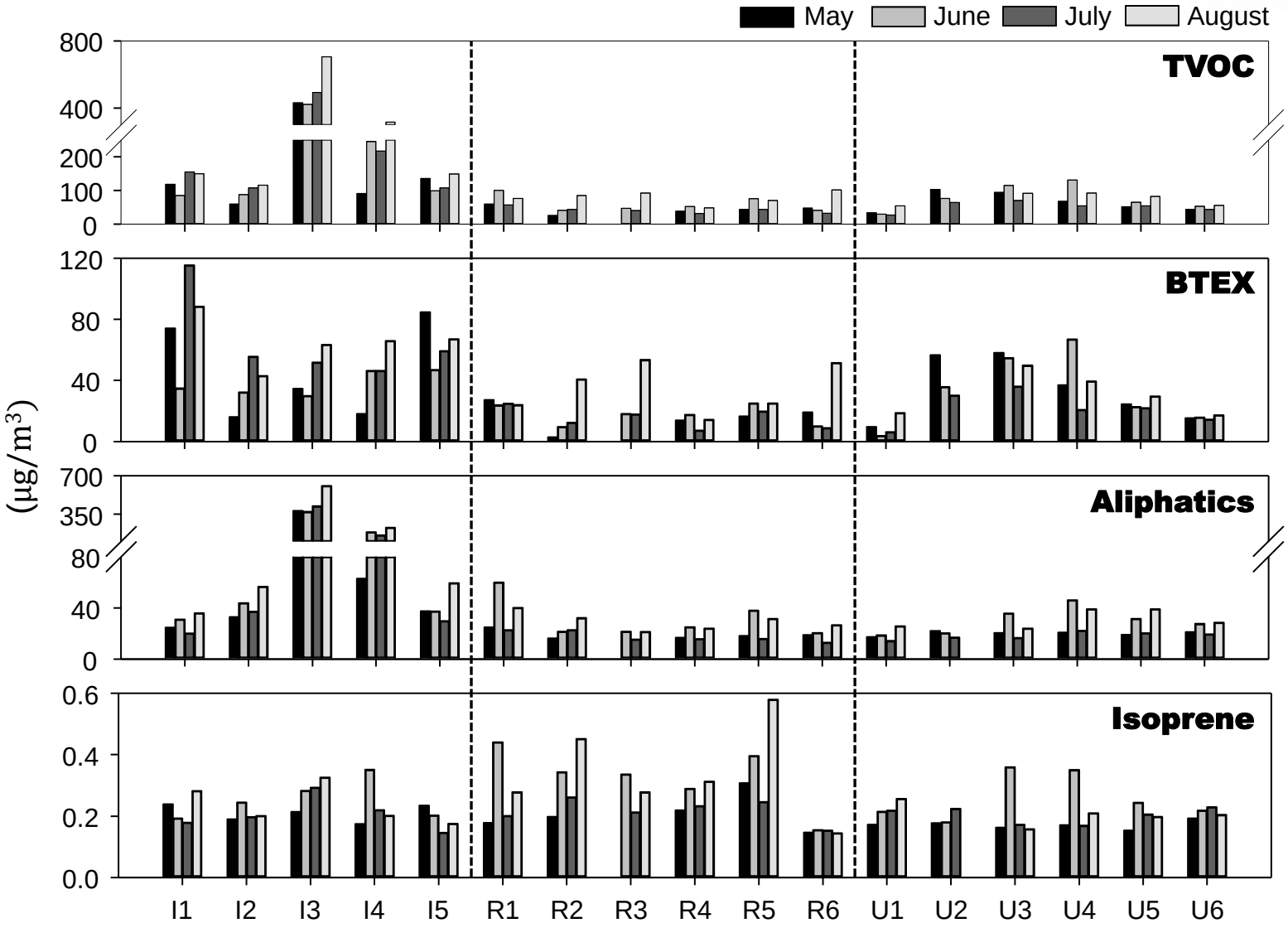

Figure 22. Monthly levels of TVOC, BTEX, aliphatics, and isoprene

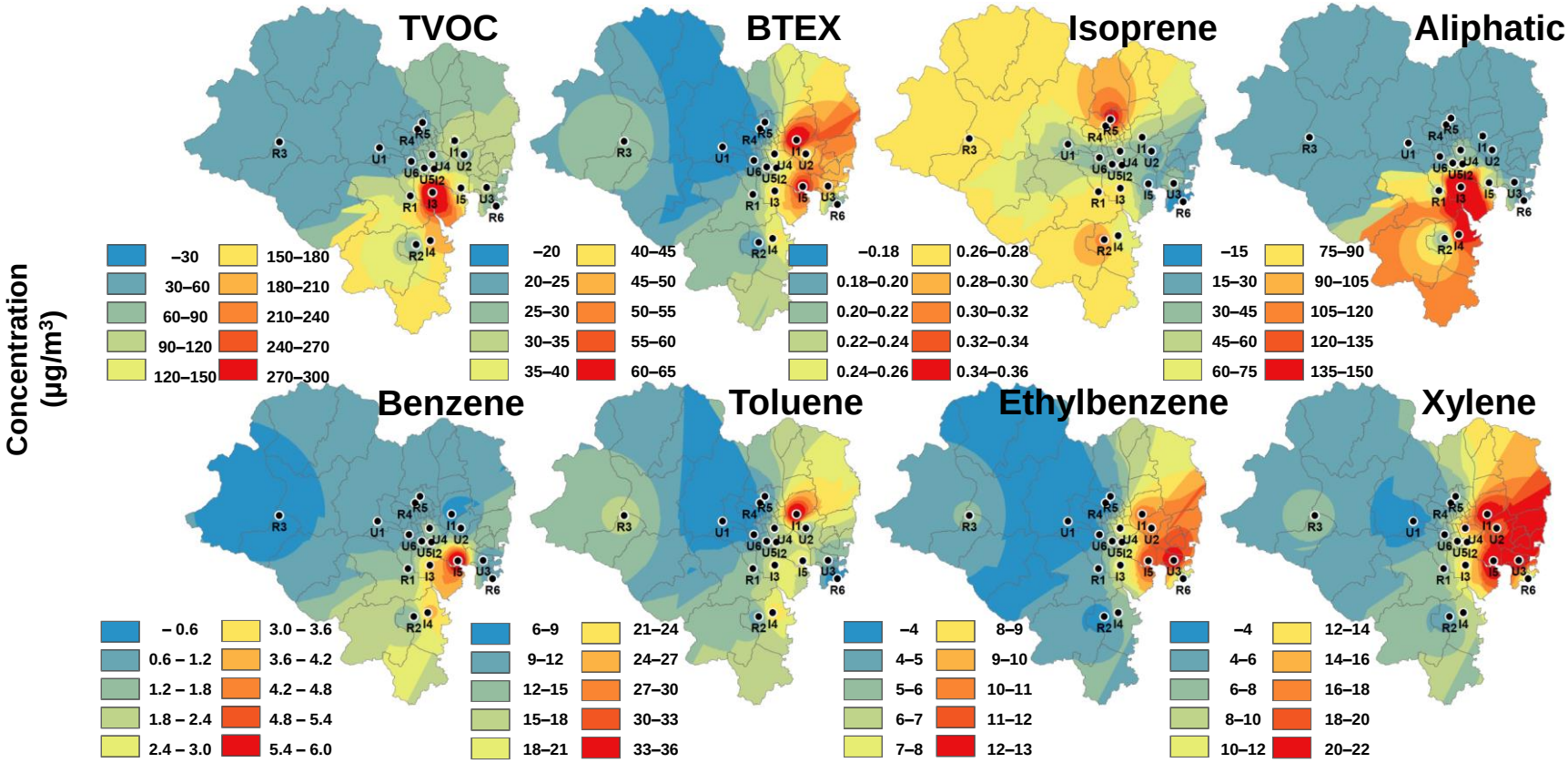

Figure 23. Spatial distributions of anthropogenic and biogenic VOCs

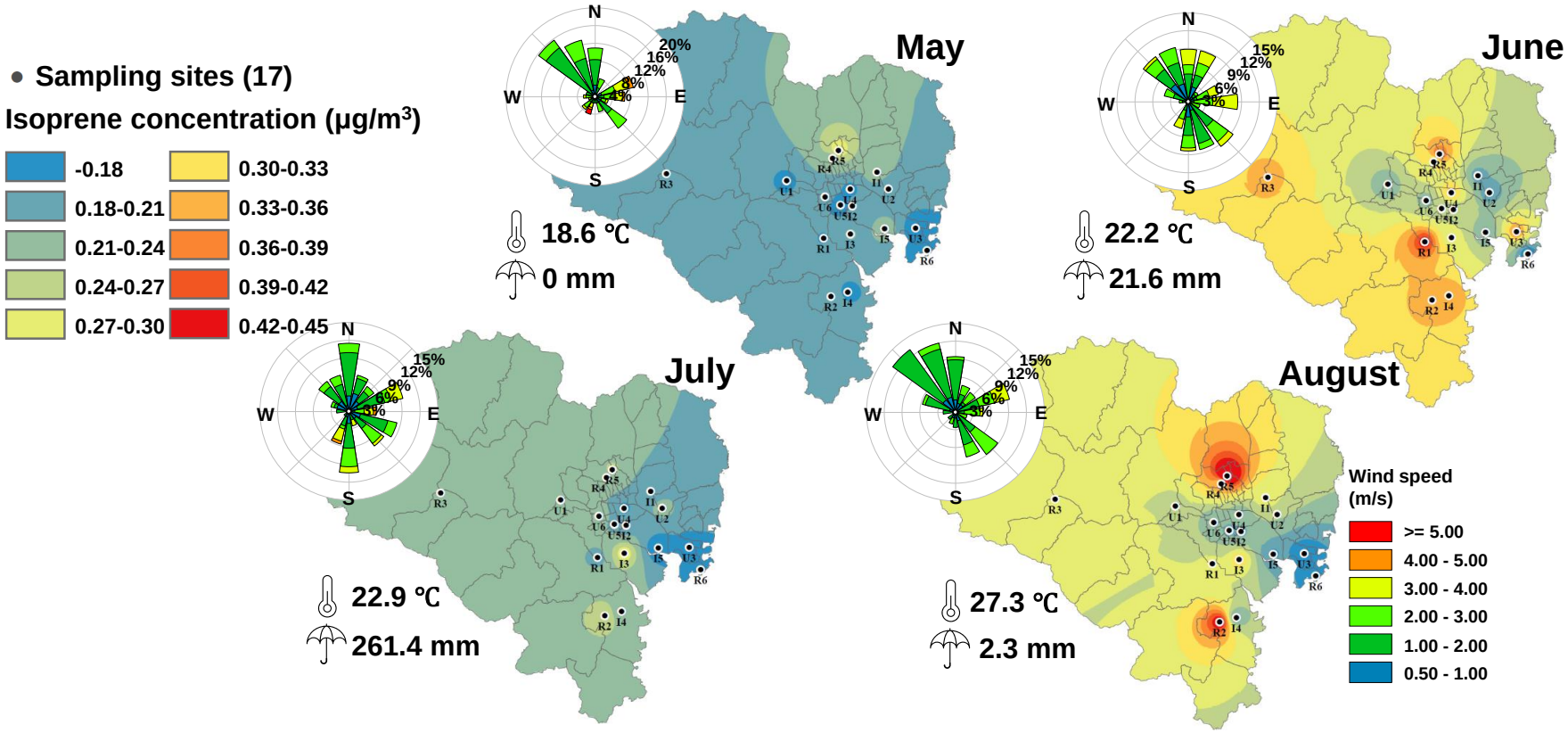

Figure 24. Monthly spatial distribution of isoprene

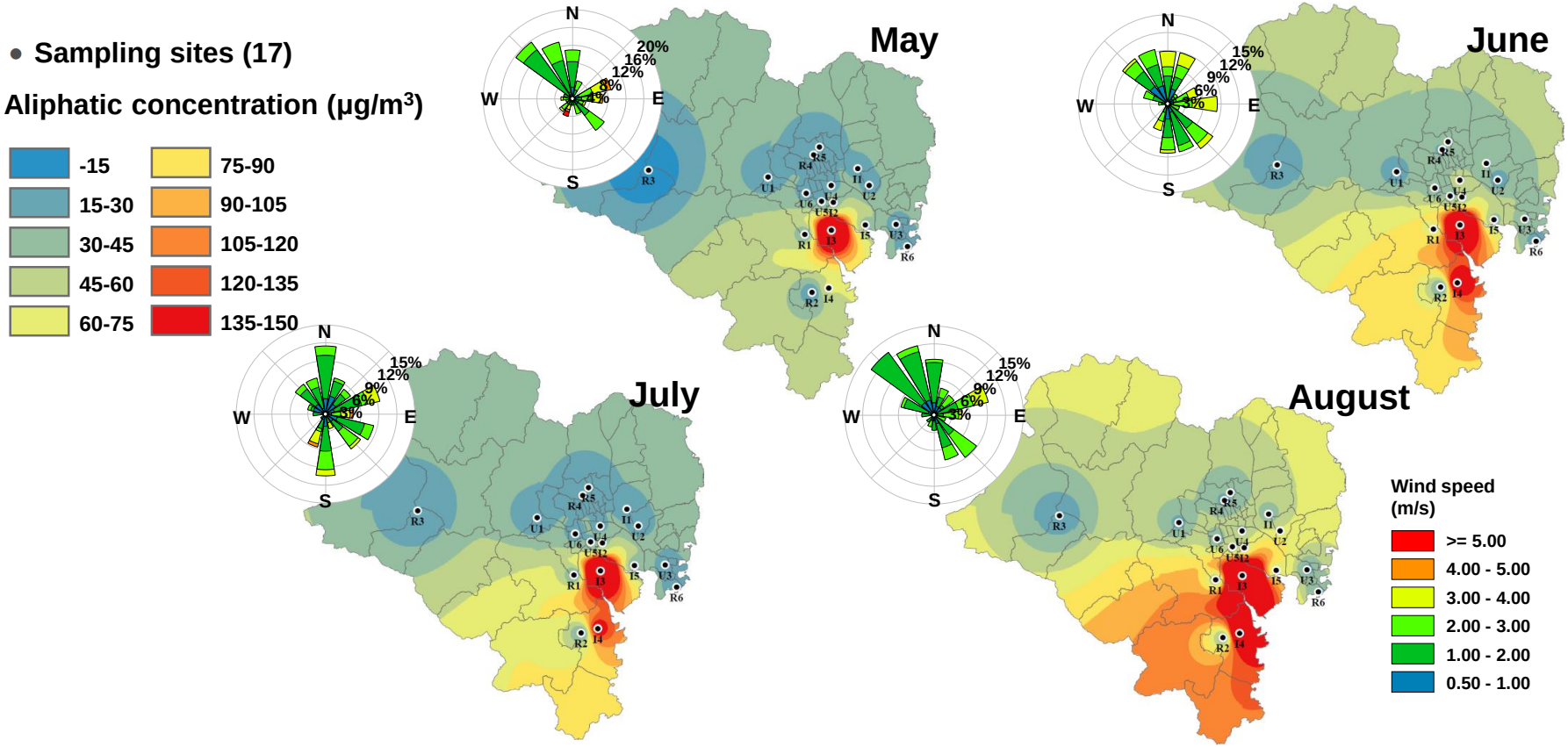

Figure 25. Monthly spatial distribution of aliphatics

3.2.2. Source and aging identification

Diagnostic ratio analysis was carried out to identify VOC sources and aging extents with BTEX concentrations at 17 sampling sites in Ulsan. Overall ratios from the 17 sites showed quite different results from those of several previous studies (Bruno et al., 2006; Gelencsér et al., 1997; Miller et al., 2011; Nelson & Quigley, 1983; Zhang et al., 2008). Average toluene/benzene (T/B) ratios was about 9, which means Ulsan was more affected by non-traffic sources such as industrial emissions rather than traffic sources in summer. Especailly, areas in the vicinity of automobile and shipbuilding industruial complexes (I1, U2, U3, and R6) had a extremely high T/B ratio because those industrial acitivities including spray painting emits large quantity of toluene into the atmosphere with ralatively low concentration of benzene. Those areas also were confirmed to be influenced by relatively fresh sources because of relatively high m,p-xylene to ethylbenzene (m,p-X/E) ratio. This means the sites are closely located to the emission sources. As a result, I1, U2, U3, and R6 were strongly influenced by the fresh and non-traffic sources from the automobile and shipbuilding industrial complexes.

Compared with the overall characteristics of source and aging identification at the rural, urban, and industrial sites, industrial areas were afftected by relatively fresh sources (average m,p-X/$E_{industirial}$: 1.04) but by both traffic and non-traffice sources. Rural sites were affected by traffic and non-traffice sources similarly to urban sites. However, the sources of rural sites were confirmed as more aged than those of urban sites (average m,p-X/E_{rural} : 0.65 , average m,p-X/E_{urban}: 0.78). This implicates the transport of air pollutants from industrial and urban sites to rural sites in Ulsan. Diurnal sea breeze results in the transport aging of air pollitants. Highly aged pollutants were characterized at the downwind areas (average m,p-X/$E_{R2, R3, R4, and U1}$: 0.41, 0.56, 0.51, and 0.42, respectively).

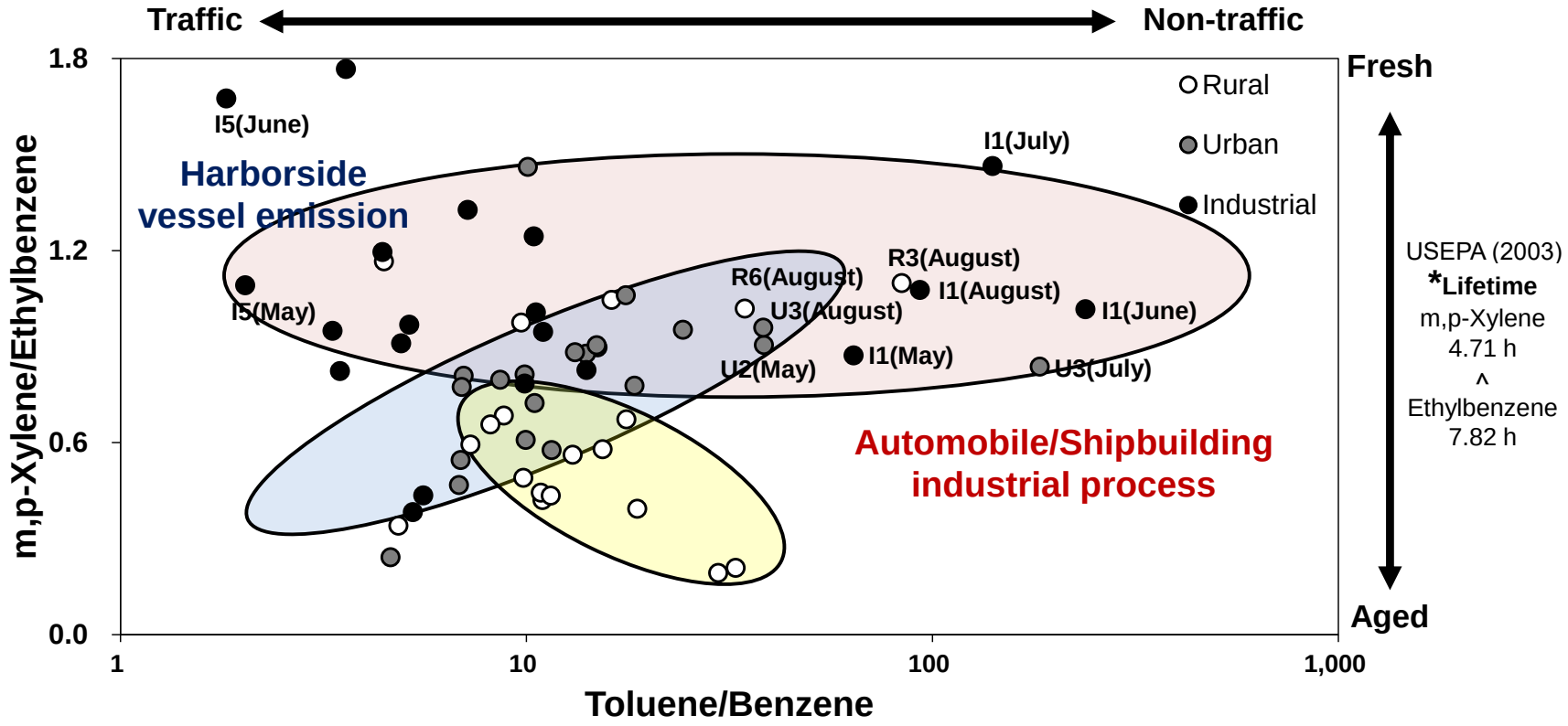

Figure 26. Diagnostic ratios of BTEX at rural, urban, and industrial sites

3.2.3. Temporal distribution of VOC concentrations

According to the result of active VOC sampling, TVOCs, BTEX, and aliphatics do not have obvious diurnal patterns (A/E/N/M) of their concentrations even if BTEX reflects morning and evening rush hour emissions ($p > 0.05$, Rank-sum test). In Figure 30, there are statistically significant differences between day (M/A) and night (E/N) concentrations of isoprene. This infers two meaningful implications of isoprene characteristics. One is that the concentration of isoprene in the atmosphere is associated with temperature and radiation dependence of its emissions. It was reported that all biogenic SOA tracers had a positive correlation with temperature in a previous study (Ding et al., 2014). As the temperature and solar radiation increase during the daytime, the concentration also increases, and vice versa. But the isoprene concentration is relatively high during the night sampling term because the night terms included the daybreak in summer. The other is that the large diurnal fluctuation in isoprene concentration shows its high reactivity and short lifetime in the air. In Table 4, the $k_{OH,isoprene}$ is 101.00 and the $lifetime_{isoprene}$ is 0.55 hrs, which are the largest reaction rate and the shortest lifetime among the target VOCs. This means the amount of isoprene that participates in oxidation reactions in the air might be underestimated and it is easy to reduce the isoprene concentration because the loss function of isoprene is liable to outweigh the production function of it at night. These diurnal high and nocturnal low patterns of isoprene were observed regardless of months and sites during Summer in Ulsan (Figure 29 and Figure 30).

A highly polluted episode was observed from 21 July to 22 July. During the morning on 21 July, the air remained stable under the anticyclone (Figure S10). While the seasonal rain front was moving north and crossed Ulsan with the 20 ℃ dewpoint line, lots of cloud formation occurred. After the sunset, the stability of the atmosphere had kept very high until the rain poured. Because of the large cloud cover and low radiation, the atmosphere temporally had an inverse layer on the surface in Ulsan and it caused the stagnation of air pollutants including CAPs and VOCs over the Ulsan on 21 to 22 July. Although the whole Ulsan area was affected by the synoptic meteorological condition, there was a substantial difference in air quality between R5 and I4 sites. The maximum concentration of TVOCs during the event was 115.4 and 413.8 $\mu g/m^3$ at R5 and I4, respectively, whereas that of $PM_{2.5}$ was 17.8 and 38.8 $\mu g/m^3$, respectively. Therefore, the areas close to the industrial complex in Ulsan have a high vulnerability of SOA and ozone formation risk from high VOC concentration when the synoptic meteorological conditions are favorable for air stagnation.

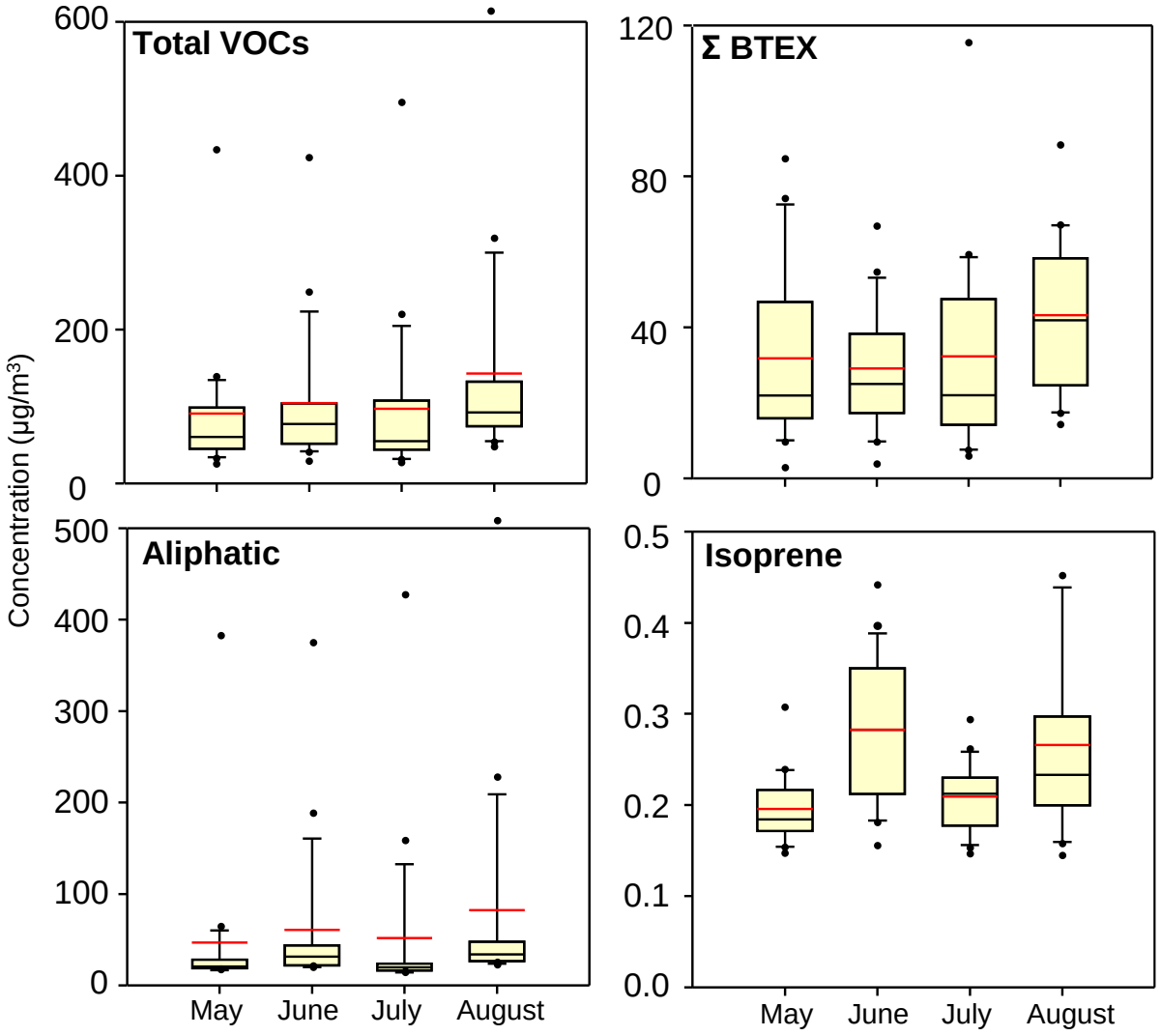

Figure 27. Monthly distribution of TVOC, BTEX, aliphatics and isoprene

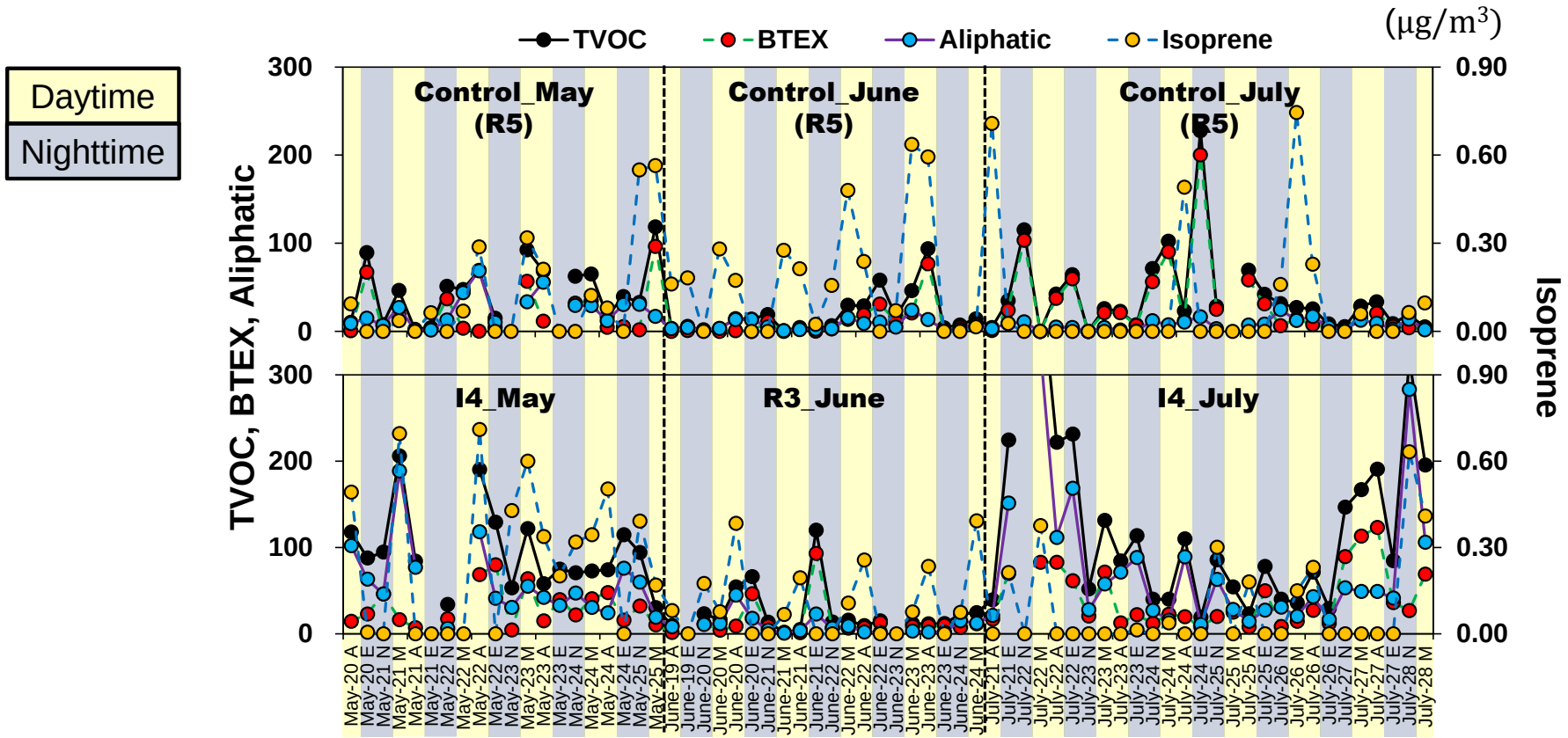

Figure 28. Diurnal patterns of TVOC, BTEX, aliphatics, and isoprene at 3 sites

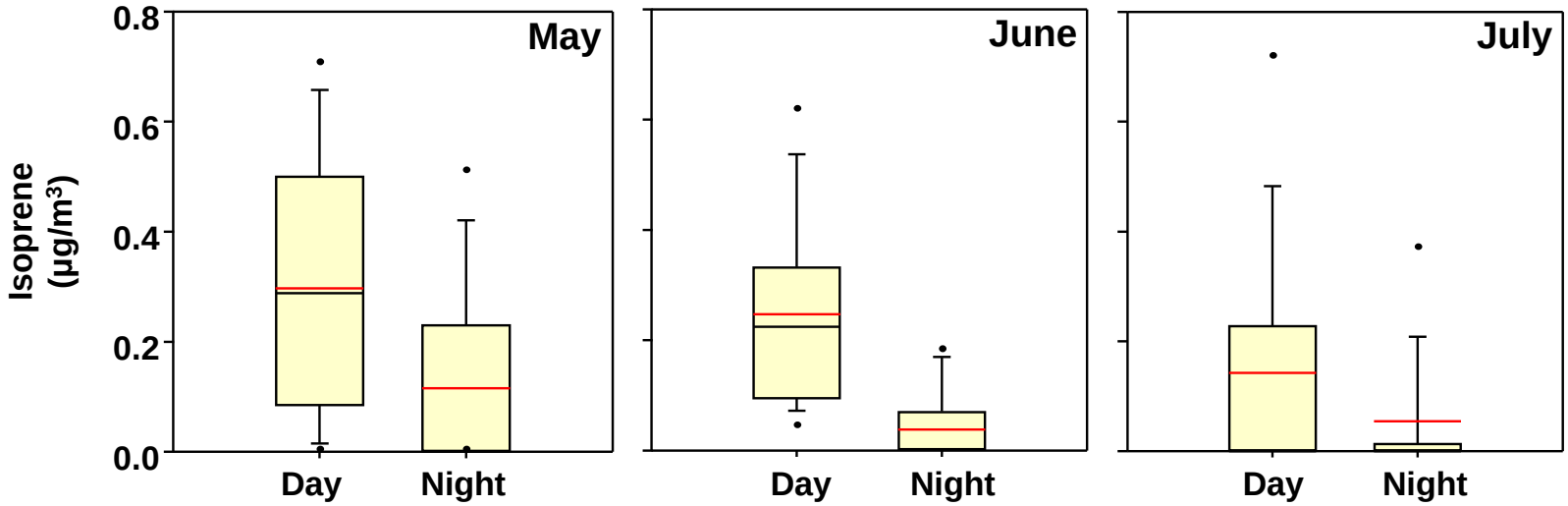

Figure 29. Monthly diurnal difference in isoprene concentrations

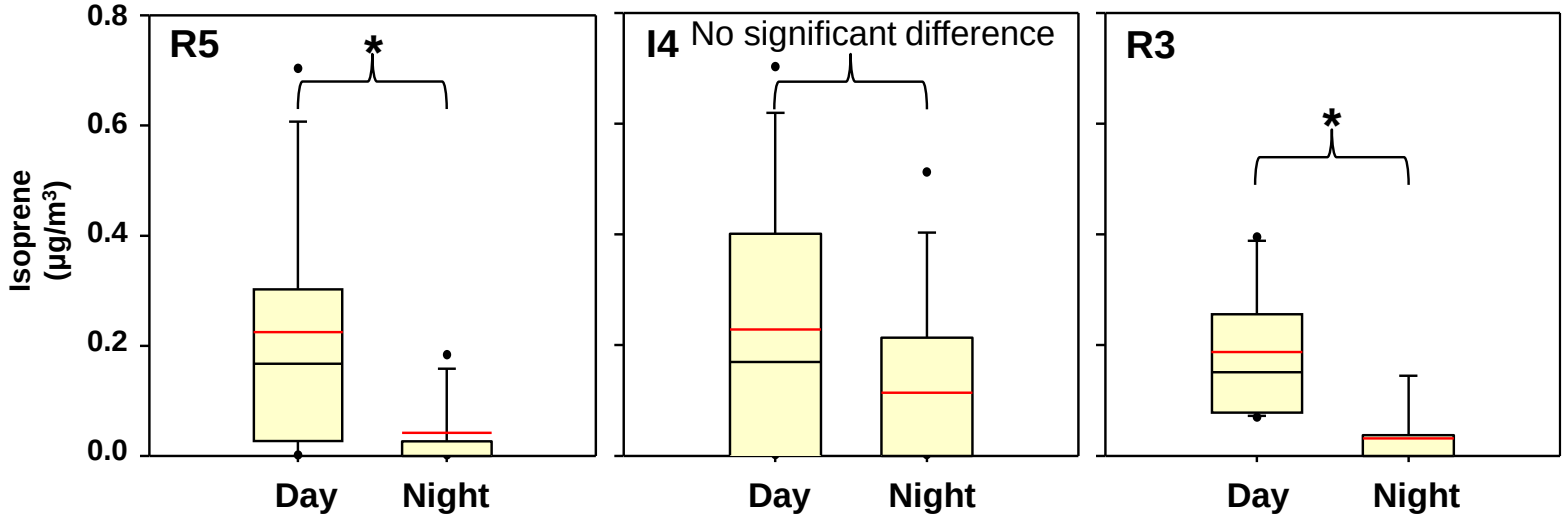

Figure 30. Diurnal difference of isoprene concentration at 3 sites

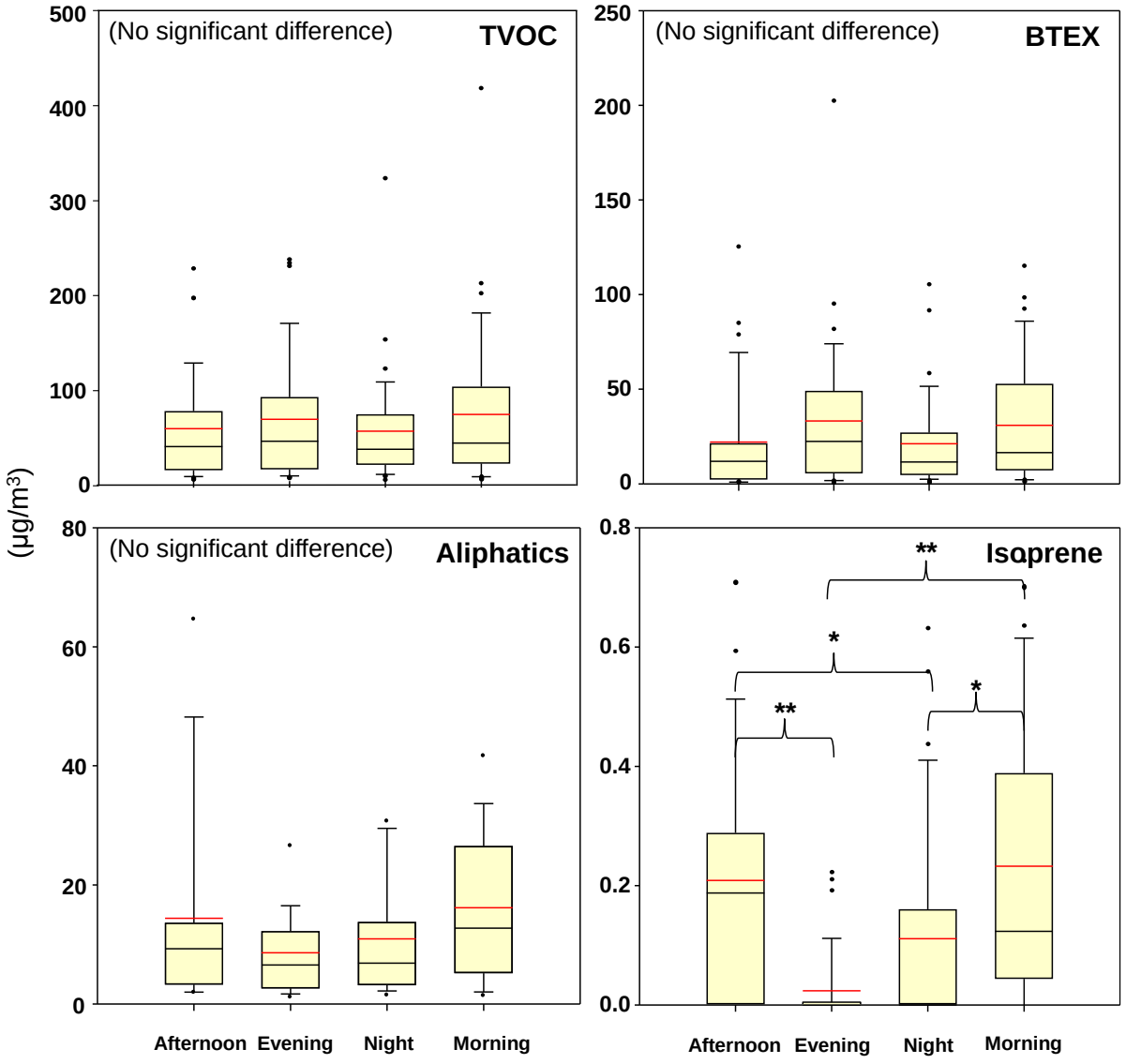

Figure 31. A/E/N/M concentration levels of TVOC, BTEX, aliphatics, and isoprene

3.3. Formation potential of SOA and ozone from VOCs

3.3.1. OFP

The top 5 contributing to total OFP were ranked for each class of areas. Most ozone formation at rural sites in Ulsan is caused by toluene (15.8%), o-xylene (10.0%), m,p-xylene (8.5%), ethylbenzene (7.0%), and 1,2,4-trimethylbenzene (6.8%), accounting for 48.1% of total OFP in the rural areas. Similarly, the OFP at urban sites was dominantly affected by m,p-xylene (13.5%), o-xylene (13.4%), toluene (12.5%), ethylbenzene (8.8%), and 1,2,4-trimethylbenzene (8.1%), which were the top 5 contributors (56.2%) of OFP. As the KORUS-AQ identified C_{7+} aromatics as dominant ozone formation contributors, the top contributors accounting for the majority of ozone formation potential in rural and urban areas are the benzene rings substituted with methyl functional groups (NIER & NASA, 2017; Schroeder et al., 2020). They are known as the constituents of gasoline and are primarily emitted into the atmosphere through the fugitive emission from gasoline fuel and the exhaust of gasoline-fueled vehicles (Atkinson et al., 2006; Farshad et al., 2013; Fraser et al., 1998; Hoekman, 1992; Olson et al., 1992). Therefore, mobile source management including traffic volume, traffic jams, and capture of fugitive emissions is required to control ozone formation in rural and urban areas.

However, the case for industrial areas is different from the rural or urban case. As represented by the pie charts in Figure 32, n-octane (21.4%), toluene (12.3%), 3-methylpentane (8.8%), m,p-xylene (8.4%), and o-xylene (6.6%) had the highest contribution to OFP among 53 target VOCs in industrial areas. Unlike rural and urban sites, about 30% OFP was created by two alkanes, n-octane, and 3-methylpentane in industrial areas. This is petrochemical industry-specific characteristics of ozone formation; a great traffic volume of heavy vehicles loading petroleum-related products and petrochemical processes including naphtha cracking and crude oil distillation are prone to emit various hydrocarbons into the ambient air while treating aliphatic hydrocarbons. We could find extensive chemical processing facilities like pipelines and tanks in the vicinity of the industrial sampling sites (I3 and I4). Factories should therefore reduce leakage of hydrocarbons while processing petrochemical sources both to minimize loss of productivity and to prevent tropospheric ozone formation in the atmospheric environment.

The high OFP from photochemical VOCs was mainly shown in the petrochemical industrial areas from May to August 2020 (Figure 33). Ulsan has consistently been affected by the VOCs emitted from the industrial areas in summer and the high ozone formation potential was concentrated on the neighborhood of the industrial facilities. The highest OFP was estimated at I3 because of aliphatic hydrocarbon emission as mentioned above. In addition, the automobile industrial complex has an

intermediate level of ozone formation potential from the large emission of toluene, o,m,p-xylene, ethylbenzene. The shipbuilding and relevant heavy industrial activities emitted the most amount of toluene, ethylbenzene, and o,m,p-xylene in Ulsan (17,239 ton/y, 986,482 ton/y, 1,834,067 ton/y, respectively) according to the 2017 PRTR data (NICS, 2018). However, their concentration at U3 and R6 was not so high due to the dilution effect from the geographical conditions of a cape of the eastern coastal area of Ulsan. Overall OFP level in Ulsan, except for I3, is similar to the level in Yeosu petrochemical industrial complex but much higher than the level in Gwangyang heavy industrial complex (Figure 33)(NIER, 2019).

Site R3, the western inland area of Ulsan, had a relatively low level of total OFP from the target VOCs. However, it does not explain the relatively high average ozone concentration (38.1 ppb) during the sampling periods in this area. Hence, a deeper investigation on the ozone chemistry including NO_X, oxidant, and radiation should be conducted to identify the mechanisms of ozone formation in the inland area of Ulsan. In addition to isoprene, other biogenic volatile organic compounds such as α,β-pinene and terpenes are required to be included in target compounds because it is known that vegetation emits a lot of the BVOCs but poorly understood in detail yet.

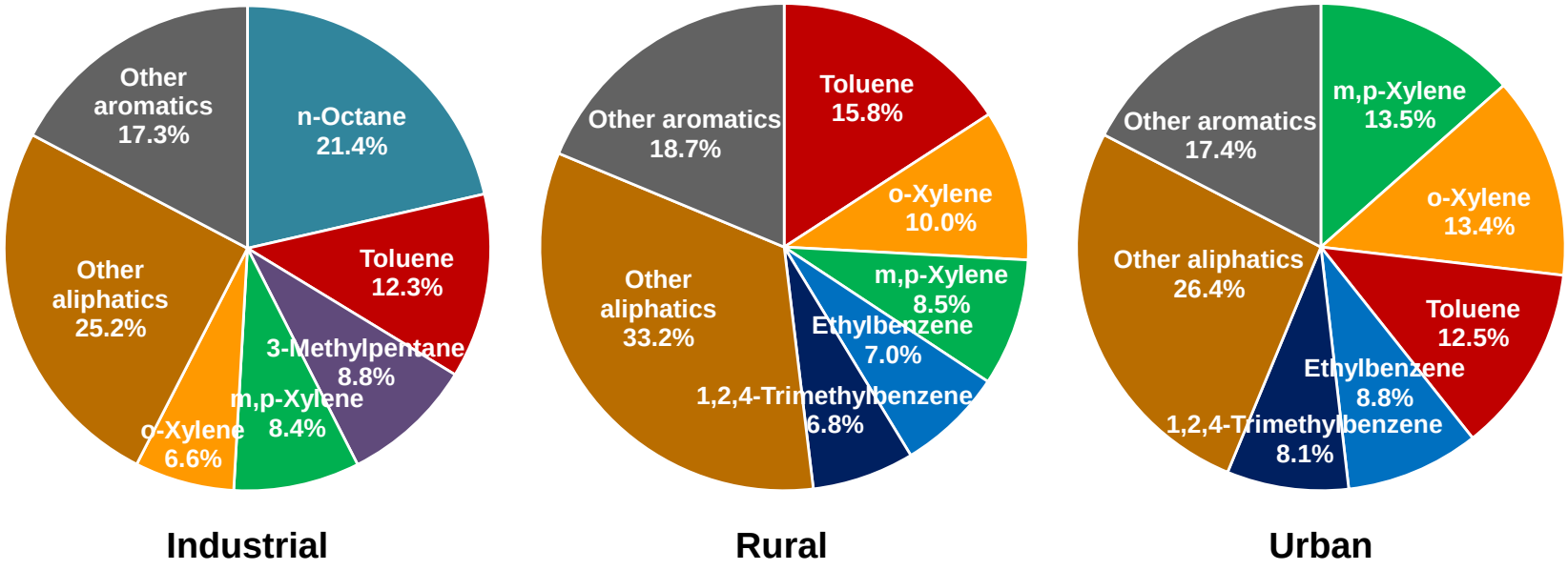

Figure 32. VOC Fraction of OFP in industrial, rural, and urban areas

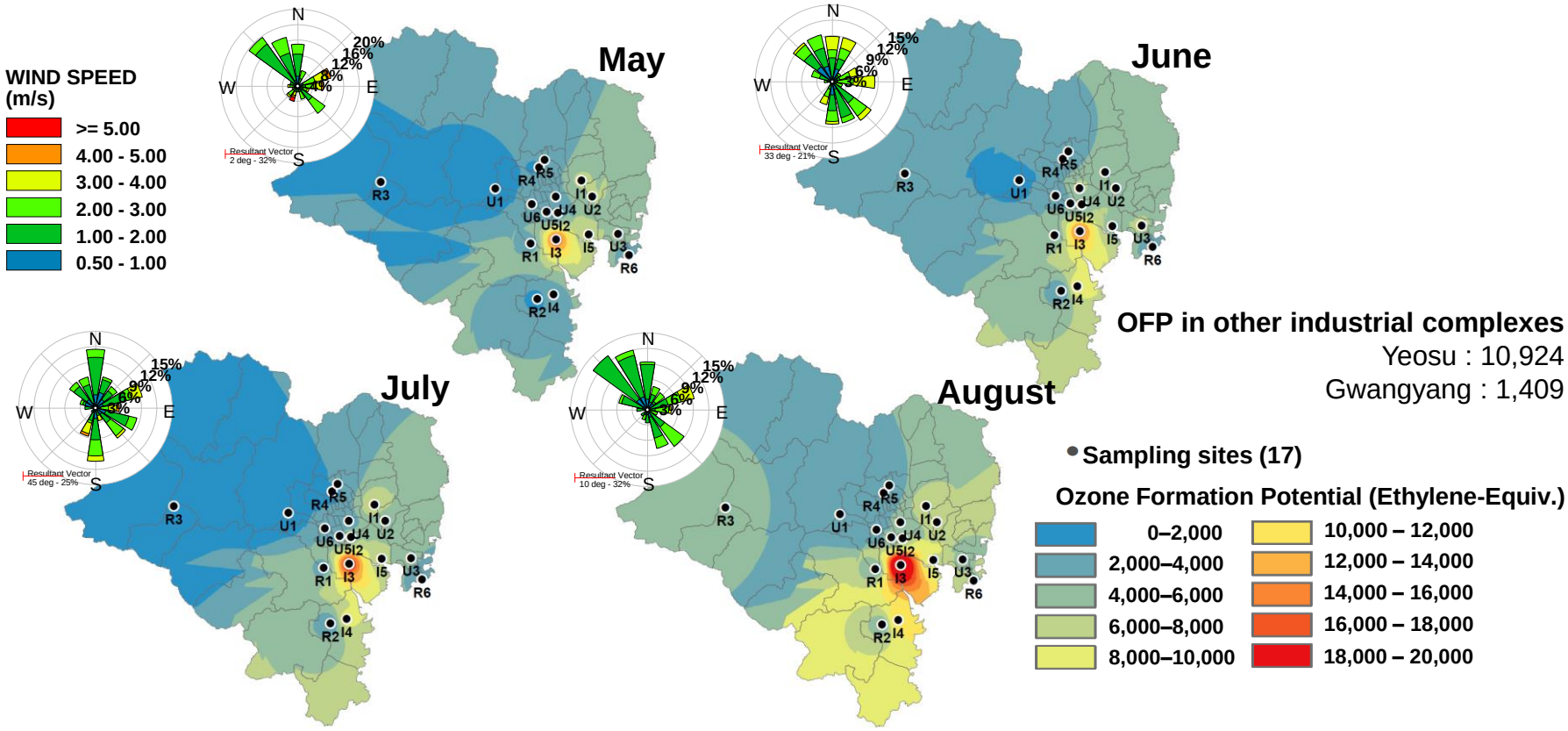

Figure 33. Monthly spatial distribution of OFP

3.3.2. SOAFP

In Figure 34, there are the top 5 VOCs that are most contributing to the potential of SOA formation in each site group. Regardless of the locations, toluene, ethylbenzene, and o,m,p-xylene accounted for more than 70% contribution to SOAFP in Ulsan in summer. The highest SOAFP was estimated around I1, U2, and U3 where the extensive automobile and shipbuilding industrial complexes are established. A tremendous amount of toluene, ethylbenzene, and o,m,p-xylene is widely used in the vehicle painting processes as a thinner to lower the viscosity of spraying paints. SOAFP was quite high in the petrochemical industrial complex because the second-highest toluene emission was reported at one of the petrochemical manufacturing companies on the 2017 PRTR (NICS, 2018). Also, xylene is known to be emitted during the loading and unloading of VOC activities, which are considered the primary evaporative emission sources from marine vessel operations (USEPA, 1994). The high concentration of toluene, ethylbenzene, and o,m,p-xylene was therefore observed over the automobile, shipbuilding, and petrochemical complexes along the eastern coastal region. This generated the distinct characteristics of SOAFP distribution in Ulsan. Overall Ulsan SOAFP level is higher than that in Yeosu petrochemical industrial and Gwangyang heavy industrial complex (Figure 35)(NIER, 2019).

Depending on meteorological conditions, the SOAFP of several urban areas was highly influenced by those industrial emissions. In June 2020, when there were some relatively strong eastern winds (> 3 m/s), U4 had the highest SOAFP. The month with the highest SOAFP was August. That is because a fire accident occurred at a chemical manufacturing factory in the petrochemical industrial complex, between R1 and I4, and dominantly resulted in the significant increment in VOC concentration and SOAFP.

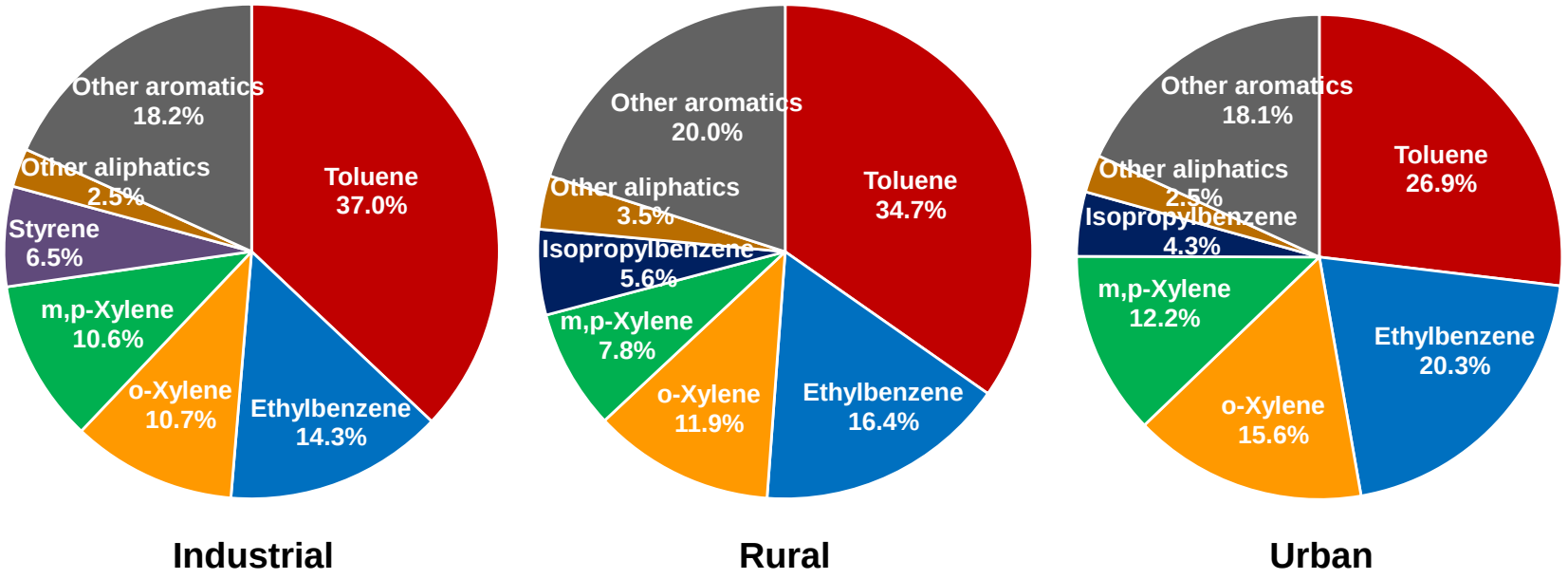

Figure 34. VOC Fraction of SOAFP in industrial, rural, and urban areas

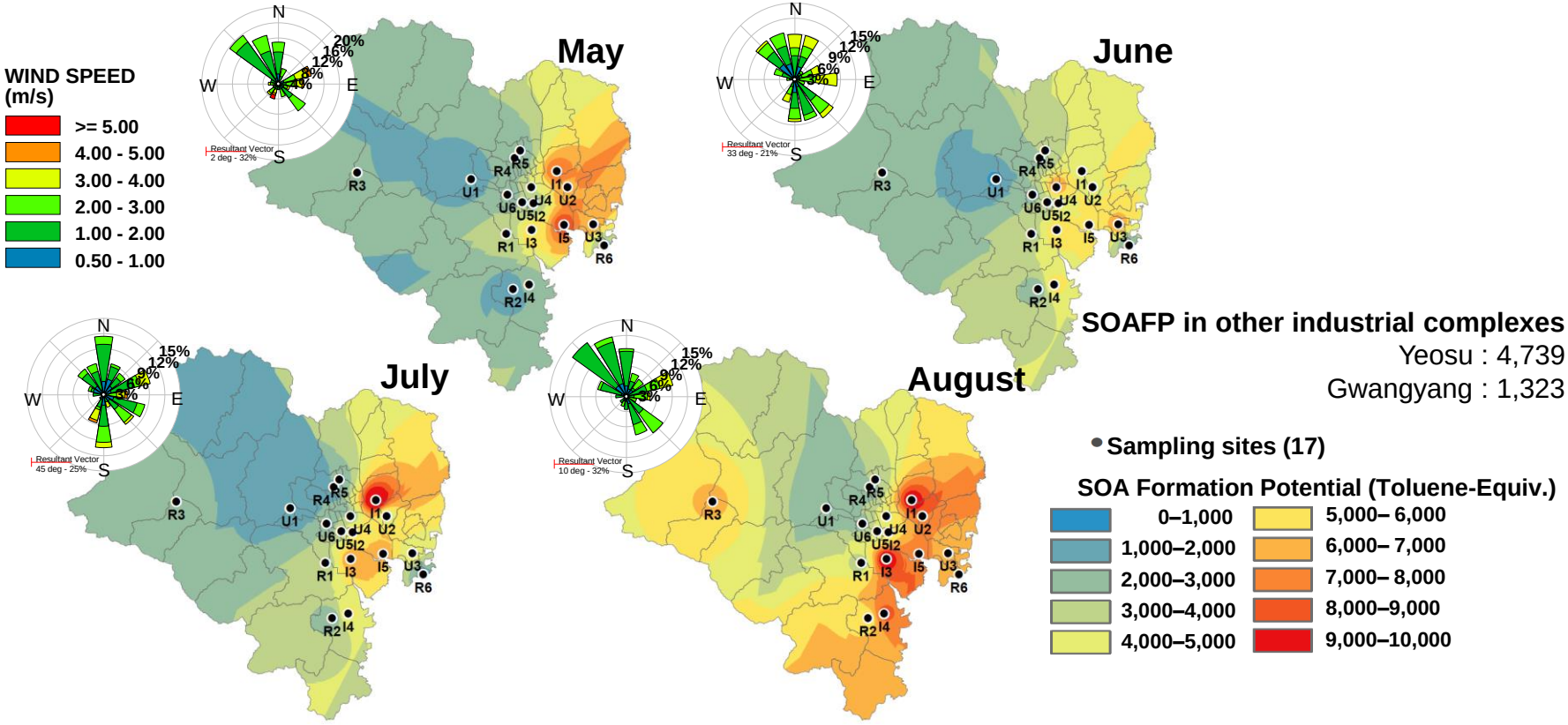

Figure 35. Monthly spatial distribution of SOAFP

3.3.3. Comparison between formation potential and concentration

The estimated formation potentials of ozone and SOA were compared with ambient ozone concentration and the $PM_{2.5}$ to PM_{10} ratio, respectively. $PM_{2.5}$ to PM_{10} ratio could be used as a reference for SOA formation. As Figure 36 shows, O_3 concentration and $PM_{2.5}/PM_{10}$ ratio had clear diurnal cycles in rural sites, high in the daytime and low in the nighttime, whereas OFP and SOAFP did not show any diurnal pattern. However, the industrial site (I4) had weak diurnal cycles in those concentrations. This means that the primary PM emissions could be a more critical factor to determine the $PM_{2.5}/PM_{10}$ ratio and the study on specific ozone chemistry in this area is required to determine how they are formed in the atmosphere.

The diurnal trend was not observed in OFP and SOAFP in Ulsan primarily because the method of the formation potential estimation in this study did not consider meteorological conditions in the field. As a result, OFP and SOAFP poorly explained ozone concentration and indirect SOA through the ratio. There are nevertheless meaningful implications that the formation reaction is nonlinear and complex and reflects a variety of conditions in a certain site. In conclusion, in order to reflect the nonlinearity of the SOA and ozone formation reactions, novel approaches such as machine learning are needed to be devised and complement the conventional linear estimation of formation potentials.

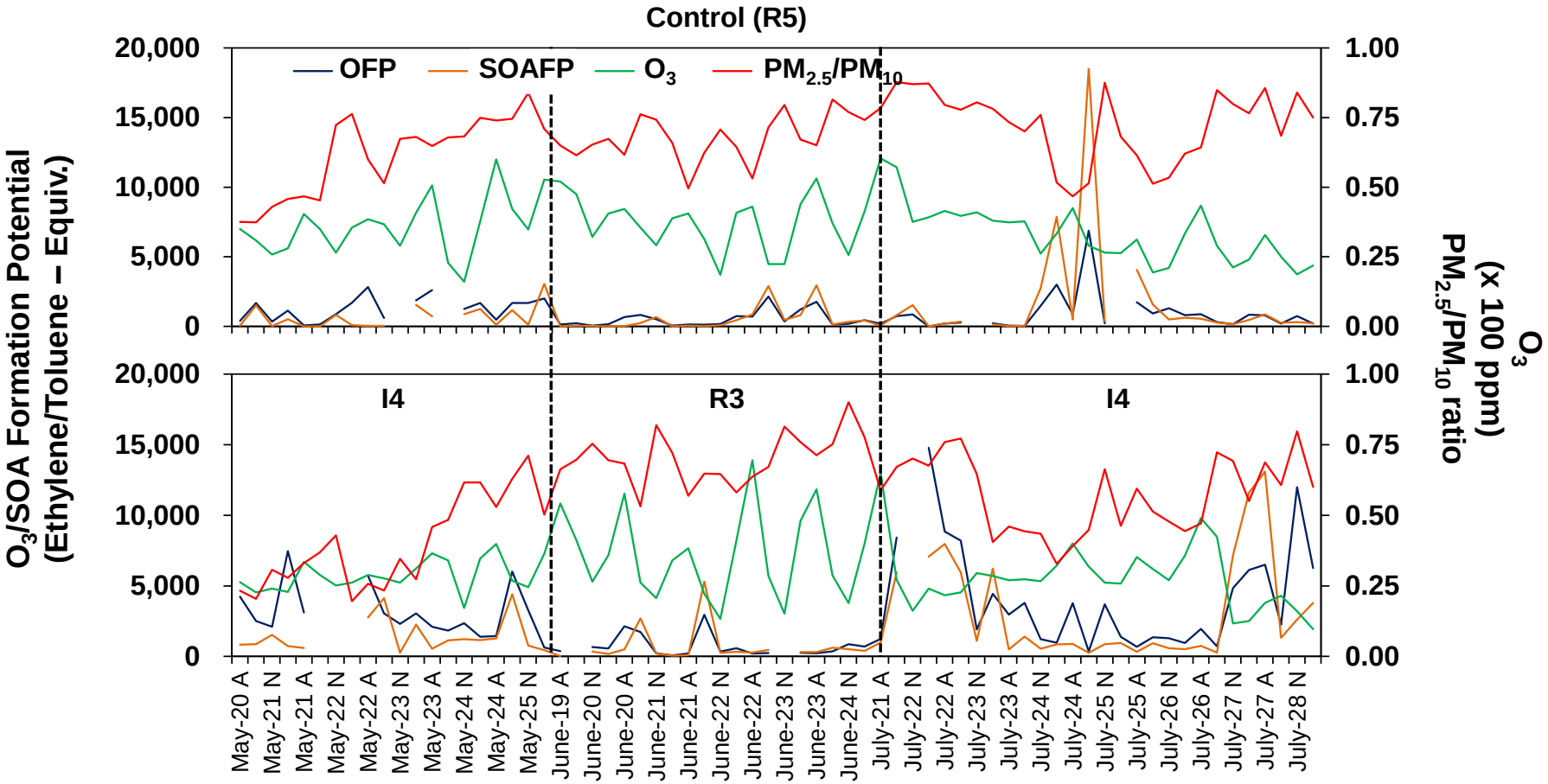

Figure 36. Difference between the estimated FP and the observed data

4. Conclusions

4.1. Implications

We have studied the formation potential during summer of SOA and ozone from anthropogenic and biogenic VOC in Ulsan, South Korea. We investigated spatial distribution and monthly concentration level of 51 VOCs (C_4-C_{12}) that could function as precursors to ozone and SOA formation with the passive monthly VOC sampling at 17 sites (5 industrial, 6 rural, and 6 urban sites) in Ulsan. Also, active 6 hr-average VOC sampling at three sites (1 control, 1 industrial, and 1 rural site) in Ulsan offered the diurnal pattern of 53 VOCs (C_3-C_{12}). The hybrid VOC sampling in Ulsan provided the VOC compositional data with both the high temporal and spatial resolutions in Ulsan for the stereological interpretations of the SOA and ozone formation potentials from the VOCs in Ulsan in summer.

Ozone formation potential of rural and urban sites in Ulsan consisted of the contributions of toluene, ethylbenzene, o,m,p-xylene, and 1,2,4-trimethylbenzene for 48.1% and 56.2%, respectively. The top contributors are the benzene substituted with methyl functional groups. They are widely used as gasoline additives, solvents, and paint and lacquer thinners (ATSDR, 2010; Farshad et al., 2013; Niaz et al., 2015; USEPA, 2005). Because they are predominantly emitted into the atmosphere from mobile vehicle sources, mobile-relevant policies such as traffic and gas station management are required to prevent ozone formation in rural and urban areas. However, additional controls are needed to reduce ozone formation potential in the industrial area since about 30% of OFP in the area resulted from the emission of aliphatic hydrocarbons from the petrochemical industrial facilities. Proper management of aliphatic hydrocarbons leakage in industrial processes could reduce not only the risk from the tropospheric ozone formation but also the economic loss.

It was confirmed that aromatic hydrocarbons mainly contributed to SOAFP over the Ulsan, as we expected from the SOAP index in Table 7. In particular, the aromatics such as toluene, ethylbenzene, and xylene isomers (TEX) are prevalently used as a spray paint and lacquer thinner for painting the surface of automobile and ship bodies. It can be assumed that substantial TEX are emitted into the atmosphere and encourage the secondary organic aerosol formation, based on Figure 34. Not only the painting processes of ships and cars but also the petrochemical and shipping activities provided considerable SOAFP contribution in the industrial area. To the best of our knowledge, it is necessary to decrease the aromatic hydrocarbon emission from traffic and industrial sources for the reduction of SOAFP in Ulsan.

In addition, meteorological conditions could enhance the formation potential in a certain area by increasing the concentration of VOCs in the atmosphere or transporting the VOCs to another place around the highly VOC polluted areas. Particularly, Ulsan is vulnerable to sea breeze transport from industrial areas to a rural or urban areas in summer because its coastal areas are highly developed as an industrial complex and the seasonal synoptic wind in summer is southeasterlies caused by North Pacific high.

4.2. Limitations

This study fills in the gap left by previous VOC monitoring research that addressed secondary organic aerosol and ozone formation in Ulsan rather than hazardous air pollutant VOC monitoring. However, there are several limitations to this study.

Conventional PAMS ozone precursor VOCs do not cover sufficiently various BVOCs. According to previous SOA tracer studies, BVOCs including isoprene, monoterpenes, and β-caryophyllene exhibited more contribution than did aromatic AVOCs (Claeys et al., 2004; Ding et al., 2014). Therefore, more various BVOCs should be monitored to estimate accurate SOA and ozone formation.

The current method for the estimation of formation potential used in this study assumes that the amount of a VOC that participates in the formation reactions is proportional to the ambient air concentration of the VOC. However, the absolute amount of the reactant VOC with high reactivity with oxidants might be underestimated with this method. In addition, meteorology was not considered as a factor while calculating the formation potential. In particular, insolation could critically affect the formation reactions and it varies with cloud cover conditions at different sites. But it is limited to reflect the spatiotemporal variation of solar radiation due to the difficulty in measurement of insulation. The way to quantify the amount of reactant VOC, therefore, is needed to consider the reactivity of reactants and meteorological key factors should be included in the calculation.

The SOA estimation from $PM_{2.5}/PM_{10}$ ratio might have large uncertainty. It assumes that the $PM_{2.5}/PM_{10}$ ratio of primary emissions is consistent over time; the atmospheric loss rates of PM_{10} and $PM_{2.5}$ including dry and wet depositions are equal to each other. Besides, the effect of PM transport ignored. The estimation method could be improved by $PM_{2.5}$ compositional analysis such as SOA tracers.

Moreover, the unexpected outbreak of the Coronavirus Disease 2019 (COVID-19) pandemic has strongly affected industrial activities in Ulsan. Even if it could result in a reduction of industrial emissions of air pollutants including VOC and NO_2, the formation potential of SOA and tropospheric ozone would not necessarily decrease because of non-linear ozone and SOA production reactions (Chameides et al., 1992; Harris et al., 1982; Kinosian, 1982; Le et al., 2020; Qian et al., 2019; Schell et al., 2001; Zhang et al., 2015). Also, the period of Changma in summer 2020 was recorded as the longest days (54 days) since KMA started weather observation in 1973 (KMA, 2020a). Since this specificity may influence atmospheric oxidation reactions, continuous futher studies on the photochemical oxidation from VOCs are required to clearly explain the SOA and ozone formation potential in Ulsan in summer.

4.3. Proposal for a further study

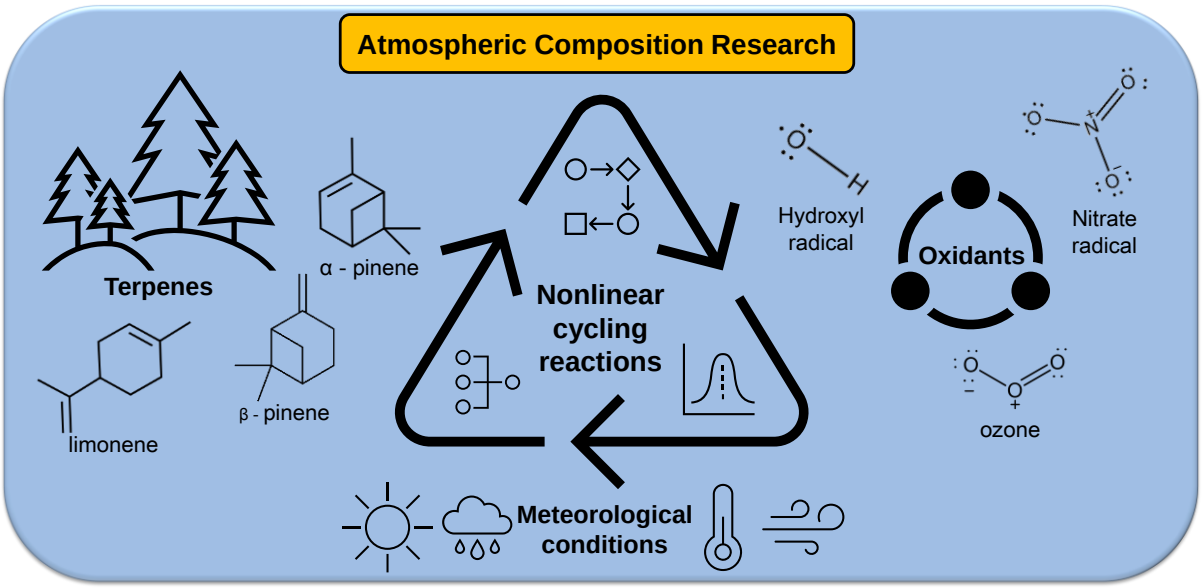

Figure 37. Blueprint for a further atmospheric composition research

The target VOCs used in this study were mostly covering the traditional PAMS ozone precursor VOCs nominated by United States Environmental Protection Agency (USEPA) which is requested from the 1990 Clean Air Act Amendment. However, the traditional PAMS ozone precursor VOCs include the only isoprene among various BVOCs; it does not include sufficient VOCs originated from vegetation even though isoprene is one of most important BVOCs in terms of ozone formation studies. For an integrated research on the atmospheric oxidation reactions related to SOA and ozone formation, it is necessary to consider other natural biogenic VOCs such as α-pinene known as a strong SOA contributor (Derwent & Malcolm, 2000). Therefore, the unprecedented broad BVOC monitoring should be researched to evaluate secondary formations from BVOCs in Ulsan in summer.

In addition to broadening the range of target compounds, the estimation methodology of SOA and O_3 formation potential from atmospheric oxidation reactions should be improved. The fundamental cause of the limitations is the non-linearity and complexity of the cycling oxidation formation reactions. Only limited parameters, including speciated VOCs, oxidants, and meteorology, could be monitored, but tremendous factors are affecting the reactions in the real atmospheric environment. It is very difficult to fully explain SOA and ozone formation within limited parameters. However, machine learning (ML) is an appropriate approach to solve non-linear problems. Although most ML approaches are black-box—i.e., being unable to show its algorithm's detail—some of them like white-box decision trees show how they use input parameters. As a result, I would like to complement the conventional understanding of SOA and ozone formation reactions with comprehensive

atmospheric compositional monitoring while using white-box machine learning approaches, providing the algorithm's structure (Atkinson & Arey, 2003).

References

Atkinson, R. (2000). Atmospheric chemistry of VOCs and NOx. *Atmospheric Environment*, *34*, 2063-2101.

Atkinson, R., & Arey, J. (2003). Gas-phase tropospheric chemistry of biogenic volatile organic compounds: a review. *Atmospheric environment*, *37*, 197-219.

Atkinson, R., Hoover, S., Arey, J., & Preston, K. (2006). *Atmospheric chemistry of gasoline-related emissions: formation of pollutants of potential concern*. https://oehha.ca.gov/media/downloads/air/document/atmoschemgas.pdf

ATSDR. (2010). Toxicological profile for ethylbenzene. *Agency for Toxic Substances and Disease Registry*.

Baek, K.-M., Kim, M.-J., Seo, Y.-K., Kang, B.-W., Kim, J.-H., & Baek, S.-O. (2020). Spatiotemporal Variations and Health Implications of Hazardous Air Pollutants in Ulsan, a Multi-Industrial City in Korea. *Atmosphere*, *11*(5), 547. https://doi.org/10.3390/atmos11050547

Bruno, P., Caselli, M., De Gennaro, G., De Gennaro, L., & Tutino, M. (2006). High spatial resolution monitoring of benzene and toluene in the urban area of Taranto (Italy). *Journal of atmospheric chemistry*, *54*(2), 177-187.

Carter, W. P. (1994). Development of ozone reactivity scales for volatile organic compounds. *Air & waste*, *44*(7), 881-899.

Chameides, W., Fehsenfeld, F., Rodgers, M., Cardelino, C., Martinez, J., Parrish, D., Lonneman, W., Lawson, D., Rasmussen, R., & Zimmerman, P. (1992). Ozone precursor relationships in the ambient atmosphere. *Journal of Geophysical Research: Atmospheres*, *97*(D5), 6037-6055.

Claeys, M., Graham, B., Vas, G., Wang, W., Vermeylen, R., Pashynska, V., Cafmeyer, J., Guyon, P., Andreae, M. O., & Artaxo, P. (2004). Formation of secondary organic aerosols through photooxidation of isoprene. *Science*, *303*(5661), 1173-1176.

Derwent, R., & Jenkin, M. (1991). Hydrocarbons and the long-range transport of ozone and PAN across Europe. *Atmospheric Environment. Part A. General Topics*, *25*(8), 1661-1678.

Derwent, R., Jenkin, M., Passant, N., & Pilling, M. (2007). Reactivity-based strategies for photochemical ozone control in Europe. *Environmental science & policy*, *10*(5), 445-453.

Derwent, R., & Malcolm, A. (2000). Photochemical generation of secondary particles in the United Kingdom. *Philosophical Transactions of the Royal Society of London. Series A: Mathematical, Physical and Engineering Sciences*, *358*(1775), 2643-2657.

Derwent, R. G., Jenkin, M. E., Utembe, S. R., Shallcross, D. E., Murrells, T. P., & Passant, N. R. (2010). Secondary organic aerosol formation from a large number of reactive man-made organic compounds. *Science of the total environment*, *408*(16), 3374-3381. https://doi.org/10.1016/j.scitotenv.2010.04.013

Ding, X., He, Q. F., Shen, R. Q., Yu, Q. Q., & Wang, X. M. (2014). Spatial distributions of secondary organic aerosols from isoprene, monoterpenes, β-caryophyllene, and aromatics over China during summer. *Journal of Geophysical Research: Atmospheres*, *119*(20), 11,877-811,891.

Farshad, A., Oliaei, H. K., Mirkazemi, R., & Bakand, S. (2013). Risk assessment of benzene, toluene, ethylbenzene, and xylenes (btex) in paint plants of two automotive industries in iran by using the coshh guideline. *European Scientific Journal*.

Fraser, M. P., Cass, G. R., & Simoneit, B. R. (1998). Gas-phase and particle-phase organic compounds emitted from motor vehicle traffic in a Los Angeles roadway tunnel. *Environmental Science & Technology*, *32*(14), 2051-2060.

Gelencsér, A., Siszler, K., & Hlavay, J. (1997). Toluene− benzene concentration ratio as a tool for characterizing the distance from vehicular emission sources. *Environmental Science & Technology*, *31*(10), 2869-2872.

Grosjean, D., & Seinfeld, J. H. (1989). Parameterization of the formation potential of secondary organic aerosols. *Atmospheric Environment (1967)*, *23*(8), 1733-1747.

Harris, G. W., Carter, W. P., Winer, A. M., Pitts, J. N., Platt, U., & Perner, D. (1982). Observations of nitrous acid in the Los Angeles atmosphere and implications for predictions of ozone-precursor relationships. *Environmental Science & Technology*, *16*(7), 414-419.

Hoekman, S. K. (1992). Speciated measurements and calculated reactivities of vehicle exhaust emissions from conventional and reformulated gasolines. *Environmental Science & Technology*, *26*(6), 1206-1216.

ICSM. (2019). *Radiello User Manual 2019*. https://www.restek.com/pdfs/radiello-manual.pdf

Jaars, K., Beukes, J., Van Zyl, P., Venter, A., Josipovic, M., Pienaar, J., Vakkari, V., Aaltonen, H., Laakso, H., & Kulmala, M. (2014). Ambient aromatic hydrocarbon measurements at Welgegund, South Africa. *Atmospheric Chemistry and Physics*, *14*(13), 7075-7089.

Kesselmeier, J., & Staudt, M. (1999). Biogenic volatile organic compounds (VOC): an overview on emission, physiology and ecology. *Journal of atmospheric chemistry*, *33*(1), 23-88.

Kim, B.-R. (2011). VOC Emissions from Automotive Painting and Their Control: A Review. *Environmental Engineering Research*, *16*(1), 1-9. https://doi.org/10.4491/eer.2011.16.1.001

Kim, H., Zhang, Q., & Heo, J. (2018). Influence of intense secondary aerosol formation and long-range transport on aerosol chemistry and properties in the Seoul Metropolitan Area during spring time: results from KORUS-AQ. *Atmospheric Chemistry & Physics*, *18*(10).

Kim, S.-J., Kwon, H.-O., Lee, M.-I., Seo, Y., & Choi, S.-D. (2019). Spatial and temporal variations of volatile organic compounds using passive air samplers in the multi-industrial city of Ulsan, Korea. *Environmental Science and Pollution Research*, *26*(6), 5831-5841.

Kim, Y. P., Na, K., & Moon, K. (1998). Air pollutant levels at ulsan, an industrial area, Korea. *Journal of Aerosol Science*(29), S237-S238.

Kinosian, J. R. (1982). Ozone-precursor relationships from EKMA diagrams. *Environmental Science & Technology*, *16*(12), 880-883.

KMA. (2020a, 9/8/2020). *Meteorological characteristics in summer 2020* http://www.kma.go.kr/notify/press/kma_list.jsp?bid=press&mode=view&num=1193919&page=1&field=subject&text=%C0%E5%B8%B6

KMA. (2020b). *Meteorological observation* https://data.kma.go.kr

Le, T., Wang, Y., Liu, L., Yang, J., Yung, Y. L., Li, G., & Seinfeld, J. H. (2020). Unexpected air pollution with marked emission reductions during the COVID-19 outbreak in China. *Science*, *369*(6504), 702-706.

Lee, G., Park, J.-H., Kim, D.-G., Koh, M. S., Lee, M., Han, J.-S., & Kim, J.-C. (2020). Current Status and Future Directions of Tropospheric Photochemical Ozone Studies in Korea. *Journal of Korean Society for Atmospheric Environment*, *36*(4), 419-441. https://doi.org/10.5572/kosae.2020.36.4.419

Liu, Y., Shao, M., Fu, L., Lu, S., Zeng, L., & Tang, D. (2008). Source profiles of volatile organic compounds (VOCs) measured in China: Part I. *Atmospheric environment*, *42*(25), 6247-6260.

Mackay, D., Shiu, W.-Y., & Lee, S. C. (2006). *Handbook of physical-chemical properties and environmental fate for organic chemicals*. CRC press.

Malherbe, L., & Mandin, C. (2007). VOC emissions during outdoor ship painting and health-risk assessment. *Atmospheric environment*, *41*(30), 6322-6330.

Miller, L., Xu, X., Grgicak-Mannion, A., Brook, J., & Wheeler, A. (2012). Multi-season, multi-year concentrations and correlations amongst the BTEX group of VOCs in an urbanized industrial city. *Atmospheric environment*, *61*, 305-315.

Miller, L., Xu, X., Wheeler, A., Atari, D. O., Grgicak-Mannion, A., & Luginaah, I. (2011). Spatial variability and application of ratios between BTEX in two Canadian cities. *TheScientificWorldJOURNAL*, *11*.

MOE. (2020). *Final air quality observation data*. MOE, Korea. https://www.airkorea.or.kr

Na, K., Kim, Y. P., Moon, K.-C., Moon, I., & Fung, K. (2001). Concentrations of volatile organic compounds in an industrial area of Korea. *Atmospheric environment*, *35*(15), 2747-2756.

Nault, B. A., Campuzano-Jost, P., Day, D. A., Schroder, J. C., Anderson, B., Beyersdorf, A. J., Blake, D. R., Brune, W. H., Choi, Y., & Corr, C. A. (2018). Secondary organic aerosol production from local emissions dominates the organic aerosol budget over Seoul, South Korea, during KORUS-AQ.

NCFDI. (2017). *National Air Pollutants Emission*. http://airemiss.nier.go.kr/mbshome/mbs/airemiss/index.do

Nelson, P., & Quigley, S. (1983). The m, p-xylenes: ethylbenzene ratio. A technique for estimating hydrocarbon age in ambient atmospheres. *Atmospheric Environment (1967)*, *17*(3), 659-662.

Niaz, K., Bahadar, H., Maqbool, F., & Abdollahi, M. (2015). A review of environmental and occupational exposure to xylene and its health concerns. *EXCLI journal*, *14*, 1167.

NICS. (2018). *Pollutant release and transfer register*. Ministry of environment. https://icis.me.go.kr/prtr/prtrInfo/unitySearch.do

NIER. (2018). *High $PM_{2.5}$ episode by the secondary photochemical formation and air stagnation in Ulsana and Busan in July 2018*. https://www.nier.go.kr/

NIER. (2019). *Annual Report of Air Quality in Korea*.

NIER, & NASA. (2017). *Introduction to the KORUS-AQ Rapid Science Synthesis Report*. https://espo.nasa.gov/korus-aq/content/KORUS-AQ

Olson, K. L., Sinkevitch, R. M., & Sloane, T. M. (1992). Speciation and quantitation of hydrocarbons in gasoline engine exhaust. *Journal of chromatographic science*, *30*(12), 500-508.

Pandis, S. N., Harley, R. A., Cass, G. R., & Seinfeld, J. H. (1992). Secondary organic aerosol formation and transport. *Atmospheric Environment. Part A. General Topics*, *26*(13), 2269-2282.

Qian, Y., Henneman, L. R., Mulholland, J. A., & Russell, A. G. (2019). Empirical development of ozone isopleths: applications to Los Angeles. *Environmental Science & Technology Letters*, *6*(5), 294-299.

Schell, B., Ackermann, I. J., Hass, H., Binkowski, F. S., & Ebel, A. (2001). Modeling the formation of secondary organic aerosol within a comprehensive air quality model system. *Journal of Geophysical Research: Atmospheres*, *106*(D22), 28275-28293.

Schroeder, J. R., Crawford, J. H., Ahn, J.-Y., Chang, L., Fried, A., Walega, J., Weinheimer, A., Montzka, D. D., Hall, S. R., & Ullmann, K. (2020). Observation-based modeling of ozone chemistry in the Seoul metropolitan area during the Korea-United States Air Quality Study (KORUS-AQ). *Elementa: Science of the Anthropocene*, *8*.

Tang, M. J., Shiraiwa, M., Pöschl, U., Cox, R. A., & Kalberer, M. (2015). Compilation and evaluation of gas phase diffusion coefficients of reactive trace gases in the atmosphere: Volume 2. Diffusivities of organic compounds, pressure-normalised mean free paths, and average Knudsen numbers for gas uptake calculations. *Atmospheric Chemistry and Physics*, *15*(10), 5585-5598. https://doi.org/10.5194/acp-15-5585-2015

Tiwari, V., Hanai, Y., & Masunaga, S. (2010). Ambient levels of volatile organic compounds in the vicinity of petrochemical industrial area of Yokohama, Japan. *Air Quality, Atmosphere & Health*, *3*(2), 65-75.

Ulsan. (2020). *About Ulsan*. Ulsan Metropolitan City. Retrieved 2020 from www.ulsan.go.kr

USEPA. (1994). *Locating and estimating air emissions from sources of xylene*. https://www3.epa.gov/ttnchie1/le/xylene.pdf

USEPA. (1995). *Federal Standards For Marine Tank Vessel Loading Operations And National Emission Standards For Hazardous Air Pollutants For Marine Tank Vessel Loading Operations*. https://nepis.epa.gov/Exe/ZyPDF.cgi/20011Z8C.PDF?Dockey=20011Z8C.PDF

USEPA. (2003). *Validation and application Protocol for Source Apportionment of photochemical assessment monitoring stations (PAMS) Ambient Volatile Organic Compound (VOC) Data*. https://www3.epa.gov/ttnamti1/archive/files/ambient/samwg/drisource.pdf

USEPA. (2005). *Toxicological Review of Toluene*.

Vivaldo, G., Masi, E., Taiti, C., Caldarelli, G., & Mancuso, S. (2017). The network of plants volatile organic compounds. *Sci Rep*, *7*(1), 11050. https://doi.org/10.1038/s41598-017-10975-x

Woolfenden, E. (2010). Sorbent-based sampling methods for volatile and semi-volatile organic compounds in air Part 1: Sorbent-based air monitoring options. *J Chromatogr A*, *1217*(16), 2674-2684. https://doi.org/10.1016/j.chroma.2009.12.042

Yang, G.-H., Jo, Y.-J., Lee, H.-J., Song, C.-K., & Kim, C.-H. (2020). Numerical Sensitivity Tests of Volatile Organic Compounds Emission to PM2. 5 Formation during Heat Wave Period in 2018 in Two Southeast Korean Cities. *Atmosphere*, *11*(4), 331. https://doi.org/10.3390/atmos11040331

Yurdakul, S., Civan, M., & Tuncel, G. (2013). Volatile organic compounds in suburban Ankara atmosphere, Turkey: sources and variability. *Atmospheric research*, *120*, 298-311.

Zhang, J., Wang, T., Chameides, W., Cardelino, C., Blake, D., & Streets, D. (2008). Source characteristics of volatile organic compounds during high ozone episodes in Hong Kong, Southern China. *Atmospheric Chemistry and Physics*, *8*(16), 4983-4996.

Zhang, R., Wang, G., Guo, S., Zamora, M. L., Ying, Q., Lin, Y., Wang, W., Hu, M., & Wang, Y. (2015). Formation of urban fine particulate matter. *Chemical Reviews*, *115*(10), 3803-3855.

Supplementary Materials

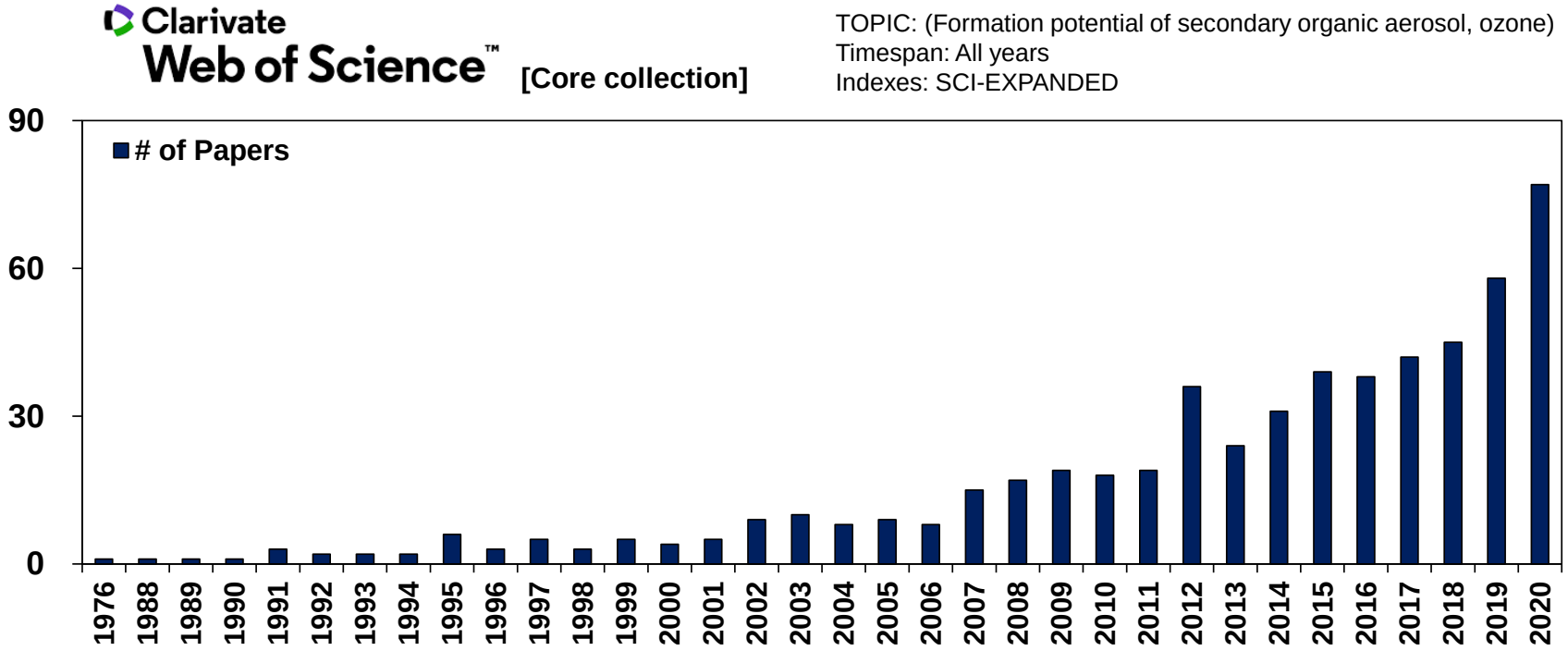

Figure S1. Trend of relevant studies

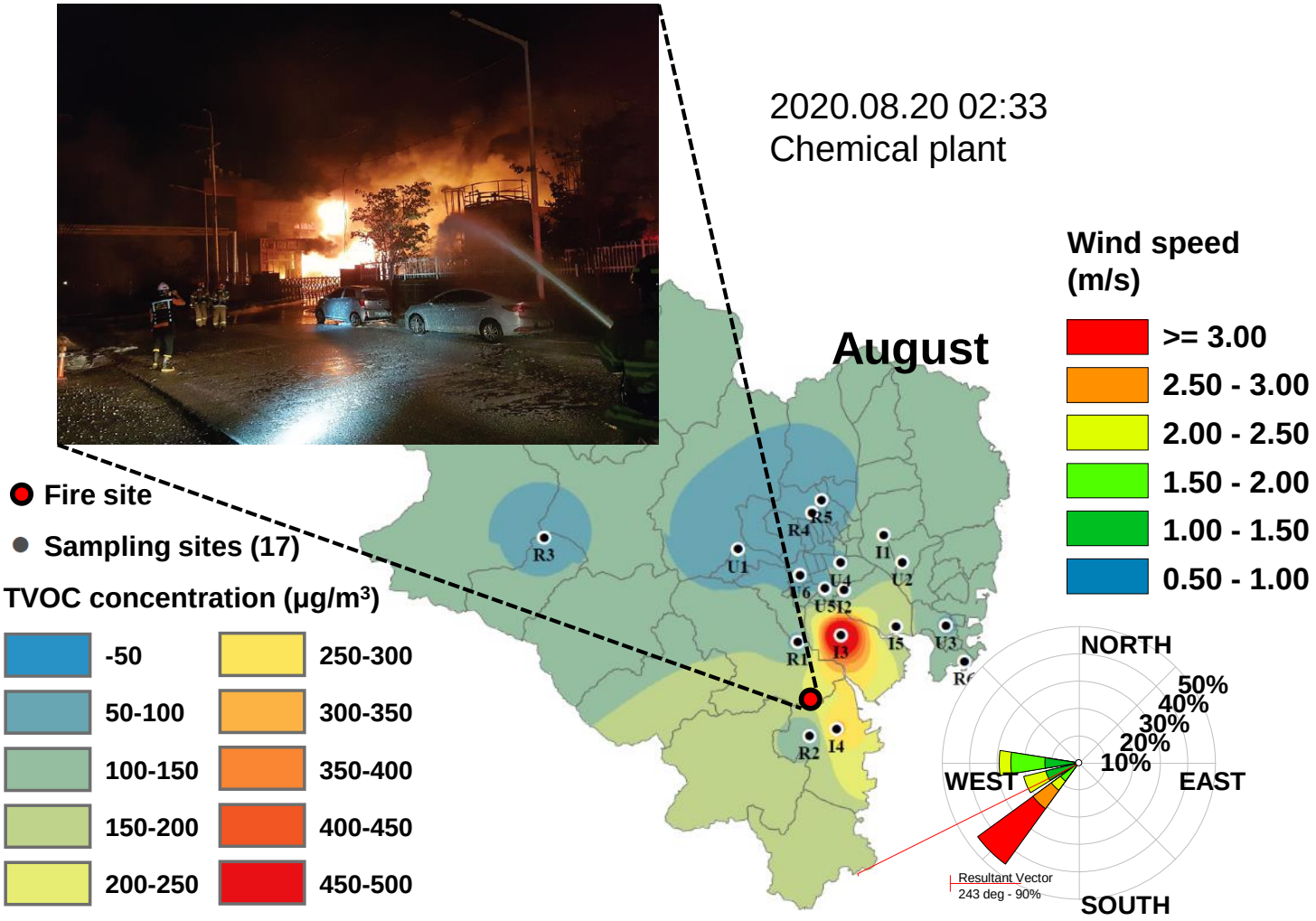

Figure S2. Industrial fire and spatial distribution of TVOC

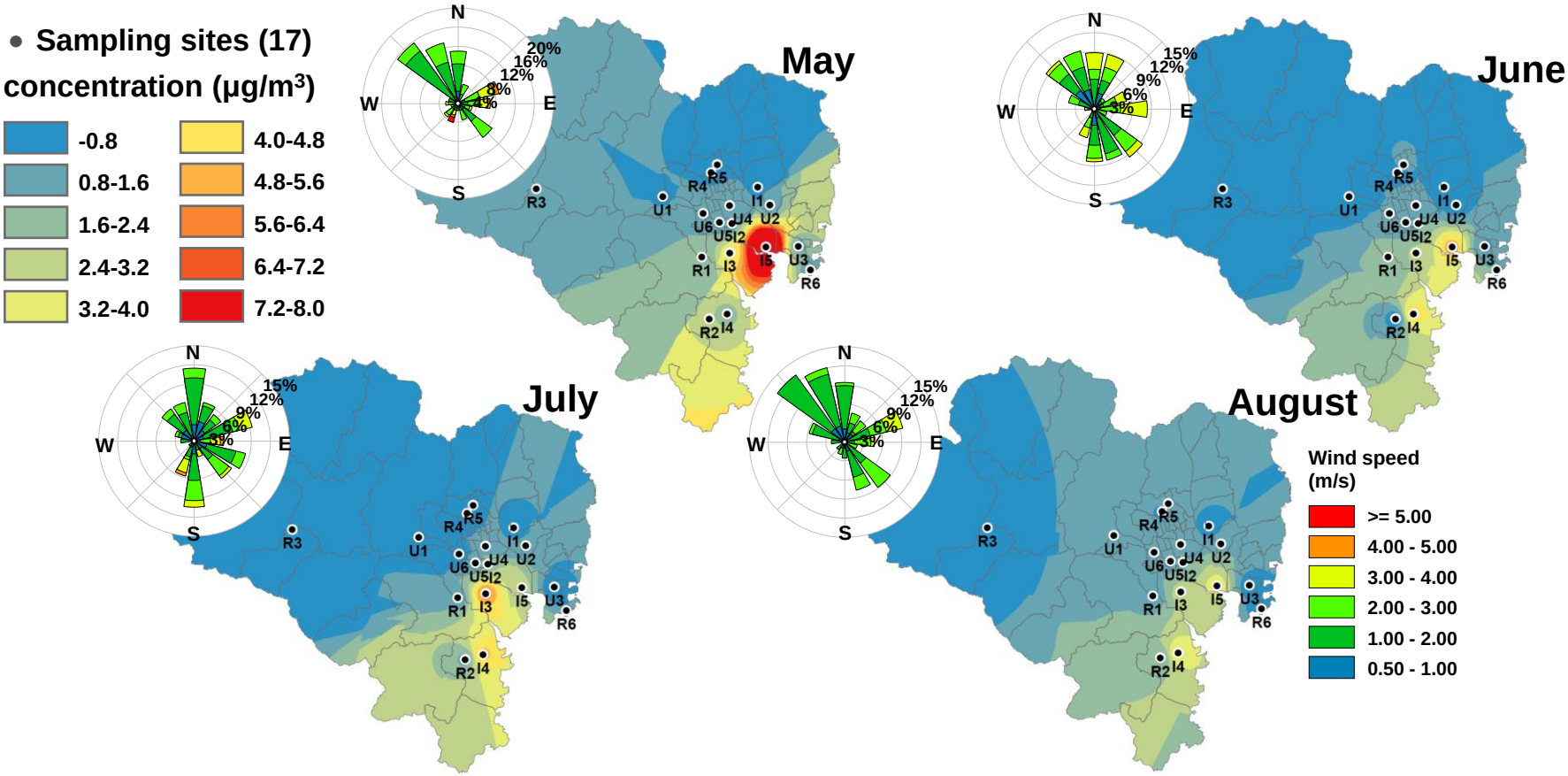

Figure S3. Monthly spatial distribution of benzene

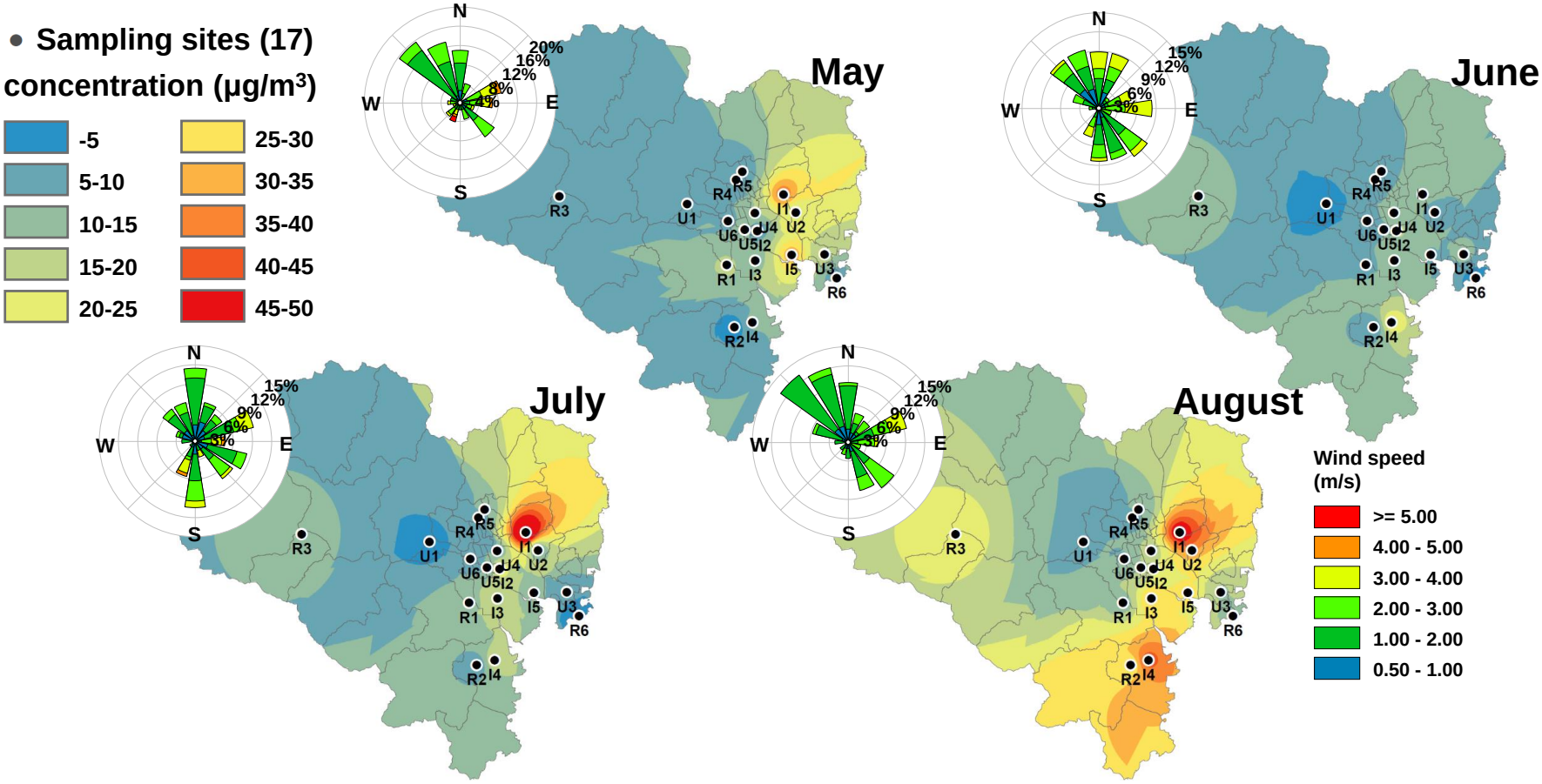

Figure S4. Monthly spatial distribution of toluene

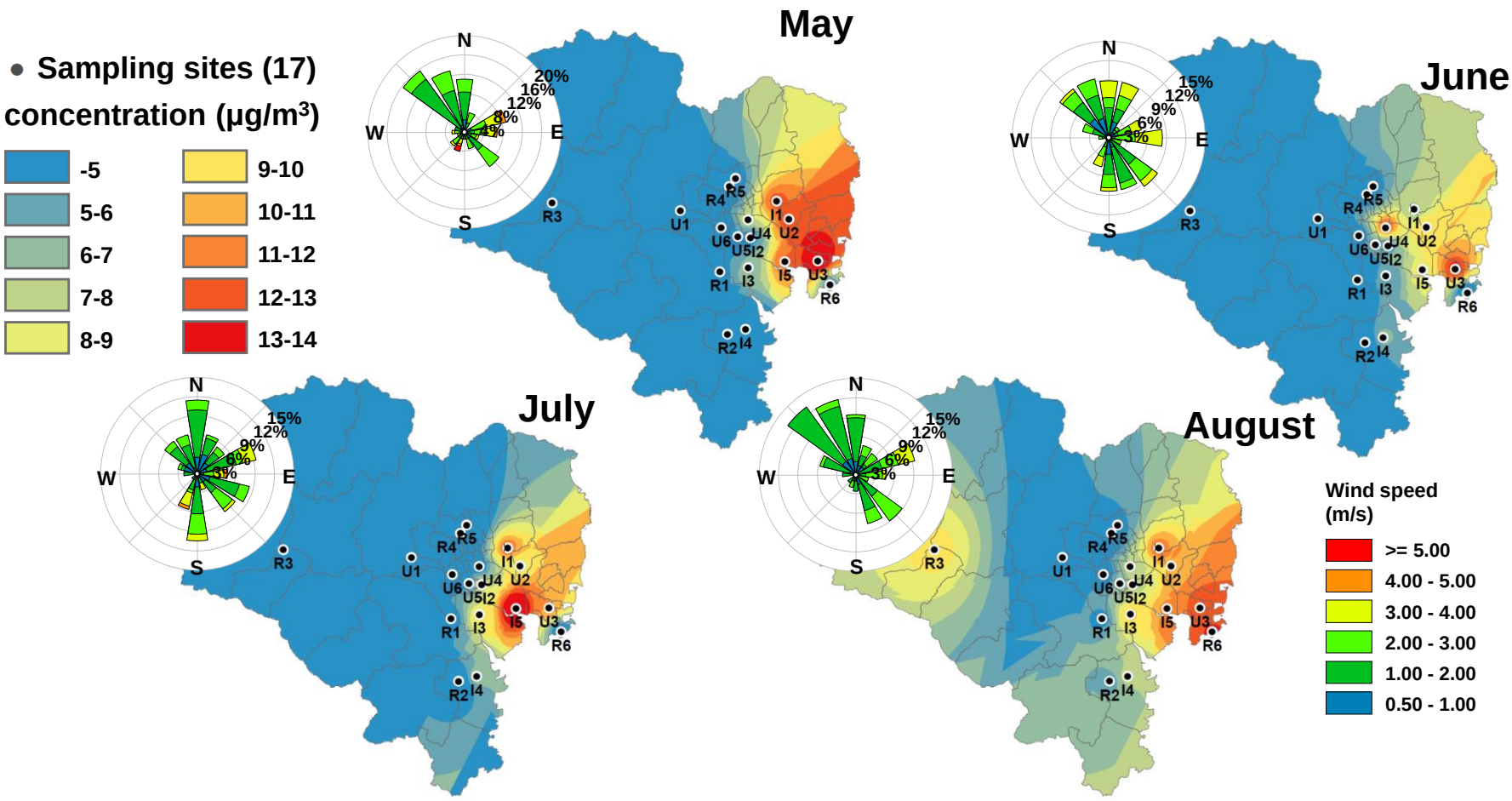

Figure S5. Monthly spatial distribution of ethylbenzene

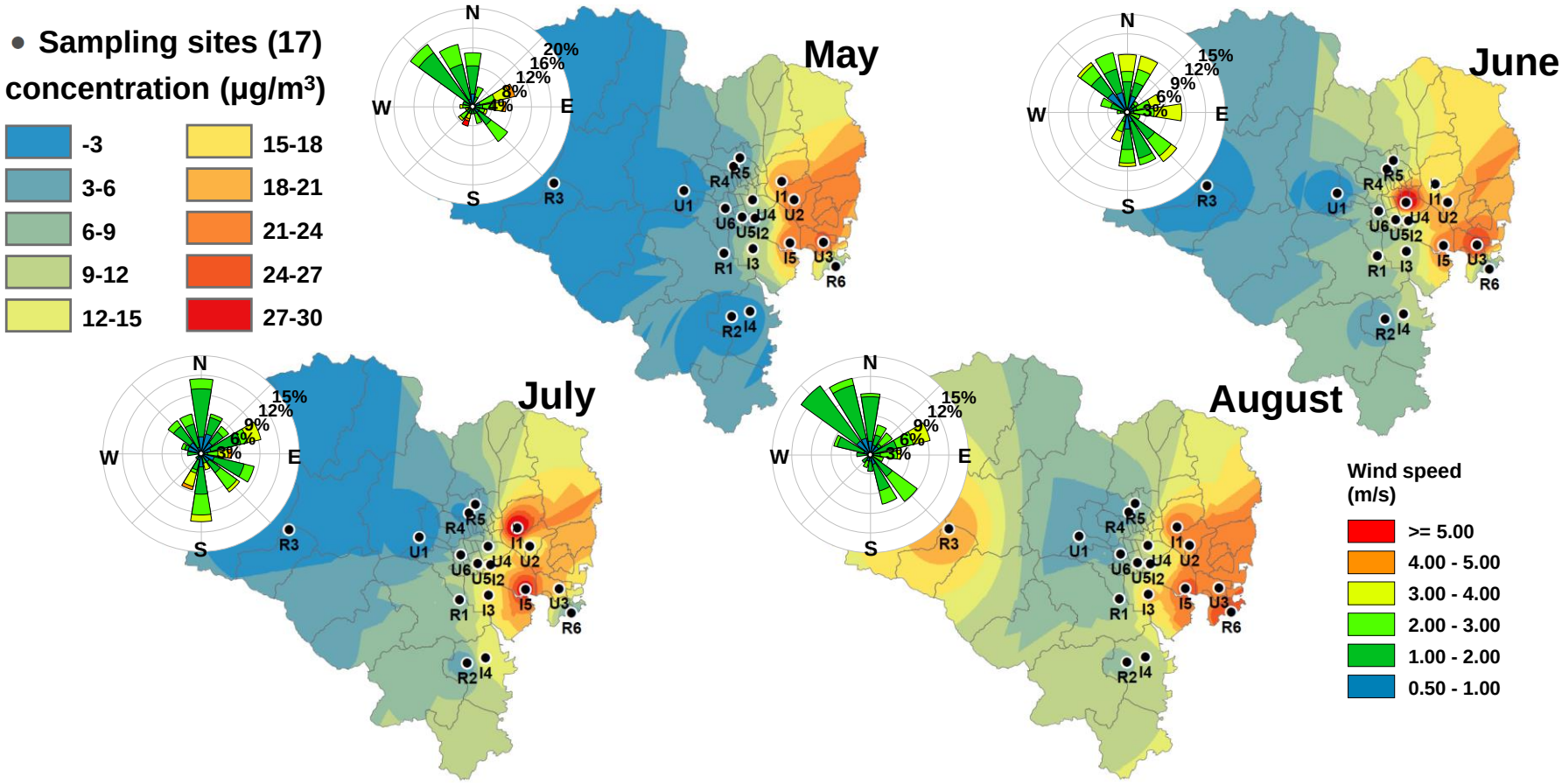

Figure S6. Monthly spatial distribution of o,m,p-xylene

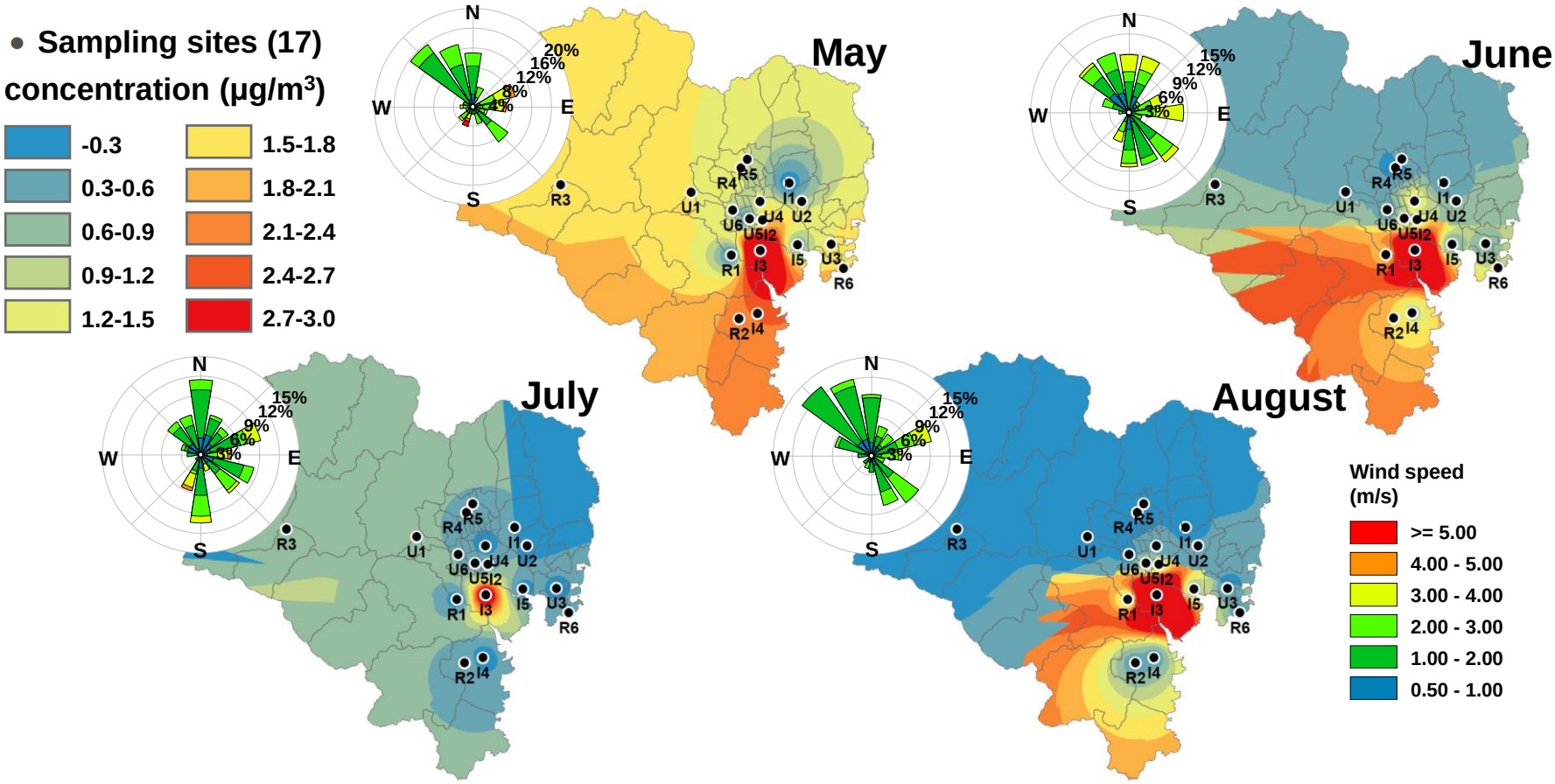

Figure S7. Monthly spatial distribution of styrene

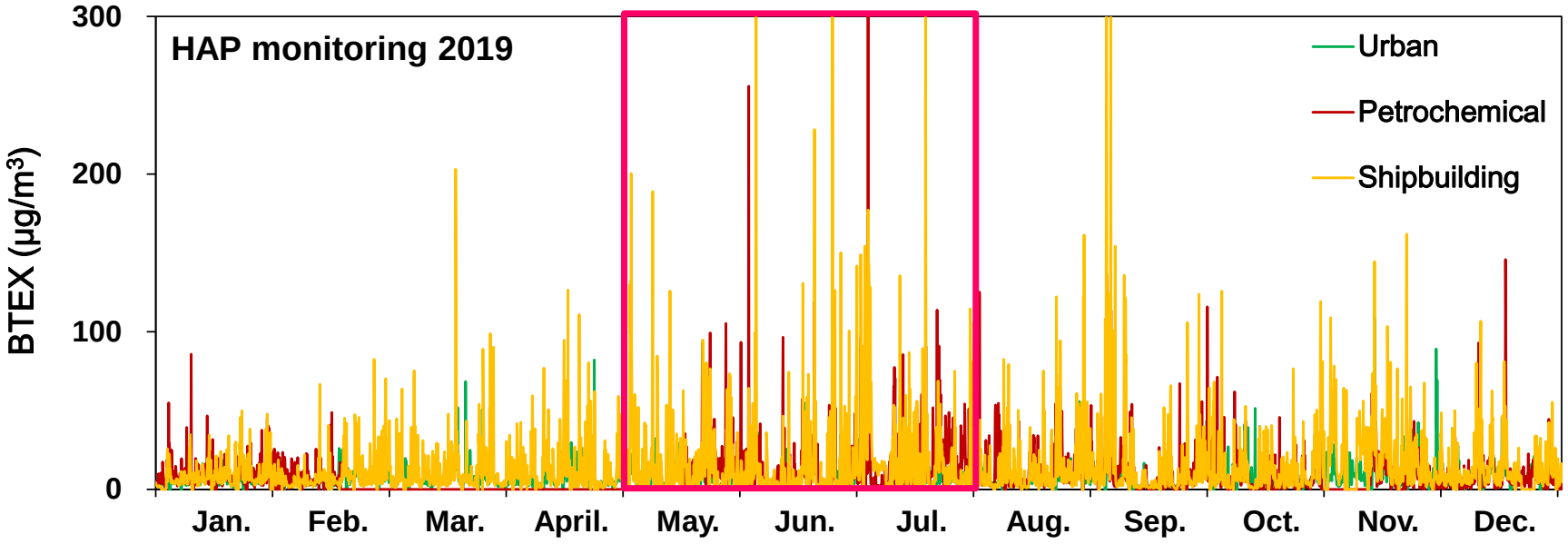

Figure S8. BTEX concentration from 3 HAP monitoring stations in Ulsan

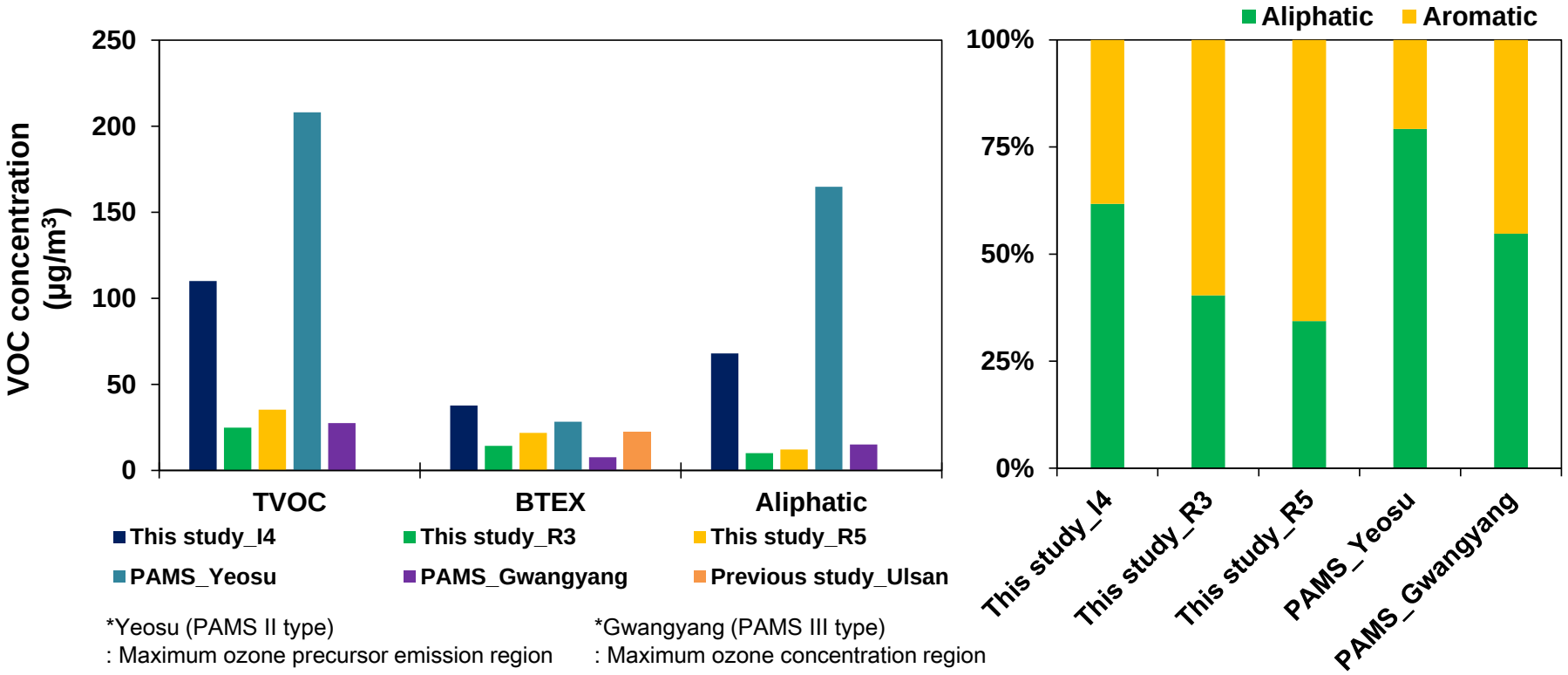

Figure S9. Levels of VOC concentration from previous VOC monitoring

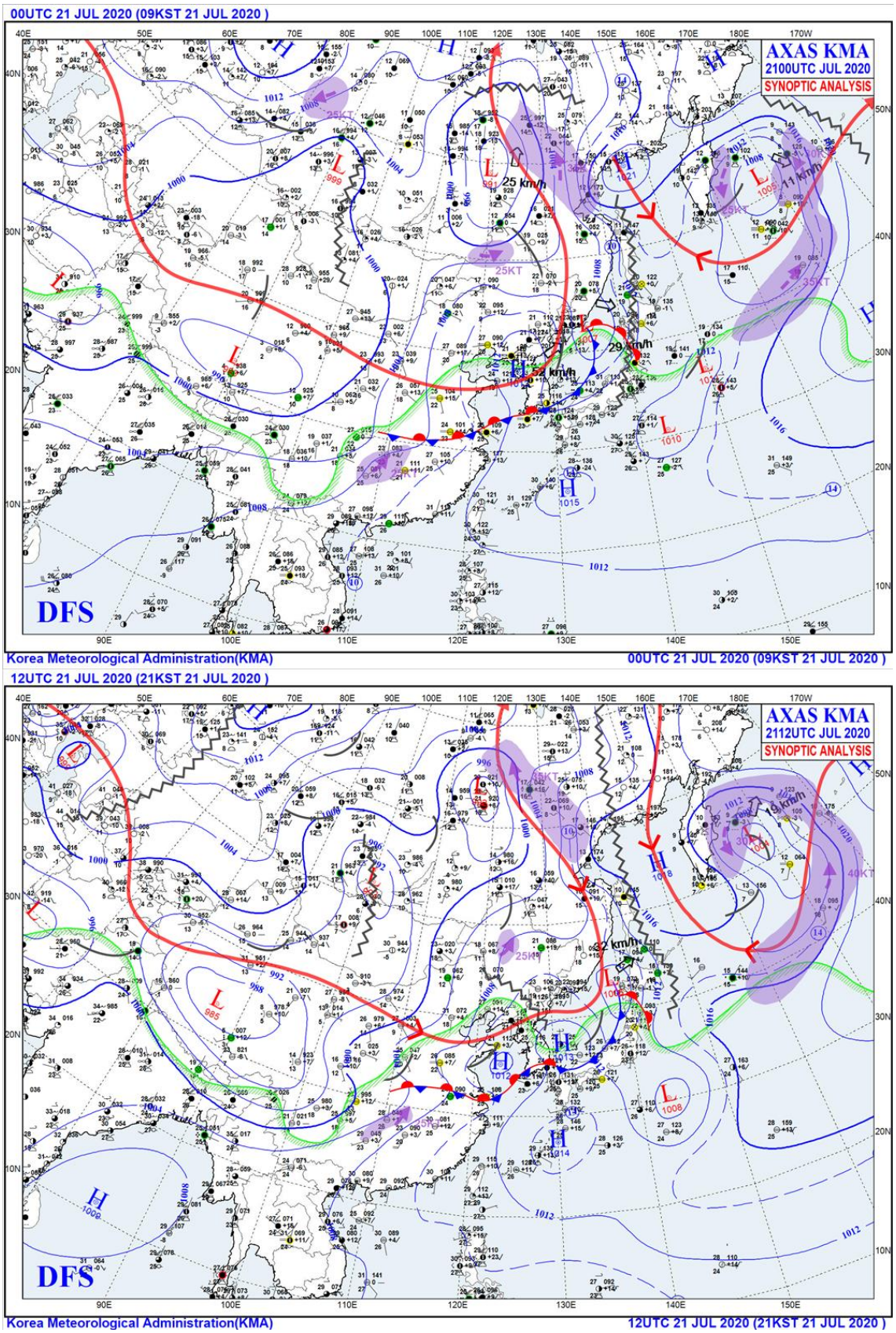

Figure S10. Weather charts on the high-pollution episode

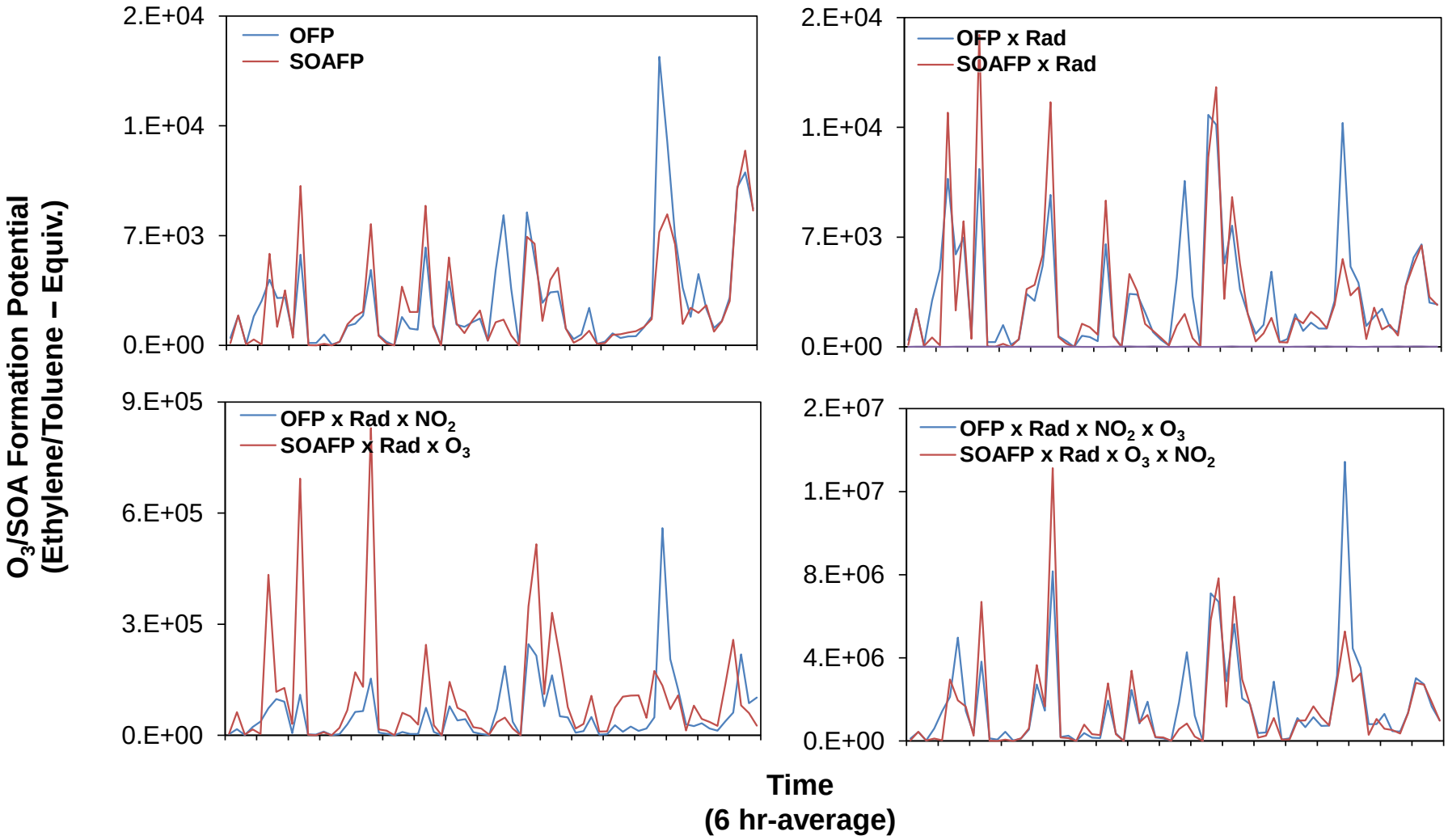

Figure S11. OFP and SOAFP estimates from various calculation methods

Acknowledgements

I would first like to appreciate that my supervisor, Professor Sung-Deuk Choi, gave me a great opportunity to learn in our lab. He stimulated my interest in environmental analytical chemistry through research on the analysis of hazardous pollutants emitted from cigarette smoke when I was a curious undergraduate intern and gave many teachings so that I could complete my master's thesis research on photochemical volatile organic compounds. Besides, I would like to express sincere gratitude to my master's thesis committee members, Professor Chang-Keun Song and Professor Sang Seo Park, who were willing to review my master's thesis and gave helpful advice for the research.

In addition, I am grateful to researchers of the UNIST Environmental Analysis Center. I would like to express deep gratitude to Chul-Su Kim who taught me from a basic knowledge of high-resolution mass spectrometry to practical instrument analysis experiments with his great enthusiasm.

I sincerely want to thank the wonderful members of EACL. Many thanks to Sang-Jin Lee who passionately informed me from sample collection to modeling, Seong-Joon Kim who inspired me through his strong attitude of leading by example and helped my master's thesis works much, Ho-Young Lee who consulted me about an undergraduate lab internship and my graduate lab life, Min-Kyu Park who has always encouraged me with a positive heart, and Ji-Min Son who helped a lot in collecting and analyzing samples. My gratitude extends to all the members of a self-supported group in EACL, named Researches & Discussions, for their insightful comments and suggestions.

Moreover, I would like to acknowledge strong supports from other UNIST members. Especially, my research sustainability was strengthened by the UNIST football club, Earth Cops (for UG)/Earth Senior (for G). Dongjun Lim and Junho Son have been the consistent inspirations for my life. My special thanks to Seonyoung Yoon for invaluable help as well as happy distraction refreshing my mind.

I would finally like to express my great gratitude to my beloved family and friends, who are the biggest support in my life, for respecting my will anytime, anywhere and giving generous assistance and encouragement so that I can do the challenging things I want to try without fear.

I think I could have graduated with a master's degree due to the many great people around me. It was a tremendous honor to be able to spend the majority of my twenties with you. In the future, I will work harder to achieve my life goals while keeping my genuine enthusiasm for contributing to society. I wish you all the best.